

Single-ion and exchange anisotropy in high-symmetry tetramer single molecule magnets

Richard A. Klemm^{1,*} and Dmitri V. Efremov^{2,†}

¹*Department of Physics, Kansas State University, Manhattan, KS 66506 USA*

²*Institut für Theoretische Physik, Technische Universität Dresden, 01062 Dresden, Germany*

(Dated: March 23, 2022)

For equal-spin s_1 tetramer single molecule magnets with ionic point groups $g = T_d, D_{4h}, D_{2d}, C_{4h}, C_{4v}$, and S_4 , we write the group-invariant single-ion, Dzaloshinskii-Moriya, and anisotropic near-neighbor and next-nearest-neighbor exchange Hamiltonians using the respective local axial and azimuthal vector groups. In the molecular representation, the symmetric anisotropic exchange interactions renormalize the near-neighbor and next-nearest-neighbor isotropic exchange interactions to \tilde{J}_g and \tilde{J}'_g . The local single-ion and symmetric anisotropic exchange interactions generate the site-independent anisotropy interactions in the molecular representation, $J_z^g(\mu_1^g)$, $J_{1,z}^g(\mu_{12}^g)$, and $J_{2,z}^g$, respectively, where μ_1^g and μ_{12}^g represent the group-consistent sets of parameters required to diagonalize the single-ion and symmetric near-neighbor and next-nearest-neighbor anisotropic exchange Hamiltonians, respectively. The site-independent group-invariant near-neighbor and next-nearest-neighbor Dzaloshinskii-Moriya interactions generally may be written as vectors of rank three and two, \mathbf{d}^g and \mathbf{d}'^g , respectively. The local anisotropy interactions also generate site-dependent single-ion, near-neighbor, and next-nearest-neighbor anisotropic exchange interactions in the molecular representation. Using our exact, compact forms for the single-ion matrix elements, we evaluate the eigenstate energies to first order in $J_z^g(\mu_1^g)$, $J_{1,z}^g(\mu_{12}^g)$, and $J_{2,z}$. There are two types of ferromagnetic (FM) ($\tilde{J}_g > 0$ and antiferromagnetic (AFM) ($\tilde{J}_g < 0$) tetramers. In Type I, $\tilde{J}'_g - \tilde{J}_g > 0$, the tetramer acts as two dimers with the maximal pair quantum numbers $s_{13} = s_{24} = 2s_1$ at low temperatures T . Type II tetramers with $\tilde{J}'_g - \tilde{J}_g < 0$ are frustrated, with minimal values of the pair quantum numbers s_{13} and s_{24} at low T . For both Type I and II AFM tetramers, we evaluate the first-order level-crossing inductions analytically for arbitrary s_1 , and illustrate the results for $s_1 = 1/2, 1, 3/2$. Accurate Hartree expressions for the thermodynamics, electron paramagnetic resonance (EPR) absorption and inelastic neutron scattering cross-section are given. A procedure to extract the effective microscopic parameters for Types I and II FM tetramers using EPR is given.

PACS numbers: 75.75.+a, 75.50.Xx, 73.22.Lp, 75.30.Gw, 75.10.Jm

I. INTRODUCTION

Single molecule magnets (SMM's) have been a topic of great interest for more than a decade,[1] because of their potential uses in quantum computing and/or magnetic storage,[2] which are possible due to magnetic quantum tunneling (MQT) and entangled states. In fits to a wealth of data, the Hamiltonian within an SMM was assumed to be the Heisenberg exchange interaction plus weaker total (global, or giant) spin anisotropy interactions, with a fixed overall total spin quantum number s . [1] MQT and entanglement were only studied in this simple model.

The simplest SMM's are dimers.[3, 4] Surprisingly, two antiferromagnetic dimers, an Fe_2 and a Ni_2 , appear to have substantial single-ion anisotropy without any appreciable total spin anisotropy.[4, 5, 6] Although the most common SMM's have ferromagnetic (FM) intramolecular interactions and contain $n \geq 8$ magnetic ions,[7] a number of intermediate-sized FM SMM's with $n = 4$ and rather simple molecular structures were recently studied. The Cu_4 tetramer $\text{Cu}_4\text{OCl}_6(\text{TPPO})_4$, where TPPO is triphenylphosphine oxide, has four spin 1/2 ions on the corners of a regular tetrahedron, with an $s = 2$ ground state and approximate T_d symmetry.[10, 11, 12]

In this case, there are no single-ion anisotropy effects, but anisotropic symmetric exchange interactions were thought to be responsible for the zero-field energy splittings.[10, 13] The Co_4 , $\text{Co}_4(\text{hmp})_4(\text{MeOH})_4\text{Cl}_4$, where hmp is hydroxymethylpyridyl, and Cr_4 , $[\text{Cr}_4\text{S}(\text{O}_2\text{CCH}_3)_8(\text{H}_2\text{O})_4](\text{NO}_3)_2 \cdot \text{H}_2\text{O}$, compounds have $s = 6$ ground states with spin 3/2 ions on the corners of tetrahedrons.[9, 14] Those compounds have S_4 and approximate D_{2d} symmetry, respectively.[9, 14] A number of high symmetry $s = 4$ ground state Ni_4 structures with spin 1 ions were reported.[15, 16, 17, 18, 19] Two of these, $[\text{Ni}(\text{hmp})(\text{ROH})\text{Cl}]_4$, where R is an alkyl group, such as methyl, ethyl, or 3,3-dimethyl-1-butyl and hmp is 2-hydroxymethylpyridyl, form tetramers with precise S_4 group symmetry.[18, 19] Two others, $\text{Ni}_4(\text{ROH})\text{L}_4$, where R is methyl or ethyl and H_2L is salicylidene-2-ethanolamine, had approximate S_4 symmetry, although the precise symmetry was only C_1 . [15] Several planar Mn_4 compounds with the Mn^{+3} spin 2 ions on the corners of squares were made, with overall $s = 8$ tetramer ground states.[20] Although two of these complexes had only approximate S_4 symmetry, one of these complexes, $\text{Mn}_4\text{Cl}_4(\text{L}')_4$, where $\text{H}_2\text{L}'$ is 4-*t*-butyl-salicylidene-2-ethanolamine, had perfect S_4 symmetry.[20] Inelastic neutron scattering (INS)

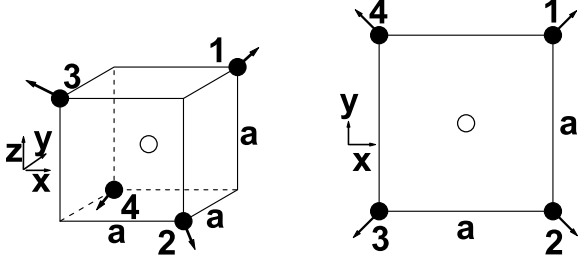


FIG. 1: T_d (left) and D_{4h} (right) ion sites (filled). Circle: origin. Arrows: local axial $\hat{z}_n^{T_d}$ (left), azimuthal $\hat{x}_n^{D_{4h}}$ (right) single-ion vectors. The axial vectors $\hat{z}_n^{D_{4h}} = \hat{z}$, normal to the ionic plane.

experiments provided strong evidence for single-ion anisotropy in Co_4 and a Ni_4 with approximate S_4 symmetry.[14, 15] The presence of single-ion or exchange anisotropy actually precludes the total spin s from being a good quantum number.[4] Fits to electron paramagnetic resonance (EPR) Ni_4 data assuming a fixed s were also problematic, suggesting single-ion or exchange anisotropy in that tetramer, as well.[21]

Recently there have been microscopic treatments of dimers,[4] trimers, and tetramers, including Zeeman g -tensor anisotropy, single-ion anisotropy, and anisotropic exchange interactions.[22] Most of those treatments and their recent extensions to more general systems expressed the single-spin matrix elements only in terms of Wigner $3j$, $6j$, and $9j$ symbols.[22, 23] While such treatments are very helpful in fitting experimental data, more compact analytic forms are desirable to study microscopic models of FM SMM's in which the MQT and entanglement issues crucial for quantum computing can be understood. We constructed the single-ion and anisotropic near-neighbor (NN) and next-nearest-neighbor (NNN) exchange SMM Hamiltonians from the respective local axial and azimuthal vector groups for equal-spin tetramer SMM's with point group symmetries $g = T_d, D_{4h}, D_{2d}, C_{4h}, C_{4v}$, and S_4 , and found compact analytic expressions for the single-spin matrix elements of four general spins. Surprisingly, each local vector group generates site-dependent molecular single-ion and exchange anisotropy. We evaluate the magnetization, specific heat, EPR and INS transitions in the Hartree approximation, and provide a procedure for extracting the effective site-independent microscopic parameters using EPR.

II. STRUCTURES AND BARE HAMILTONIAN

For SMM's with ionic site point groups $g = T_d, D_{4h}$, we assume the four equal-spin s_1 ions sit on opposite corners of a cube or square of side a centered at the origin, as

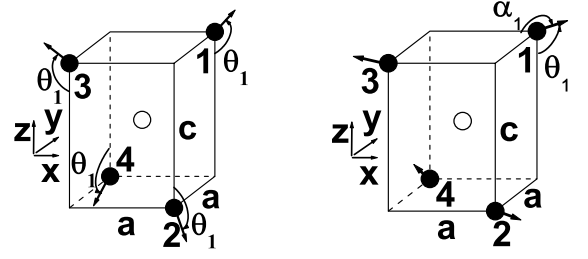


FIG. 2: D_{2d} (left) and S_4 (right) ion sites (filled). Circle: origin. Arrows: local axial single-ion vectors. The $g = D_{2d}, S_4$ axial vectors \hat{z}_1^g make the angles θ_1^g with the z axis, and the S_4 axial vector $\hat{z}_1^{S_4}$ also makes the angle α_1 with the x axis, where $\cos \alpha_1 = \sin \theta_1^{S_4} \cos \phi_1^{S_4}$.

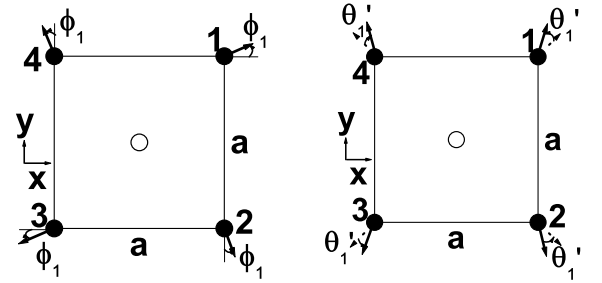


FIG. 3: C_{4h} (left) and C_{4v} (right) ion sites (filled). Circle: origin. Arrows: local azimuthal $\hat{x}_n^{C_{4h}}$ (left) axial $\hat{z}_n^{C_{4v}}$ (right) single-ion vectors. The axial vectors $\hat{z}_n^{C_{4h}} = \hat{z}$. The C_{4v} axial vectors each make the angle $\theta_1 = \pi/2 - \theta'_1$ with z axis. The dotted arrows (equivalent to the D_{4h} azimuthal single-ion vectors $\hat{x}_n^{D_{4h}}$) are their projections in the xy plane.

pictured in Fig. 1. For SMM's with $g = D_{2d}, S_4$, we take the ions to sit on opposite corners of a tetragonal prism with sides (a, a, c) centered at the origin, as in Fig. 2. The ions for $g = C_{4h}, C_{4v}$ also sit on the corners of a square of side a centered at the origin, as pictured in Fig. 3, but the ligand groups have different symmetries than for the simpler D_{4h} case pictured in Fig. 1. In each case, we take the origin to be at the geometric center, so that $\sum_{n=1}^4 \mathbf{r}_n = 0$, where the relative ion site vectors

$$\mathbf{r}_n = \frac{a}{2}[-\gamma_n^+ \hat{x} + \gamma_n^- \hat{y}] - \frac{c}{2}(-1)^n \hat{z}, \quad (1)$$

$$\gamma_n^\pm = \epsilon_n^+ (-1)^{n/2} \pm \epsilon_n^- (-1)^{(n+1)/2}, \quad (2)$$

and $\epsilon_n^\pm = [1 \pm (-1)^n]/2$. [24] For clarity, the values of ϵ_n^\pm and γ_n^\pm are given in Table 1. In tetrahedrons with $g = T_d$, $c/a = 1$, approximately as in Cu_4 . [10] In squares with $g = D_{4h}, C_{4h}$, or C_{4v} , $c = 0$. The high D_{4h} symmetry is approximately exhibited by the square Nd_4 compound, $\text{Nd}_4(\text{OR})_{12}$, where R is 2,2-dimethyl-1-propyl, in which the Nd^{+3} ions have equal total angular momentum $j = 9/2$. [25, 26] We note that the Mn_4 SMM's with

n	ϵ_n^+	ϵ_n^-	γ_n^+	γ_n^-
1	0	1	-1	1
2	1	0	-1	-1
3	0	1	1	-1
4	1	0	1	1

TABLE I: Values of ϵ_n^\pm and γ_n^\pm .

approximate or exact S_4 symmetry also have $c = 0$. [20] In tetragonal prisms with $g = D_{2d}$ or S_4 , $c/a > 1$, approximately as in Co_4 , [14] or $c/a < 1$, as in Mn_4 and a Ni_4 . [16, 20] $\hat{x}, \hat{y}, \hat{z}$ are the molecular (or laboratory) axes of each SMM.

The most general Hamiltonian quadratic in the four spin operators \mathbf{S}_n may be written for group g as

$$\mathcal{H}^g = -\mu_B \sum_{n=1}^4 \mathbf{B} \cdot \overleftrightarrow{\mathbf{g}}_n^g \cdot \mathbf{S}_n + \sum_{n,n'=1}^4 \mathbf{S}_n \cdot \overleftrightarrow{\mathbf{D}}_{n,n'}^g \cdot \mathbf{S}_{n'}, \quad (3)$$

where μ_B is the Bohr magneton and $\mathbf{B} = B(\sin \theta \cos \phi, \sin \theta \sin \phi, \cos \theta)$ is the magnetic induction at an arbitrary direction (θ, ϕ) relative to the molecular coordinates $(\hat{x}, \hat{y}, \hat{z})$. [22, 27]

The exchange matrices $\overleftrightarrow{\mathbf{D}}_{n,n'}^g$ for $n' \neq n$ can have antisymmetric terms, which are the Dzyaloshinskii-Moriya (DM) interactions. Of the six molecular group symmetries under study, the DM interactions are non-vanishing for all but the highest group symmetry, T_d . [28, 29] For the other five group symmetries, the DM interactions lead to weak perturbations to the eigenstate energies. Inequivalent ions or ligands, or local structural distortions from the ideal point group symmetry, as commonly occur in real systems, [30] break these g symmetries, introducing stronger DM interactions. Such lower symmetry groups will be discussed elsewhere. [31]

For simplicity, we take $\overleftrightarrow{\mathbf{g}}_n^g$ to be diagonal, isotropic, and site-independent, so that the Zeeman interaction may be written in terms of a single gyromagnetic ratio $\gamma \approx 2\mu_B$. Thus in the following, g only refers to the molecular group. We separate $\overleftrightarrow{\mathbf{D}}_{n,n'}^g$ into its symmetric and antisymmetric parts, $\overleftrightarrow{\mathbf{D}}_{n,n'}^g = \overleftrightarrow{\mathbf{D}}_{n,n'}^{g,s} + \overleftrightarrow{\mathbf{D}}_{n,n'}^{g,a}$, respectively. For $n' = n$, the single-ion $\overleftrightarrow{\mathbf{D}}_{n,n}^g$ is necessarily symmetric, so $\overleftrightarrow{\mathbf{D}}_{n,n}^{g,a} = 0$. For each g , the four $\overleftrightarrow{\mathbf{D}}_{n,n}^{g,s}$ contain the local single-ion structural information, and the six distinct symmetric $\overleftrightarrow{\mathbf{D}}_{n,n'}^{g,s}$ contain the local symmetric exchange structural information, which lead to the isotropic, or Heisenberg, exchange interactions, and the remaining symmetric anisotropic exchange interactions. The six distinct antisymmetric $\overleftrightarrow{\mathbf{D}}_{n,n'}^{g,a}$ contain additional local structural information which lead to the DM interactions. Physically, the symmetric anisotropic exchange interactions also contain the dipole-dipole interactions, which can be even larger in magnitude than the terms originating from actual anisotropic exchange. [27]

As is well known, each of the symmetric rank-three tensors (or matrices) can be diagonalized by three rotations: a rotation by the angle $\phi_{n,n'}^g$ about the molecular z axis, then a rotation by the angle $\theta_{n,n'}^g$ about the rotated \tilde{x} axis, followed by a rotation by the angle $\psi_{n,n'}^g$ about the rotated \tilde{z} axis. [32] This necessarily leads to the three principal axes $\hat{\mathbf{x}}_{n,n'}^g, \hat{\mathbf{y}}_{n,n'}^g$, and $\hat{\mathbf{z}}_{n,n'}^g$. For the single-ion axes with $n' = n$, we denote these principal axes to be $\hat{\mathbf{x}}_n^g, \hat{\mathbf{y}}_n^g$, and $\hat{\mathbf{z}}_n^g$, respectively, which are written explicitly in Sec. III. The non-vanishing matrix elements in these locally-diagonalized symmetric matrix coordinates are $\tilde{D}_{n,n'}^{g,s,xx}, \tilde{D}_{n,n'}^{g,s,yy}$ and $\tilde{D}_{n,n'}^{g,s,zz}$. Since the structural information in each of the $\overleftrightarrow{\mathbf{D}}_{n,n'}^{g,s}$ depends upon the local environment, in the absence of molecular group g symmetry, each of these angles would in principle be different from one another. We characterize the single-ion and symmetric anisotropic exchange vector sets by those for the spin at site 1, the NN pair at sites 1 and 2, and the NNN pair at sites 1 and 3, respectively,

$$\{\mu_1^g\} = (\theta_1^g, \phi_1^g, \psi_1^g), \quad (4)$$

$$\{\mu_{12}^g\} = (\theta_{12}^g, \phi_{12}^g, \psi_{12}^g), \quad (5)$$

$$\{\mu_{13}^g\} = (\theta_{13}^g, \phi_{13}^g, \psi_{13}^g), \quad (6)$$

respectively, where $\theta_1^g = \theta_{1,1}^g$, $\theta_{12}^g = \theta_{1,2}^g$, and $\theta_{13}^g = \theta_{1,3}^g$.

Since the antisymmetric exchange matrix cannot generally be diagonalized, instead of writing a different general set of exchange vectors, we first employ the Moriya rules for the interactions between each pair of spins in the molecular representation, [27, 29] and then impose the group operations in that representation. This leads to an additional set of as many as five parameters for the NN and NNN DM interactions, which we write as the three- and two-vectors, \mathbf{d}^g and \mathbf{d}_\perp^g , respectively.

For the six high-symmetry groups under study, we analyze the effects of molecular group symmetry upon these coordinates. As shown in the following, the molecular group symmetry can greatly simplify the theoretical analysis of the measurable quantities, so that only the various interaction magnitudes and these five angular sets are required. Some group symmetries impose severe restrictions upon the elements of the angular sets.

In the absence of any anisotropy interactions, the bare Hamiltonian \mathcal{H}_0^g is given by the Zeeman and Heisenberg interactions,

$$\begin{aligned} \mathcal{H}_0^g = & -\gamma \mathbf{B} \cdot \mathbf{S} - J'_g (\mathbf{S}_1 \cdot \mathbf{S}_3 + \mathbf{S}_2 \cdot \mathbf{S}_4) \\ & - J_g (\mathbf{S}_1 \cdot \mathbf{S}_2 + \mathbf{S}_2 \cdot \mathbf{S}_3 + \mathbf{S}_3 \cdot \mathbf{S}_4 + \mathbf{S}_4 \cdot \mathbf{S}_1), \end{aligned} \quad (7)$$

which can be rewritten as

$$\mathcal{H}_0^g = -\frac{J_g}{2} \mathbf{S}^2 - \gamma \mathbf{B} \cdot \mathbf{S} - \frac{(J'_g - J_g)}{2} (\mathbf{S}_{13}^2 + \mathbf{S}_{24}^2), \quad (8)$$

where we have dropped the irrelevant constants, and

$$J'_{T_d} = J_{T_d}, \quad (9)$$

$$J'_g \neq J_g \quad (10)$$

for $g = D_{2d}, S_4, D_{4h}, C_{4h}$, and C_{4v} . In terms of the diagonalized matrix elements, $-2J_g = \tilde{D}_{1,2,xx}^{g,s} + \tilde{D}_{1,2,yy}^{g,s}$ and $-2J'_g = \tilde{D}_{1,3,xx}^{g,s} + \tilde{D}_{1,3,yy}^{g,s}$, for instance.

We note that for $c/a < 1$, $-J_g$ and $-J'_g$ are the NN and NNN Heisenberg interactions for D_{2d}, S_4 , as for C_{4v}, C_{4h} and D_{4h} with $c = 0$, but for $c/a > 1$, $-J_g$ and $-J'_g$ are the NNN and NN Heisenberg interactions, respectively, for D_{2d} and S_4 . In Eq. (8), $\mathbf{S}_{13} = \mathbf{S}_1 + \mathbf{S}_3$, $\mathbf{S}_{24} = \mathbf{S}_2 + \mathbf{S}_4$, and $\mathbf{S} = \mathbf{S}_{13} + \mathbf{S}_{24}$ is the total spin operator.[26]

III. THE SINGLE-ION AND ANISOTROPIC EXCHANGE HAMILTONIANS

In order to properly take account of the molecular group g symmetries, it is useful to describe the single-ion and symmetric anisotropic exchange interactions in terms of the *local* coordinates. We write the local Hamiltonian for these interactions, and require that it must be invariant under all λ operations \mathcal{O}_λ^g of g . As noted above, we write the antisymmetric exchange interactions in the molecular representation, employing the group symmetry interactions relevant to the particular pair involved in each exchange, and then impose the overall group symmetry. In Secs. IV-IX, we then impose the group symmetries on these interactions for $C_{4h}, D_{4h}, C_{4v}, S_4, D_{2d}$, and T_d molecular group symmetries, respectively.

A. Local single-ion Hamiltonian

To do so for the single-ion anisotropy, we first define the vector bases for each group g . We define the local axial vector basis to be $\{\hat{\mathbf{z}}_n^g\}$ for each g , and the orthogonal azimuthal vector bases to be $\{\hat{\mathbf{x}}_n^g\}$ and $\{\hat{\mathbf{y}}_n^g\}$. The elements of these bases are the vectors that diagonalize the single ion matrix from $\overset{\leftrightarrow}{D}_{n,n}^g$ to $\overset{\leftrightarrow}{D}_{n,n}^g$. [32] Since we employ these vectors repeatedly, we write them here for simplicity of presentation. The diagonalized vectors $\hat{\mathbf{x}}_n^g$, etc., may be written in the molecular $(\hat{\mathbf{x}}, \hat{\mathbf{y}}, \hat{\mathbf{z}})$ representation as

$$\hat{\mathbf{x}}_n^g = \begin{pmatrix} \cos \phi_n^g \cos \psi_n^g - \cos \theta_n^g \sin \phi_n^g \sin \psi_n^g \\ \cos \psi_n^g \sin \phi_n^g + \cos \theta_n^g \cos \phi_n^g \sin \psi_n^g \\ \sin \theta_n^g \sin \psi_n^g \end{pmatrix}, \quad (11)$$

$$\hat{\mathbf{y}}_n^g = \begin{pmatrix} -\cos \phi_n^g \sin \psi_n^g - \cos \theta_n^g \sin \phi_n^g \cos \psi_n^g \\ -\sin \psi_n^g \sin \phi_n^g + \cos \theta_n^g \cos \phi_n^g \cos \psi_n^g \\ \sin \theta_n^g \cos \psi_n^g \end{pmatrix} \quad (12)$$

$$\hat{\mathbf{z}}_n^g = \begin{pmatrix} \sin \theta_n^g \sin \phi_n^g \\ -\sin \theta_n^g \cos \phi_n^g \\ \cos \theta_n^g \end{pmatrix}, \quad (13)$$

which satisfy $\hat{\mathbf{x}}_n^g \times \hat{\mathbf{y}}_n^g = \hat{\mathbf{z}}_n^g$. We then write the most general quadratic single-ion anisotropy interaction as

$$\mathcal{H}_{si}^{g,\ell} = - \sum_{n=1}^4 \left(J_{a,n}^g (\mathbf{S}_n \cdot \hat{\mathbf{z}}_n^g)^2 + J_{e,n}^g [(\mathbf{S}_n \cdot \hat{\mathbf{x}}_n^g)^2 - (\mathbf{S}_n \cdot \hat{\mathbf{y}}_n^g)^2] \right), \quad (14)$$

in terms of the site-dependent axial and azimuthal interactions $J_{a,n}^g, J_{e,n}^g$, analogous in notation to that for homoionic dimers.[4] In terms of the diagonalized matrix elements, $-J_{a,n}^g = \tilde{D}_{n,n,zz}^{g,s} - (\tilde{D}_{n,n,xx}^{g,s} + \tilde{D}_{n,n,yy}^{g,s})/2$ and $-J_{e,n}^g = (\tilde{D}_{n,n,xx}^{g,s} - \tilde{D}_{n,n,yy}^{g,s})/2$.

We require $\mathcal{H}_{si}^{g,\ell}$ to be invariant under all allowed g symmetries. As we shall see for the six high-symmetry cases under study, this forces $J_{a,n}^g$ and $J_{e,n}^g$ to be independent of n for each g in these local coordinates, and places constraints upon the single-ion parameter set $\{\theta_n^g, \phi_n^g, \psi_n^g\}$.

B. Local symmetric anisotropic exchange Hamiltonian

In addition to the single-ion interactions, the other microscopic anisotropic interactions are the anisotropic exchange interactions, which include the dipole-dipole interactions. We neglect intermolecular dipole-dipole interactions, which can be important at very low temperatures.[33] As for the single-ion interactions, we first construct the symmetric anisotropic exchange Hamiltonian \mathcal{H}_{ae}^g in the local group coordinates. In this case, there are distinct local vector sets for the NN and NNN exchange interactions. Diagonalization of the symmetric anisotropic exchange matrix $\overset{\leftrightarrow}{D}_{n,n'}^{g,s}$ leads to $\overset{\leftrightarrow}{D}_{n,n'}^{g,s}$ and the vector basis $\{\hat{\mathbf{x}}_{n,n'}^g, \hat{\mathbf{y}}_{n,n'}^g, \hat{\mathbf{z}}_{n,n'}^g\}$, given by Eqs. (11)-(13) with the subscript n replaced by n, n' .

The local symmetric anisotropic exchange Hamiltonian $\mathcal{H}_{ae}^{g,\ell}$ is then generally given by

$$\mathcal{H}_{ae}^{g,\ell} = - \sum_{m=1}^2 \sum_{n=1}^{6-2m} \left[J_{n,n+m}^{f,g} (\mathbf{S}_n \cdot \hat{\mathbf{z}}_{n,n+m}^g) (\mathbf{S}_{n+m} \cdot \hat{\mathbf{z}}_{n,n+m}^g) + J_{n,n+m}^{c,g} \left((\mathbf{S}_n \cdot \hat{\mathbf{x}}_{n,n+m}^g) (\mathbf{S}_{n+m} \cdot \hat{\mathbf{x}}_{n,n+m}^g) - (\mathbf{S}_n \cdot \hat{\mathbf{y}}_{n,n+m}^g) (\mathbf{S}_{n+m} \cdot \hat{\mathbf{y}}_{n,n+m}^g) \right) \right], \quad (15)$$

where we define $\mathbf{S}_5 \equiv \mathbf{S}_1$, as if the four NN spins were on a ring. In Eq. (15), the axial and azimuthal interaction strengths $-J_{n,n'}^{f,g} = \tilde{D}_{n,n',zz}^{g,s} - (\tilde{D}_{n,n',xx}^{g,s} + \tilde{D}_{n,n',yy}^{g,s})/2$ and $-J_{n,n'}^{c,g} = (\tilde{D}_{n,n',xx}^{g,s} - \tilde{D}_{n,n',yy}^{g,s})/2$, as for the single-ion interaction strengths, but in this case $n' = n + m$, where $m = 1, 2$.

Since the structures allow for two distinct bond lengths, with four NN's and 2 NNN's for $c/a < 1$, there

are two sets of local axial and azimuthal coordinates. The vector sets $\{\hat{\mathbf{z}}_{n,n+1}^g\}$, $\{\hat{\mathbf{x}}_{n,n+1}^g\}$, and $\{\hat{\mathbf{y}}_{n,n+1}^g\}$ each have four elements, and are the bases for the NN axial and azimuthal symmetric anisotropic exchange vectors. In addition, the vector sets $\{\hat{\mathbf{z}}_{n,n+2}^g\}$, $\{\hat{\mathbf{x}}_{n,n+2}^g\}$, and $\{\hat{\mathbf{y}}_{n,n+2}^g\}$ each have two elements, and are the NNN symmetric anisotropic exchange vector bases. These are both different from the single-ion vector bases.

For the six high-symmetry groups under study, the groups symmetries force the interaction strengths $J_{n,n+m}^{f,g}$ and $J_{n,n+m}^{c,g}$ to be independent of n , but are generally different for NN ($m = 1$) and NNN ($m = 2$) interactions. The group symmetries also place restrictions upon the NN and NNN symmetric anisotropic exchange parameter sets $\{\theta_{n,n+m}^g, \phi_{n,n+m}^g, \psi_{n,n+m}^g\}$ for $m = 1, 2$. These restrictions are much stronger for the NNN parameter set than for the NN parameter set.

C. Antisymmetric anisotropic exchange Hamiltonian

As noted above, since the antisymmetric anisotropic exchange matrix with three real distinct matrix elements cannot generally be diagonalized by a unitary transformation, there is no particular vector basis resulting from the diagonalization. We therefore write the antisymmetric anisotropic exchange, or DM, Hamiltonian \mathcal{H}_{DM}^g in the molecular representation,[27]

$$\mathcal{H}_{DM}^g = \sum_{m=1}^2 \sum_{n=1}^{6-2m} \mathbf{d}_{n,n+m}^g \cdot (\mathbf{S}_n \times \mathbf{S}_{n+m}). \quad (16)$$

We note that in these molecular coordinates, the DM interaction three-vectors $\mathbf{d}_{n,n+m}^g$ depend explicitly upon the exchange bond indices $n, n+m$ for each group g . We then employ the local group symmetries to relate them to one another.

The rules for the directions of the $\mathbf{d}_{n,n+m}^g$ were given by Moriya,[29] and were employed for a dimer example by Bencini and Gatteschi,[27] The Moriya rules are: (1) $\mathbf{d}_{n,n'}^g$ vanishes if a center of inversion connects \mathbf{r}_n and $\mathbf{r}_{n'}$. (2) When a mirror plane contains \mathbf{r}_n and $\mathbf{r}_{n'}$, $\mathbf{d}_{n,n'}^g$ is normal to the mirror plane. (3) When a mirror plane is the perpendicular bisector of $\mathbf{r}_n - \mathbf{r}_{n'}$, $\mathbf{d}_{n,n'}^g$ lies in the mirror plane. (4) When a two-fold rotation axis is the perpendicular bisector of $\mathbf{r}_n - \mathbf{r}_{n'}$, then $\mathbf{d}_{n,n'}^g$ is orthogonal to $\mathbf{r}_n - \mathbf{r}_{n'}$. (5) When $\mathbf{r}_n - \mathbf{r}_{n'}$ is a p -fold rotation axis with $p > 2$, then $\mathbf{d}_{n,n'}^g$ is parallel to $\mathbf{r}_n - \mathbf{r}_{n'}$. As noted above, we shall incorporate these rules in the molecular representation.

In the following, we impose the Moriya rules on each anisotropic exchange pair, and then impose the required group symmetries on the six pairs. For each g , the symmetries relate the NN and NNN DM interactions to one another, greatly restricting the number of parameters. For the six groups under study, the group symmetries

place restrictions upon the $\mathbf{d}_{n,n+m}^g$, causing them to be independent of n , so that only the two three-vectors \mathbf{d}_{12}^g and \mathbf{d}_{13}^g can describe the full DM interactions of each tetramer group. However, some components of the DM interaction vectors can have site-dependent signs.

In Sections IV-IX, we evaluate \mathcal{H}_{si}^g , \mathcal{H}_{ae}^g , and \mathcal{H}_{DM}^g for $g = C_{4h}, D_{4h}, C_{4v}, S_4, D_{2d}$, and T_d , respectively.

IV. C_{4h} GROUP SYMMETRY

We first discuss the simplest group symmetries, C_{4h} . Besides the trivial identity operation, the allowed group operations $\mathcal{O}_\lambda^{C_{4h}}$ for $\lambda = 1, 2, 3$ are clockwise and counterclockwise rotations by $\pi/2$ about the z axis, and reflections in the xy plane.[24] These operations are represented respectively by the matrices

$$\mathcal{O}_{1,2}^{C_{4h}} = \begin{pmatrix} 0 & \pm 1 & 0 \\ \mp 1 & 0 & 0 \\ 0 & 0 & 1 \end{pmatrix}, \quad (17)$$

$$\mathcal{O}_3^{C_{4h}} = \begin{pmatrix} 1 & 0 & 0 \\ 0 & 1 & 0 \\ 0 & 0 & -1 \end{pmatrix}. \quad (18)$$

C_{4h} single-ion anisotropy

We require $\mathcal{O}_\lambda^{C_{4h}} \mathcal{H}_{si}^{C_{4h}} = \mathcal{H}_{si}^{C_{4h}}$ for $\lambda = 1, 2, 3$. We first consider the effects of $\mathcal{O}_1^{C_{4h}}$. We note that $\mathcal{O}_1^{C_{4h}} \mathbf{r}_n = \mathbf{r}_{n+1}$. Hence, this operation rotates the crystal by $\pi/4$ about the z axis. Graphically, this is accomplished by relabelling Fig. 3(a) with $n \rightarrow n-1$, so that \mathbf{S}_1 is now at \mathbf{r}_2 , etc. Thus,

$$\begin{aligned} \mathcal{O}_1^{C_{4h}} \mathcal{H}_{si}^{C_{4h},\ell} = & - \sum_{n=1}^4 \left(J_{a,n}^{C_{4h}} (\mathbf{S}_n \cdot \hat{\mathbf{z}}_{n+1}^{C_{4h}})^2 \right. \\ & \left. + J_{e,n}^{C_{4h}} [(\mathbf{S}_n \cdot \hat{\mathbf{x}}_{n+1}^{C_{4h}})^2 - (\mathbf{S}_n \cdot \hat{\mathbf{y}}_{n+1}^{C_{4h}})^2] \right), \end{aligned} \quad (19)$$

where $\mathcal{O}_1^{C_{4h}} \hat{\mathbf{z}}_n^{C_{4h}} = \hat{\mathbf{z}}_{n+1}^{C_{4h}}$, etc. In order that the axial part of $\mathcal{H}_{si}^{C_{4h},\ell}$ is invariant under the transformation, we require

$$J_{a,n}^{C_{4h}} = J_{a,n-1}^{C_{4h}} = J_a \quad (20)$$

and

$$\sin \theta_n^{C_{4h}} \sin \phi_n^{C_{4h}} = -\sin \theta_{n-1}^{C_{4h}} \cos \phi_{n-1}^{C_{4h}}, \quad (21)$$

$$\sin \theta_n^{C_{4h}} \cos \phi_n^{C_{4h}} = \sin \theta_{n-1}^{C_{4h}} \sin \phi_{n-1}^{C_{4h}}, \quad (22)$$

$$\cos \theta_n^{C_{4h}} = \cos \theta_{n-1}^{C_{4h}}. \quad (23)$$

There are two possible solutions for these recursion relations. One possibility is

$$\theta_n^{C_{4h}} = 0, \pi, \quad (24)$$

$$\phi_n^{C_{4h}} = \text{arbitrary}. \quad (25)$$

The second possible solution is

$$\theta_n^{C_{4h}} = \theta_{n-1}^{C_{4h}}, \quad (26)$$

$$\phi_n^{C_{4h}} = \phi_{n-1}^{C_{4h}} - \frac{\pi}{2}. \quad (27)$$

However, imposition of the xy mirror plane symmetry, $\mathcal{O}_3^{C_{4h}}$, such as setting $\mathcal{O}_3^{C_{4h}} \hat{z}_n^{C_{4h}} = \pm \hat{z}_n^{C_{4h}}$ forces either the even parity $\theta_n^{C_{4h}} = 0$ or the odd parity $\theta_n^{C_{4h}} = \pi$. We choose the odd parity solution, setting

$$\theta_n^{C_{4h}} = 0, \quad (28)$$

which implies $\hat{z}_n^{C_{4h}} = \hat{z}$, the axis of high symmetry.

Now, we also must also require the azimuthal part of $\mathcal{H}_{si}^{C_{4h}, \ell}$ to be invariant under $\mathcal{O}_1^{C_{4h}}$. Using Eq. (28), we see from Eqs. (11) and (12) that $\hat{x}_n^{C_{4h}} = \hat{y} \sin \chi_n^{C_{4h}} + \hat{x} \cos \chi_n^{C_{4h}}$, etc., where

$$\chi_n^{C_{4h}} = \phi_n^{C_{4h}} + \psi_n^{C_{4h}}. \quad (29)$$

Then, invariance of $\mathcal{H}_{si}^{C_{4h}, \ell}$ under $\mathcal{O}_1^{C_{4h}}$ requires

$$J_{e,n}^{C_{4h}} = J_{e,n-1}^{C_{4h}} = J_e \quad (30)$$

and

$$\cos \chi_n^{C_{4h}} = \sin \chi_{n-1}^{C_{4h}}, \quad (31)$$

$$\sin \chi_n^{C_{4h}} = -\cos \chi_{n-1}^{C_{4h}}, \quad (32)$$

or that

$$\chi_n^{C_{4h}} = \chi_{n-1}^{C_{4h}} - \frac{\pi}{2}. \quad (33)$$

We note that for these vector groups, $\mathcal{H}_{si}^{C_{4h}, \ell}$ is automatically invariant under $\mathcal{O}_2^{C_4}$ and $\mathcal{O}_3^{C_4}$. In the latter case, $\mathcal{O}_3^{C_4} \hat{z}_n^{C_{4h}} = -\hat{z}_n^{C_{4h}}$ has odd parity.

Since $\mathcal{O}_1^{C_{4h}}$ interchanges the x and y components of the azimuthal vectors, it is useful to define the functions

$$\delta_n^+(\phi) = \epsilon_n^+(-1)^{n/2} \sin \phi + \epsilon_n^-(-1)^{(n+1)/2} \cos \phi, \quad (34)$$

$$\delta_n^-(\phi) = \epsilon_n^+(-1)^{n/2} \cos \phi - \epsilon_n^-(-1)^{(n+1)/2} \sin \phi. \quad (35)$$

We note that $\delta_n^\pm(\pi/4) = \gamma_n^\pm/\sqrt{2}$ and $\delta_n^\pm(3\pi/4) = \pm \gamma_n^\mp/\sqrt{2}$. For clarity, these new functions are listed in Table II. Some useful relations are

$$\left(\delta_n^+(\phi)\right)^2 + \left(\delta_n^-(\phi)\right)^2 = 1, \quad (36)$$

$$\left(\delta_n^+(\phi)\right)^2 - \left(\delta_n^-(\phi)\right)^2 = (-1)^n \cos(2\phi), \quad (37)$$

$$\delta_n^+(\phi) \delta_n^-(\phi) = \frac{(-1)^n}{2} \sin(2\phi). \quad (38)$$

n	$\delta_n^+(\phi)$	$\delta_n^-(\phi)$
1	$-\cos \phi$	$\sin \phi$
2	$-\sin \phi$	$-\cos \phi$
3	$\cos \phi$	$-\sin \phi$
4	$\sin \phi$	$\cos \phi$

TABLE II: Values of the functions $\delta_n^\pm(\phi)$.

Hence, the single-ion vector groups for $g = C_{4h}$ symmetry are $\{\hat{x}_n^{C_{4h}}\}$, $\{\hat{y}_n^{C_{4h}}\}$, $\{\hat{z}_n^{C_{4h}}\}$, where the elements are given by

$$\hat{x}_n^{C_{4h}} = -\delta_n^+(\chi_1^{C_{4h}}) \hat{x} + \delta_n^-(\chi_1^{C_{4h}}) \hat{y}, \quad (39)$$

$$\hat{y}_n^{C_{4h}} = -\delta_n^-(\chi_1^{C_{4h}}) \hat{x} - \delta_n^+(\chi_1^{C_{4h}}) \hat{y}, \quad (40)$$

$$\hat{z}_n^{C_{4h}} = \hat{z}. \quad (41)$$

The single-ion parameter set for $g = C_{4h}$ is

$$\{\mu_1^{C_{4h}}\} = (0, \chi_1^{C_{4h}}), \quad (42)$$

$$\chi_1^{C_{4h}} = \phi_1^{C_{4h}} + \psi_1^{C_{4h}}. \quad (43)$$

C_{4h} symmetric anisotropic exchange

The construction of the symmetric anisotropic exchange vector groups is entirely analogous to those of the single-ion anisotropy. We find

$$J_{n,n+m}^{f,C_{4h}} = J_f^{n-1,n+m-1} = J_{f,m}, \quad (44)$$

$$\equiv J_{f,m}, \quad (45)$$

$$J_{n,n+m}^{c,C_{4h}} = J_c^{n-1,n+m-1} = J_{c,m}, \quad (46)$$

$$\equiv J_{c,m}, \quad (47)$$

and the near-neighbor and next-nearest-neighbor vector groups are

$$\hat{x}_{n,n+1}^{C_{4h}} = -\delta_n^+(\chi_{12}^{C_{4h}}) \hat{x} + \delta_n^-(\chi_{12}^{C_{4h}}) \hat{y}, \quad (48)$$

$$\hat{y}_{n,n+1}^{C_{4h}} = -\delta_n^-(\chi_{12}^{C_{4h}}) \hat{x} - \delta_n^+(\chi_{12}^{C_{4h}}) \hat{y}, \quad (49)$$

$$\hat{z}_{n,n+1}^{C_{4h}} = \hat{z}, \quad (50)$$

and

$$\hat{x}_{n,n+2}^{C_{4h}} = -\delta_n^+(\chi_{13}^{C_{4h}}) \hat{x} + \delta_n^-(\chi_{13}^{C_{4h}}) \hat{y}, \quad (51)$$

$$\hat{y}_{n,n+2}^{C_{4h}} = -\delta_n^-(\chi_{13}^{C_{4h}}) \hat{x} - \delta_n^+(\chi_{13}^{C_{4h}}) \hat{y}, \quad (52)$$

$$\hat{z}_{n,n+2}^{C_{4h}} = \hat{z}, \quad (53)$$

respectively, where

$$\chi_{1p}^{C_{4h}} \equiv \chi_{1,p}^{C_{4h}} = \phi_{1p}^{C_{4h}} + \psi_{1p}^{C_{4h}} \quad (54)$$

for $p = 2, 3$.

C. C_{4h} antisymmetric exchange interactions

With antisymmetric exchange, we first impose the Moriya rules for C_{4h} symmetry. We first note that $\mathcal{O}_1^{C_{4h}} \mathcal{O}_1^{C_{4h}} = -\mathcal{O}_3^{C_{4h}}$, so that the origin is a center of inversion for the next-nearest neighbor bonds with $g = C_{4h}$. [24] This implies

$$d_{n,n+2}^{C_{4h}} = 0. \quad (55)$$

Since all four spins lie in the xy mirror plane, $\mathcal{O}_3^{C_{4h}}$, we have

$$d_{n,n+1}^{C_{4h}} = d_{n,n+1}^{C_{4h}} \hat{z}. \quad (56)$$

Then, imposing the $\mathcal{O}_1^{C_{4h}}$ rotational symmetry on $\mathcal{H}_{DM}^{C_{4h}}$, we find

$$d_{n,n+1}^{C_{4h}} = d_{n-1,n}^{C_{4h}} \quad (57)$$

$$\equiv d_z \quad (58)$$

is a scalar independent of n . Thus, the antisymmetric anisotropic exchange interaction for C_{4h} symmetry is simply

$$\mathcal{H}_{DM}^{C_{4h}} = d_z \sum_{n=1}^4 \hat{z} \cdot (\mathbf{S}_n \times \mathbf{S}_{n+1}). \quad (59)$$

V. D_{4h} GROUP SYMMETRY

We now consider the higher symmetry $g = D_{4h}$. This group contains the three symmetries of C_{4h} , so that $\mathcal{O}_\lambda^{D_{4h}} = \mathcal{O}_\lambda^{C_{4h}}$ for $\lambda = 1, 2, 3$. In addition, there are four two-fold rotations about axes normal to the principle z axis. These rotation axes are the x and y axes and the $y = \pm x$ diagonals. These D_{4h} operations are represented by

$$\mathcal{O}_{4,5}^{D_{4h}} = \begin{pmatrix} \pm 1 & 0 & 0 \\ 0 & \mp 1 & 0 \\ 0 & 0 & -1 \end{pmatrix}, \quad (60)$$

$$\mathcal{O}_{6,7}^{D_{4h}} = \begin{pmatrix} 0 & \pm 1 & 0 \\ \pm 1 & 0 & 0 \\ 0 & 0 & -1 \end{pmatrix}. \quad (61)$$

A. D_{4h} single-ion anisotropy

We begin with the same invariances of $\mathcal{H}_{si}^{D_{4h},\ell}$ as for C_{4h} symmetry, leading to the single-ion vector groups given by Eqs. (39)-(41) with $C_{4h} \rightarrow D_{4h}$. As for C_{4h} symmetry, $J_a^{D_{4h}} = J_{a,n-1}^{D_{4h}} = J_a$ and $J_e^{D_{4h}} = J_{e,n-1}^{D_{4h}} = J_e$. We then impose the additional symmetries $\mathcal{O}_\lambda^{D_{4h}}$ for $\lambda = 4 - 7$. We note that $\mathcal{O}_6^{D_{4h}} \mathbf{r}_1 = \mathbf{r}_1$, for example.

Hence, we require $\mathcal{O}_4^{D_{4h}} \hat{\mathbf{x}}_{1,3} = \pm \hat{\mathbf{x}}_{2,4}$, $\mathcal{O}_5^{D_{4h}} \hat{\mathbf{x}}_{1,2} = \pm \hat{\mathbf{x}}_{4,3}$, $\mathcal{O}_6^{D_{4h}} \hat{\mathbf{x}}_{1,3} = \pm \hat{\mathbf{x}}_{1,3}$, $\mathcal{O}_6^{D_{4h}} \hat{\mathbf{x}}_{2,4} = \pm \hat{\mathbf{x}}_{4,2}$, and $\mathcal{O}_7^{D_{4h}} \hat{\mathbf{x}}_{1,3} = \pm \hat{\mathbf{x}}_{3,1}$, $\mathcal{O}_7^{D_{4h}} \hat{\mathbf{x}}_{2,4} = \pm \hat{\mathbf{x}}_{2,4}$. The even (odd) parity choices lead to $\sin \chi_1^{D_{4h}} = \pm \cos \chi_1^{D_{4h}}$, and we make the even parity choice,

$$\chi_1^{D_{4h}} = \pi/4, \quad (62)$$

consistent with Fig. 1. We then obtain the single-ion vector sets for D_{4h} symmetry,

$$\hat{\mathbf{x}}_n^{D_{4h}} = \frac{1}{\sqrt{2}}(-\gamma_n^+ \hat{\mathbf{x}} + \gamma_n^- \hat{\mathbf{y}}), \quad (63)$$

$$\hat{\mathbf{y}}_n^{D_{4h}} = -\frac{1}{\sqrt{2}}(\gamma_n^- \hat{\mathbf{x}} + \gamma_n^+ \hat{\mathbf{y}}), \quad (64)$$

$$\hat{\mathbf{z}}_n^{D_{4h}} = \hat{\mathbf{z}}, \quad (65)$$

$$\{\mu_1^{D_{4h}}\} = (0, \pi/4), \quad (66)$$

where the second entry refers to $\chi_1^{D_{4h}} = \phi_1^{D_{4h}} + \psi_1^{D_{4h}} = \pi/4$. We note that $\hat{\mathbf{x}}_n^{D_{4h}} = \hat{\mathbf{r}}_n$, as pictured in Fig. 1.

B. D_{4h} symmetric anisotropic exchange

As for the single-ion interactions, we begin with the symmetric anisotropic exchange vector groups for C_{4h} . As for C_{4h} symmetry, we have $J_{n,n+m}^{c,D_{4h}} = J_{n-1,n+m-1}^{c,D_{4h}} = J_{c,m}$ and $J_{n,n+m}^{f,D_{4h}} = J_{n-1,n+m-1}^{f,D_{4h}} = J_{f,m}$. We then impose the additional symmetries, setting $\mathcal{O}_4 \hat{\mathbf{x}}_{12}^{D_{4h}} = \hat{\mathbf{x}}_{21}^{D_{4h}} = -\hat{\mathbf{x}}_{12}^{D_{4h}}$ and $\mathcal{O}_4 \hat{\mathbf{x}}_{13}^{D_{4h}} = \hat{\mathbf{x}}_{24}^{D_{4h}}$, for examples. Thus, it is elementary to obtain the restrictions

$$\cos \chi_{12}^{D_{4h}} = 0, \quad (67)$$

$$\cos \chi_{13}^{D_{4h}} = \sin \chi_{12}^{D_{4h}}, \quad (68)$$

and we choose the solutions

$$\chi_{12}^{D_{4h}} = \frac{\pi}{2}, \quad (69)$$

$$\chi_{13}^{D_{4h}} = \frac{\pi}{4}. \quad (70)$$

These solutions are consistent with the remaining symmetries $\mathcal{O}_\lambda^{D_{4h}}$ for $\lambda = 5, 6, 7$. Thus, we obtain the near-neighbor and next-nearest-neighbor D_{4h} symmetric anisotropic exchange vector groups,

$$\hat{\mathbf{x}}_{n,n+1}^{D_{4h}} = -\frac{1}{2}(\gamma_n^+ + \gamma_n^-) \hat{\mathbf{x}} + \frac{1}{2}(\gamma_n^- - \gamma_n^+) \hat{\mathbf{y}}, \quad (71)$$

$$\hat{\mathbf{y}}_{n,n+1}^{D_{4h}} = \frac{1}{2}(\gamma_n^+ - \gamma_n^-) \hat{\mathbf{x}} - \frac{1}{2}(\gamma_n^+ + \gamma_n^-) \hat{\mathbf{y}}, \quad (72)$$

$$\hat{\mathbf{y}}_{n,n+1}^{D_{4h}} = \hat{\mathbf{z}}, \quad (73)$$

and

$$\hat{\mathbf{x}}_{n,n+2}^{D_{4h}} = \frac{1}{\sqrt{2}}(-\gamma_n^+ \hat{\mathbf{x}} + \gamma_n^- \hat{\mathbf{y}}), \quad (74)$$

$$\hat{\mathbf{y}}_{n,n+2}^{D_{4h}} = -\frac{1}{\sqrt{2}}(\gamma_n^- \hat{\mathbf{x}} + \gamma_n^+ \hat{\mathbf{y}}), \quad (75)$$

$$\hat{\mathbf{z}}_{n,n+2}^{D_{4h}} = \hat{\mathbf{z}}, \quad (76)$$

respectively.

C. D_{4h} antisymmetric anisotropic exchange

For D_{4h} symmetry, the origin is a center of inversion for the next-nearest-neighbor DM interactions, forcing them to vanish, as for C_{4h} . Moreover, it is easy to show that tetramers with D_{4h} symmetry, the near-neighbor exchange given by Eq. (59) also is invariant under $\mathcal{O}_\lambda^{D_{4h}}$. Hence, the most general antisymmetric anisotropic exchange Hamiltonian for D_{4h} symmetry is

$$\mathcal{H}_{DM}^{D_{4h}} = d_z \sum_{n=1}^4 \hat{\mathbf{z}} \cdot (\mathbf{S}_n \times \mathbf{S}_{n+1}), \quad (77)$$

precisely the same as for C_{4h} symmetry.

VI. C_{4v} GROUP SYMMETRY

For C_{4v} , the group operations $\mathcal{O}_\lambda^{C_{4v}}$ for $\lambda = 1, \dots, 6$ are clockwise and counterclockwise rotations by $\pi/2$ about the z axis (equivalent to $\mathcal{O}_{1,2}^{C_{4h}}$ in Eq. (17)), and reflections in the xz , yz , and diagonal mirror planes containing the z axis and the lines $y = \pm x$. [24] The additional operations are represented respectively by the matrices

$$\mathcal{O}_{3,4}^{C_{4v}} = \begin{pmatrix} \pm 1 & 0 & 0 \\ 0 & \mp 1 & 0 \\ 0 & 0 & 1 \end{pmatrix}, \quad (78)$$

$$\mathcal{O}_{5,6}^{C_{4v}} = \begin{pmatrix} 0 & \pm 1 & 0 \\ \pm 1 & 0 & 0 \\ 0 & 0 & 1 \end{pmatrix}, \quad (79)$$

where the upper signs refer to the lower subscript numbers.

A. C_{4v} single-ion anisotropy

As for C_{4h} and D_{4h} symmetries, we first impose the $\mathcal{O}_1^{C_{4v}}$ invariance, the rotation by $\pi/2$ about the z axis. This again leads to $J_{a,n}^{C_{4v}} = J_{a,n-1}^{C_{4v}} = J_a$ and $J_{e,n}^{C_{4v}} = J_{e,n-1}^{C_{4v}} = J_e$, independent of n . As for the axial single-ion anisotropy with C_{4h} symmetry, this leads to Eqs. (21)-(23), with the two choices for the recursion relations for $\theta_n^{C_{4v}}$ and $\phi_n^{C_{4v}}$. However, with C_{4v} symmetry, the xy plane is not a mirror plane. Instead, we impose the xz mirror plane operation $\mathcal{O}_3^{C_{4v}}$, and require $\mathcal{O}_3^{C_{4v}} \hat{\mathbf{z}}_2^{C_{4v}} = \pm \hat{\mathbf{z}}_1^{C_{4v}}$. Choosing the even parity case leads to the equation

$$\sin \theta_1^{C_{4v}} \sin \phi_1^{C_{4v}} = -\sin \theta_1^{C_{4v}} \cos \phi_1^{C_{4v}}, \quad (80)$$

which is satisfied by either choosing $\sin \theta_1^{C_{4v}} = 0$ or $\sin \phi_1^{C_{4v}} = -\cos \phi_1^{C_{4v}}$. The former solution is appropriate for the higher-symmetry C_{4h} , D_{4h} cases in which the xy plane is a molecular mirror plane, pictured in the right panel of Fig. 1, but this is not required for the most general tetramers exhibiting C_{4v} symmetry, for which the ligands on opposite sides of the ring may be different. We therefore choose the more general case, setting $\phi_1^{C_{4v}} = 3\pi/4$, and leaving $\theta_1^{C_{4v}}$ arbitrary. We then construct $\hat{\mathbf{z}}_3^{C_{4v}}$ and $\hat{\mathbf{z}}_4^{C_{4v}}$ from $\mathcal{O}_1^{C_{4v}} \hat{\mathbf{z}}_2^{C_{4v}} = \hat{\mathbf{z}}_3^{C_{4v}}$ and $\mathcal{O}_1^{C_{4v}} \hat{\mathbf{z}}_3^{C_{4v}} = \hat{\mathbf{z}}_4^{C_{4v}}$. The resulting vector group $\{\hat{\mathbf{z}}_n^{C_{4v}}\}$ is invariant under the diagonal mirror plane operations $\mathcal{O}_{5,6}^{C_{4v}}$, as $\mathcal{O}_5^{C_{4v}} \hat{\mathbf{z}}_{2,4}^{C_{4v}} = \hat{\mathbf{z}}_{4,2}^{C_{4v}}$, $\mathcal{O}_5^{C_{4v}} \hat{\mathbf{z}}_{1,3}^{C_{4v}} = \hat{\mathbf{z}}_{1,3}^{C_{4v}}$, and $\mathcal{O}_6^{C_{4v}} \hat{\mathbf{z}}_{2,4}^{C_{4v}} = \hat{\mathbf{z}}_{2,4}^{C_{4v}}$, $\mathcal{O}_6^{C_{4v}} \hat{\mathbf{z}}_{1,3}^{C_{4v}} = \hat{\mathbf{z}}_{3,1}^{C_{4v}}$. Hence, these diagonal mirror planes introduce no restrictions upon $\theta_1^{C_{4v}}$. We also note that the yz mirror plane operations $\mathcal{O}_4 \hat{\mathbf{z}}_{1,4}^{C_{4v}} = \hat{\mathbf{z}}_{4,1}^{C_{4v}}$ and $\mathcal{O}_4 \hat{\mathbf{z}}_{2,3}^{C_{4v}} = \hat{\mathbf{z}}_{3,2}^{C_{4v}}$.

Similarly, from $\hat{\mathbf{x}}_1^{C_{4v}}$ given by Eq. (11) with $n = 1$, $g = C_{4v}$, we construct $\hat{\mathbf{x}}_2^{C_{4v}} = \mathcal{O}_1^{C_{4v}} \hat{\mathbf{x}}_1^{C_{4v}} = \mathcal{O}_2^{C_{4v}} \hat{\mathbf{x}}_1^{C_{4v}}$. After imposing our choice $\phi_1^{C_{4v}} = 3\pi/4$, we find that these two equations are only satisfied if $\cos \psi_1^{C_{4v}} = 0$. We therefore choose $\psi_1^{C_{4v}} = -\pi/2$, so that $\chi_1^{C_{4v}} = \phi_1^{C_{4v}} + \psi_1^{C_{4v}} = \pi/4$, as for D_{4h} symmetry.

By successive applications of $\mathcal{O}_1^{C_{4v}}$ and $\mathcal{O}_3^{C_{4v}}$, we obtain the three vector groups $\{\hat{\mathbf{x}}_n^{C_{4v}}\}$, $\{\hat{\mathbf{y}}_n^{C_{4v}}\}$ and $\{\hat{\mathbf{z}}_n^{C_{4v}}\}$, with the elements

$$\hat{\mathbf{x}}_n^{C_{4v}} = \frac{1}{\sqrt{2}} \begin{pmatrix} -\gamma_n^+ \cos \theta_1^{C_{4v}} \\ \gamma_n^- \cos \theta_1^{C_{4v}} \\ -\sqrt{2} \sin \theta_1^{C_{4v}} \end{pmatrix}, \quad (81)$$

$$\hat{\mathbf{y}}_n^{C_{4v}} = -\frac{1}{\sqrt{2}} \begin{pmatrix} \gamma_n^- \\ \gamma_n^+ \\ 0 \end{pmatrix}, \quad (82)$$

$$\hat{\mathbf{z}}_n^{C_{4v}} = \frac{1}{\sqrt{2}} \begin{pmatrix} -\gamma_n^+ \sin \theta_1^{C_{4v}} \\ \gamma_n^- \sin \theta_1^{C_{4v}} \\ \sqrt{2} \cos \theta_1^{C_{4v}} \end{pmatrix}, \quad (83)$$

where the γ_m^\pm are given in Eq. (2) and Table I. These forms are also consistent with the yz and diagonal mirror plane operations ($\mathcal{O}_\lambda^{C_{4v}}$ operations for $\lambda = 4, 5, 6$), and leave Eq. (14) invariant. [24] We note that some of the reflections of some of the $\hat{\mathbf{y}}_n^{C_{4v}}$ have odd parity. We also note that these vectors reduce to those for D_{4h} symmetry, Eqs. (63)-(65) in the $\theta_1^{C_{4v}} \rightarrow 0$ limit. We reiterate that the C_{4v} group symmetry imposes restrictions upon $\phi_1^{C_{4v}}$ and $\psi_1^{C_{4v}}$, leading to

$$\{\mu_1^{C_{4v}}\} = (\theta_1^{C_{4v}}, 3\pi/4, -\pi/2). \quad (84)$$

B. C_{4v} symmetric anisotropic exchange

As for C_{4h} and D_{4h} symmetry, we first impose the invariance of $\mathcal{H}_{ae}^{C_{4v}}$ under $\pi/2$ rotations about the z axis, $\mathcal{O}_1^{C_{4v}}$. For the axial part of $\mathcal{H}_{ae}^{C_{4v}}$, this leads to

$$J_{n,n+m}^{f,C_{4v}} = J_{n-1,n+m-1}^{f,C_{4v}} = J_{f,m}, \quad (85)$$

$$J_{n,n+m}^{c,C_{4v}} = J_{n-1,m+m-1}^{c,C_{4v}} = J_{c,m}, \quad (86)$$

plus restrictions upon $\theta_{n,n+m}^{C_{4v}}$, $\phi_{n,n+m}^{C_{4v}}$, and $\psi_{n,n+m}^{C_{4v}}$, precisely as for C_{4h} and D_{4h} symmetries.

Now, we impose the mirror plane restrictions of C_{4v} . The diagonal mirror plane containing the z axis and the line $y = -x$, $\mathcal{O}_6^{C_{4v}}$ requires $\mathcal{O}_6^{C_{4v}} \hat{\mathbf{z}}_{12}^{C_{4v}} = \pm \hat{\mathbf{z}}_{32}^{C_{4v}} = \mp \hat{\mathbf{z}}_{23}^{C_{4v}}$. By analogy with C_{4h} and D_{4h} , we choose $\theta_{12}^{C_{4v}} = 0$, leaving $\phi_{12}^{C_{4v}}$ unrestricted. This leads to $\hat{\mathbf{x}}_{12}^{C_{4v}} = \cos \chi_{12}^{C_{4v}} \hat{\mathbf{x}} + \sin \chi_{12}^{C_{4v}} \hat{\mathbf{y}}$, where $\chi_{12}^{C_{4v}} = \phi_{12}^{C_{4v}} + \psi_{12}^{C_{4v}}$. Imposing the xz mirror plane restriction, $\mathcal{O}_3^{C_{4v}} \hat{\mathbf{x}}_{12}^{C_{4v}} = \pm \hat{\mathbf{x}}_{12}^{C_{4v}}$ leads to either $\cos \chi_{12}^{C_{4v}} = 0$ or $\sin \chi_{12}^{C_{4v}} = 0$. We then choose $\chi_{12}^{C_{4v}} = 0$. A similar procedure is carried out separately for the next-nearest-neighbor interactions.

After checking all of the mirror plane operations of C_{4v} symmetry, we find that the C_{4v} symmetric anisotropic exchange vector group elements may be written as

$$\hat{\mathbf{x}}_{n,n+1}^{C_{4v}} = -\frac{1}{2}(\gamma_n^+ - \gamma_n^-) \hat{\mathbf{x}} + \frac{1}{2}(\gamma_n^+ + \gamma_n^-) \hat{\mathbf{y}}, \quad (87)$$

$$\hat{\mathbf{y}}_{n,n+1}^{C_{4v}} = \frac{1}{2}(\gamma_n^+ + \gamma_n^-) \hat{\mathbf{x}} + \frac{1}{2}(\gamma_n^+ - \gamma_n^-) \hat{\mathbf{y}}, \quad (88)$$

$$\hat{\mathbf{z}}_{n,n+1}^{C_{4v}} = \hat{\mathbf{z}}, \quad (89)$$

and the matrix diagonalization parameters satisfy

$$\{\mu_{12}^{C_{4v}}\} = (\theta_{12}^{C_{4v}}, \chi_{12}^{C_{4v}}) = (0, 0). \quad (90)$$

The next-nearest-neighbor vector group elements can similarly be shown to satisfy

$$\hat{\mathbf{x}}_{n,n+2}^{C_{4v}} = \frac{1}{\sqrt{2}}(-\gamma_n^+ \hat{\mathbf{x}} + \gamma_n^- \hat{\mathbf{y}}), \quad (91)$$

$$\hat{\mathbf{y}}_{n,n+2}^{C_{4v}} = -\frac{1}{\sqrt{2}}(\gamma_n^- \hat{\mathbf{x}} + \gamma_n^+ \hat{\mathbf{y}}), \quad (92)$$

$$\hat{\mathbf{z}}_{n,n+2}^{C_{4v}} = \hat{\mathbf{z}}, \quad (93)$$

and the matrix diagonalization parameters satisfy

$$\{\mu_{13}^{C_{4v}}\} = (\theta_{13}^{C_{4v}}, \chi_{13}^{C_{4v}}) = (0, \frac{\pi}{4}). \quad (94)$$

C. C_{4v} antisymmetric exchange

We first consider the next-nearest-neighbor antisymmetric exchange interactions, $\mathbf{d}_{13}^{C_{4v}} \cdot (\mathbf{S}_1 \times \mathbf{S}_3) + \mathbf{d}_{24}^{C_{4v}} \cdot (\mathbf{S}_2 \times \mathbf{S}_4)$. The relevant mirror planes are the diagonal mirror planes containing the z axis and the lines

$y = \pm x$, $\mathcal{O}_{5,6}^{C_{4v}}$. The Moriya rules require that $\mathbf{d}_{13}^{C_{4v}}$ and $\mathbf{d}_{24}^{C_{4v}}$ are perpendicular to the respective mirror planes containing the interacting spin sites. Thus, we write $\mathbf{d}_{13}^{C_{4v}} = d_{13}(\hat{\mathbf{y}} - \hat{\mathbf{x}})/\sqrt{2}$ and $\mathbf{d}_{24}^{C_{4v}} = d_{24}(\hat{\mathbf{x}} + \hat{\mathbf{y}})/\sqrt{2}$. Then, we impose the invariance under $\pi/2$ rotations about the z axis, $\mathcal{O}_1^{C_{4v}}$. This operation satisfies $\mathcal{O}_1^{C_{4v}} \mathbf{S}_n = \mathbf{S}_{n+1}$ and the coordinates transformations $\mathcal{O}_1^{C_{4v}} \hat{\mathbf{x}} = -\hat{\mathbf{y}}$ and $\mathcal{O}_1^{C_{4v}} \hat{\mathbf{y}} = \hat{\mathbf{x}}$. This symmetry then forces $d_{13} = d_{24}$.

For the next-nearest-neighbor antisymmetric exchange interactions, the relevant mirror planes are the xz and yz mirror planes, which bisect the respective near-neighbor interaction sites. The Moriya rules dictate that $\mathbf{d}_{12}^{C_{4v}}$ and $\mathbf{d}_{34}^{C_{4v}}$ lie in the xz plane, and that $\mathbf{d}_{23}^{C_{4v}}$ and $\mathbf{d}_{41}^{C_{4v}}$ lie in the yz plane. We therefore write $\mathbf{d}_{12}^{C_{4v}} = d_{12x} \hat{\mathbf{x}} + d_{12z} \hat{\mathbf{z}}$, $\mathbf{d}_{23}^{C_{4v}} = d_{23y} \hat{\mathbf{y}} + d_{23z} \hat{\mathbf{z}}$, $\mathbf{d}_{34}^{C_{4v}} = d_{34x} \hat{\mathbf{x}} + d_{34z} \hat{\mathbf{z}}$, and $\mathbf{d}_{41}^{C_{4v}} = d_{41y} \hat{\mathbf{y}} + d_{41z} \hat{\mathbf{z}}$. We then impose the cyclic rotation symmetry $\mathcal{O}_1^{C_{4v}}$, as for the next-nearest-neighbor interactions. Invariance of the Hamiltonian under this symmetry then requires $d_{12x} = -d_{23y} = -d_{34x} = d_{41y}$ and $d_{12z} = d_{23z} = d_{34z} = d_{41z}$.

Thus, the combined antisymmetric exchange interaction for tetramers with C_{4v} symmetry may be written as

$$\begin{aligned} \mathcal{H}_{DM}^{C_{4v}} = & \sum_{n=1}^4 \left(d_z \hat{\mathbf{z}} + \frac{d_{\perp}}{2} [(\gamma_n^- - \gamma_n^+) \hat{\mathbf{x}} + (\gamma_n^+ + \gamma_n^-) \hat{\mathbf{y}}] \right) \\ & \cdot (\mathbf{S}_n \times \mathbf{S}_{n+1}) \\ & + d' \sum_{n=1}^2 \left(\hat{\mathbf{y}} + (-1)^n \hat{\mathbf{x}} \right) \cdot (\mathbf{S}_n \times \mathbf{S}_{n+2}), \end{aligned} \quad (95)$$

where the three scalar parameters are $d' = d_{13}\sqrt{2}$, $d_z = d_{12z}$, and $d_{\perp} = d_{12x}$. Thus, for C_{4v} symmetry, there are both site-independent and site-dependent DM interactions. The site-independent DM interactions are the same as for C_{4h} and D_{4h} symmetry.

VII. S_4 GROUP SYMMETRY

For S_4 , the group operations are clockwise and counterclockwise operation rotations by $\pi/4$ followed by a reflection in the xy plane.[24] The structure is pictured in Fig. 2(b). These operations are represented by the matrices

$$\mathcal{O}_{1,2}^{S_4} = \begin{pmatrix} 0 & \pm 1 & 0 \\ \mp 1 & 0 & 0 \\ 0 & 0 & -1 \end{pmatrix}. \quad (96)$$

A. S_4 single-ion anisotropy

We then construct the vector groups from the site 1 vectors by successive operations of $\mathcal{O}_1^{S_4}$, setting $\hat{\mathbf{v}}_{n+1}^{S_4} =$

$\mathcal{O}_1^{S_4} \hat{\mathbf{v}}_n^{S_4}$, where $\hat{\mathbf{v}}_n^{S_4} = \hat{\mathbf{x}}_n^{S_4}, \hat{\mathbf{y}}_n^{S_4}$ and $\hat{\mathbf{z}}_n^{S_4}$. The inverse operations of $\mathcal{O}_2^{S_4}$ are automatically satisfied. With S_4 symmetry, there are no mirror planes to satisfy. However, the improper rotation $\mathcal{O}_1^{S_4}$ interchanges the x and y vector components, complicating the most general vector forms. However, we still obtain $J_{a,n}^{S_4} = J_{a,n-1}^{S_4} = J_a$ and $J_{e,n}^{S_4} = J_{e,n-1}^{S_4} = J_e$, both independent of n , as for the three planar symmetries discussed previously.

Hence, the group vectors for S_4 symmetry contain the elements

$$\hat{\mathbf{x}}_n^{S_4} = \begin{pmatrix} -\cos \psi_1^{S_4} \delta_n^+(\phi_1^{S_4}) - \cos \theta_1^{S_4} \sin \psi_1^{S_4} \delta_n^-(\phi_1^{S_4}) \\ \cos \psi_1^{S_4} \delta_n^-(\phi_1^{S_4}) - \cos \theta_1^{S_4} \sin \psi_1^{S_4} \delta_n^+(\phi_1^{S_4}) \\ (-1)^{n+1} \sin \psi_1^{S_4} \sin \theta_1^{S_4} \end{pmatrix}, \quad (97)$$

$$\hat{\mathbf{y}}_n^{S_4} = \begin{pmatrix} \sin \psi_1^{S_4} \delta_n^+(\phi_1^{S_4}) - \cos \theta_1^{S_4} \cos \psi_1^{S_4} \delta_n^-(\phi_1^{S_4}) \\ -\sin \psi_1^{S_4} \delta_n^-(\phi_1^{S_4}) - \cos \theta_1^{S_4} \cos \psi_1^{S_4} \delta_n^+(\phi_1^{S_4}) \\ (-1)^{n+1} \cos \psi_1^{S_4} \sin \theta_1^{S_4} \end{pmatrix}, \quad (98)$$

$$\hat{\mathbf{z}}_n^{S_4} = \begin{pmatrix} \sin \theta_1^{S_4} \delta_n^-(\phi_1^{S_4}) \\ \sin \theta_1^{S_4} \delta_n^+(\phi_1^{S_4}) \\ (-1)^{n+1} \cos \theta_1^{S_4} \end{pmatrix}, \quad (99)$$

where

$$\{\mu_1^{S_4}\} = (\theta_1^{S_4}, \phi_1^{S_4}, \psi_1^{S_4}) \quad (100)$$

is unrestricted by the group symmetry, and $\delta_n^\pm(\phi)$ are given by Eqs. (34) and (35).

B. S_4 symmetric anisotropic exchange

We now consider the most general symmetric anisotropic exchange vector groups for S_4 symmetry. As for C_{4v} we begin with the near-neighbor axial vector $\hat{\mathbf{z}}_{12}^{S_4}$ using the general Eq. (13) with $\theta_1^{C_{4v}} \rightarrow \theta_{12}^{S_4}$ and $\phi_1^{C_{4v}} \rightarrow \phi_{12}^{S_4}$. We construct the near-neighbor axial symmetric anisotropic exchange vector group by successive operations of $\mathcal{O}_1^{S_4}$, setting $\hat{\mathbf{z}}_{23}^{S_4} = \mathcal{O}_1^{S_4} \hat{\mathbf{z}}_{12}^{S_4}$, etc. The same procedure can be applied to construct the azimuthal symmetric anisotropic exchange vector group. The group symmetry imposes no restrictions upon the three near-neighbor bond angles $\theta_{12}^{S_4}$, $\phi_{12}^{S_4}$, and $\psi_{12}^{S_4}$, because the fourth operation, $\mathcal{O}_1^{S_4} \hat{\mathbf{v}}_{41}^{S_4} = \hat{\mathbf{v}}_{12}^{S_4}$ is automatically satisfied for $\hat{\mathbf{v}}^{S_4} = \hat{\mathbf{x}}^{S_4}, \hat{\mathbf{y}}^{S_4}$, and $\hat{\mathbf{z}}^{S_4}$. Thus, the near-neighbor anisotropic exchange vector groups with S_4 symmetry are fully general, with $\hat{\mathbf{x}}_{n,n+1}^{S_4}$, $\hat{\mathbf{y}}_{n,n+1}^{S_4}$, and $\hat{\mathbf{z}}_{n,n+1}^{S_4}$ obtained from the single-ion $\hat{\mathbf{x}}_n^{S_4}$, $\hat{\mathbf{y}}_n^{S_4}$, and $\hat{\mathbf{z}}_n^{S_4}$ vectors in Eqs. (97)-(99) by replacing $\theta_1^{S_4} \rightarrow \theta_{12}^{S_4}$, $\phi_1^{S_4} \rightarrow \phi_{12}^{S_4}$, and $\psi_1^{S_4} \rightarrow \psi_{12}^{S_4}$, respectively. Thus,

$$\{\mu_{12}^{S_4}\} = (\theta_{12}^{S_4}, \phi_{12}^{S_4}, \psi_{12}^{S_4}) \quad (101)$$

is unrestricted by the group symmetry.

However, the next-nearest-neighbor symmetric anisotropic exchange vector groups are different. We first set $\hat{\mathbf{z}}_{13}^{S_4}$ equal to Eq. (13) with $\theta_1^{C_{4v}} \rightarrow \theta_{13}^{S_4}$ and $\phi_1^{C_{4v}} \rightarrow \phi_{13}^{S_4}$, and construct $\hat{\mathbf{z}}_{24}^{S_4}$ from $\mathcal{O}_1^{S_4} \hat{\mathbf{z}}_{13}^{S_4} = \hat{\mathbf{z}}_{24}^{S_4}$. But we then require $\mathcal{O}_1^{S_4} \hat{\mathbf{z}}_{24}^{S_4} = \hat{\mathbf{z}}_{31}^{S_4} = -\hat{\mathbf{z}}_{13}^{S_4}$. This forces $\cos \theta_{13}^{S_4} = 0$, and we take $\theta_{13}^{S_4} = \pi/2$. However, $\phi_{13}^{S_4}$ is unrestricted by the group symmetry.

Performing the same construction of the azimuthal symmetric next-nearest-neighbor exchange vector groups, there is a restriction upon $\psi_{13}^{S_4}$, which can be satisfied by choosing either $\sin \psi_{13}^{S_4} = 0$ or $\cos \psi_{13}^{S_4} = 0$. We choose $\sin \psi_{13}^{S_4} = 0$. We thus obtain

$$\hat{\mathbf{x}}_{n,n+2}^{S_4} = -\delta_n^+(\phi_{13}^{S_4}) \hat{\mathbf{x}} + \delta_n^-(\phi_{13}^{S_4}) \hat{\mathbf{y}}, \quad (102)$$

$$\hat{\mathbf{y}}_{n,n+2}^{S_4} = (-1)^{n+1} \hat{\mathbf{z}}, \quad (103)$$

$$\hat{\mathbf{z}}_{n,n+2}^{S_4} = \delta_n^-(\phi_{13}^{S_4}) \hat{\mathbf{x}} + \delta_n^+(\phi_{13}^{S_4}) \hat{\mathbf{y}}, \quad (104)$$

and

$$\{\mu_{13}^{S_4}\} = (\pi/2, \phi_{13}^{S_4}, 0). \quad (105)$$

We note that the axial symmetric anisotropic exchange vectors are not necessarily collinear with the bond directions. If all of these anisotropic exchange interactions arose solely from dipole-dipole interactions, the axial anisotropic exchange vectors would lie along the bond directions, and the azimuthal anisotropic exchange vectors would be irrelevant. This would imply $\phi_{13}^{S_4} = 3\pi/4$ for the next-nearest-neighbor interactions, and $\theta_{12}^{S_4} = c/a$ and $\phi_{12}^{S_4} = \pi$ for the near-neighbor interactions. However, the group symmetry does not require this, and if some amount of physical anisotropic exchange (not arising from dipolar interactions) were also present, more general $\phi_{13}^{S_4}, \theta_{12}^{S_4}$ and $\phi_{12}^{S_4}$ would be allowed, and the azimuthal anisotropic exchange vectors would be relevant, with general $\psi_{13}^{S_4}$ and $\psi_{12}^{S_4}$, respectively.

C. S_4 antisymmetric exchange

We begin with the next-nearest-neighbor antisymmetric exchange Hamiltonian, which may generally be written as $\mathbf{d}_{13}^{S_4} \cdot (\mathbf{S}_1 \times \mathbf{S}_3) + \mathbf{d}_{24}^{S_4} \cdot (\mathbf{S}_2 \times \mathbf{S}_4)$, where nominally $\mathbf{d}_{13}^{S_4}$ and $\mathbf{d}_{24}^{S_4}$ are three-vectors. Using the relations $\mathcal{O}_1^{S_4} \mathbf{S}_n = \mathbf{S}_{n+1}$, $\mathcal{O}_1^{S_4} \hat{\mathbf{x}} = -\hat{\mathbf{y}}$, $\mathcal{O}_1^{S_4} \hat{\mathbf{y}} = \hat{\mathbf{x}}$, and $\mathcal{O}_1^{S_4} \hat{\mathbf{z}} = -\hat{\mathbf{z}}$, we find that the components satisfy $d_{13z}^{S_4} = d_{24z}^{S_4} = 0$, $d_{13y}^{S_4} = d_{24x}^{S_4}$, and $d_{13x}^{S_4} = -d_{24y}^{S_4}$. There are no mirror planes to satisfy. There are therefore two distinct parameters for the next-nearest-neighbor antisymmetric exchange.

For the near-neighbor antisymmetric exchange, we nominally set $\mathbf{d}_{n,n+1}^{S_4}$ to be general three-vectors. Then, requiring the near-neighbor antisymmetric exchange Hamiltonian to be invariant under the improper rotation $\mathcal{O}_1^{S_4}$, we then find that the components satisfy $d_{12x}^{S_4} =$

$-d_{23y}^{S_4} = -d_{34x}^{S_4} = d_{41y}^{S_4}$, $d_{12y}^{S_4} = d_{23x}^{S_4} = -d_{34y}^{S_4} = -d_{41x}^{S_4}$, and $d_{12z}^{S_4} = -d_{23z}^{S_4} = d_{34z}^{S_4} = -d_{41z}^{S_4}$. Thus, three parameters describe the near-neighbor antisymmetric exchange for S_4 symmetry.

Combining the near-neighbor and next-nearest-neighbor antisymmetric exchange interactions, we find

$$\begin{aligned} \mathcal{H}_{DM}^{S_4} = & d_z \hat{z} \cdot \left(\sum_{n=1}^4 (-1)^{n+1} \mathbf{S}_n \times \mathbf{S}_{n+1} \right) \\ & + \mathbf{d}_\perp \cdot \left(\mathbf{S}_1 \times \mathbf{S}_2 - \mathbf{S}_3 \times \mathbf{S}_4 \right) \\ & + (\mathbf{d}_\perp \times \hat{z}) \cdot \left(\mathbf{S}_2 \times \mathbf{S}_3 - \mathbf{S}_4 \times \mathbf{S}_1 \right) \\ & + \mathbf{d}'_\perp \cdot (\mathbf{S}_1 \times \mathbf{S}_3) + (\mathbf{d}'_\perp \times \hat{z}) \cdot (\mathbf{S}_2 \times \mathbf{S}_4), \end{aligned} \quad (106)$$

where d_z is a scalar, and \mathbf{d}_\perp and \mathbf{d}'_\perp are two-vectors in the xy plane.

Thus, there are only site-dependent and site-independent DM interactions for S_4 symmetry. The NN DM interactions average to zero, but the NNN DM interactions generally do not.

VIII. D_{2d} GROUP SYMMETRY

We now consider the interesting case of D_{2d} symmetry pictured in Fig. 2. In this case, the operations $\mathcal{O}_\lambda^{D_{2d}}$ $\lambda = 1, \dots, 9$ are rotations by π about the x , y , and z axes ($\lambda = 1, 2, 3$, respectively), and the two diagonal mirror planes associated with the principal rotation axis, z . [24] The first of these is

$$\mathcal{O}_1^{D_{2d}} = \begin{pmatrix} 1 & 0 & 0 \\ 0 & -1 & 0 \\ 0 & 0 & -1 \end{pmatrix}, \quad (107)$$

and the $\lambda = 2, 3$ cases have the single $+1$ in the yy and zz positions, respectively. The two mirror planes associated with the principal z axis rotation are the planes containing the z axis and the lines $y = \pm x$, respectively, $\mathcal{O}_{4,5}^{D_{2d}} = \mathcal{O}_{5,6}^{C_{4v}}$, given by Eq. (79). We note, for example, that the plane bisecting the sites 1,2 and passing through the sites 3,4 is not a mirror plane unless $c = a$, which we assume not to be true for D_{3d} symmetry.

We first try to generate the most general axial vector set satisfying D_{2d} symmetry. Taking $\hat{\mathbf{z}}_1^{D_{2d}}$ to have the general form of Eq. (13), we then require it to be invariant under $\mathcal{O}_4^{D_{2d}}$, which leaves $\hat{\mathbf{r}}_1$ invariant. It is then easy to see that we must have $\phi_1^{D_{2d}} = 3\pi/4$, but $\theta_1^{D_{2d}}$ is unrestricted. We then generate the remaining $\hat{\mathbf{z}}_n^{D_{2d}}$ from $\mathcal{O}_1^{D_{2d}} \hat{\mathbf{z}}_1 = \hat{\mathbf{z}}_2$, $\mathcal{O}_2^{D_{2d}} \hat{\mathbf{z}}_1 = \hat{\mathbf{z}}_4$, and $\mathcal{O}_3^{D_{2d}} \hat{\mathbf{z}}_1 = \hat{\mathbf{z}}_3$. This is consistent with the invariance of the axial part of the single-ion Hamiltonian, and also leads to the results that $J_{a,n}^{D_{2d}} = J_a$, independent of n .

We then construct the azimuthal single-ion vectors, beginning with $\hat{\mathbf{x}}_1^{D_{2d}}$ from Eq. (11), using our result that $\theta_1^{D_{2d}}$ is arbitrary and $\phi_1^{D_{2d}} = 3\pi/4$. Requiring the invariance of the azimuthal part of the single-ion Hamiltonian under the mirror plane represented by $\mathcal{O}_4^{D_{2d}}$, we find that $\cos \psi_1^{D_{2d}} = 0$, and we choose the solution $\psi_1^{D_{2d}} = -\pi/2$, so that $\phi_1^{D_{2d}} + \psi_1^{D_{2d}} = \pi/4$. Then, we generate the remaining $\hat{\mathbf{x}}_n^{D_{2d}}$ from rotations of $\hat{\mathbf{x}}_1^{D_{2d}}$ about the x , y , and z axes. This of course leads to $J_{e,n}^{D_{2d}} = J_e$, independent of n .

We then find that the single-ion vector group elements for D_{2d} symmetry are

$$\hat{\mathbf{x}}_n^{D_{2d}} = \frac{1}{\sqrt{2}} \begin{pmatrix} -\gamma_n^+ \cos \theta_1^{D_{2d}} \\ \gamma_n^- \cos \theta_1^{D_{2d}} \\ \sqrt{2}(-1)^n \sin \theta_1^{D_{2d}} \end{pmatrix}, \quad (108)$$

$$\hat{\mathbf{y}}_n^{D_{2d}} = \frac{(-1)^n}{\sqrt{2}} \begin{pmatrix} \gamma_n^- \\ \gamma_n^+ \\ 0 \end{pmatrix}, \quad (109)$$

$$\hat{\mathbf{z}}_n^{D_{2d}} = \frac{1}{\sqrt{2}} \begin{pmatrix} -\gamma_n^+ \sin \theta_1^{D_{2d}} \\ \gamma_n^- \sin \theta_1^{D_{2d}} \\ \sqrt{2}(-1)^{n+1} \cos \theta_1^{D_{2d}} \end{pmatrix}, \quad (110)$$

and the associated single-ion parameters are

$$\{\mu_1^{D_{2d}}\} = (\theta_1^{D_{2d}}, \frac{3\pi}{4}, -\frac{\pi}{2}). \quad (111)$$

B. D_{2d} symmetric anisotropic exchange

We first consider the near-neighbor axial exchange vector between sites 1 and 2, writing $\hat{\mathbf{z}}_{12}$ in the form of Eq. (13). Since we require it to be either odd or even under rotations about the x axis, $\mathcal{O}_1^{D_{2d}} \hat{\mathbf{z}}_{12} = \mp \hat{\mathbf{z}}_{12}$, we then find that $\sin \phi_{12}^{D_{2d}} = 0$, and we choose $\phi_{12}^{D_{2d}} = 0$ with $\theta_{12}^{D_{2d}}$ arbitrary. We then employ $\mathcal{O}_3^{D_{2d}} \hat{\mathbf{z}}_{12} = \hat{\mathbf{z}}_{34}$, $\mathcal{O}_2^{D_{2d}} \hat{\mathbf{z}}_{12} = -\hat{\mathbf{z}}_{34}$, and $\mathcal{O}_4^{D_{2d}} \hat{\mathbf{z}}_{12} = -\hat{\mathbf{z}}_{41}$ to generate the axial near-neighbor symmetric anisotropic exchange vector group.

We then consider the azimuthal near-neighbor symmetric anisotropic exchange vector $\hat{\mathbf{x}}_{12}^{D_{2d}}$, using Eq. (11). Demanding invariance of the exchange Hamiltonian under $\mathcal{O}_1^{D_{2d}}$, or that $\mathcal{O}_1^{D_{2d}} \hat{\mathbf{x}}_{12}^{D_{2d}} = \mp \hat{\mathbf{x}}_{12}^{D_{2d}}$, we then require $\cos \psi_{12}^{D_{2d}} = 0$, and choose $\psi_{12}^{D_{2d}} = \pi/2$. We then generate the remainder of the azimuthal near-neighbor symmetric anisotropic exchange vector group as above. We thus obtain

$$\hat{\mathbf{x}}_{n,n+1}^{D_{2d}} = -\frac{1}{2} \begin{pmatrix} (\gamma_n^+ + \gamma_n^-) \cos \theta_{12}^{D_{2d}} \\ (\gamma_n^+ - \gamma_n^-) \cos \theta_{12}^{D_{2d}} \\ (-1)^n \sin \theta_{12}^{D_{2d}} \end{pmatrix}, \quad (112)$$

$$\hat{\mathbf{y}}_{n,n+1}^{D_{2d}} = \frac{(-1)^n}{2} \begin{pmatrix} (\gamma_n^- - \gamma_n^+) \\ (\gamma_n^+ + \gamma_n^-) \\ 0 \end{pmatrix}, \quad (113)$$

$$\hat{\mathbf{z}}_{n,n+1}^{D_{2d}} = \frac{1}{2} \begin{pmatrix} (\gamma_n^+ + \gamma_n^-) \sin \theta_{12}^{D_{2d}} \\ (\gamma_n^+ - \gamma_n^-) \sin \theta_{12}^{D_{2d}} \\ (-1)^{n+1} \cos \theta_{12}^{D_{2d}} \end{pmatrix}, \quad (114)$$

and the associated parameter set is

$$\{\mu_{12}^{D_{2d}}\} = (\theta_{12}^{D_{2d}}, 0, \frac{\pi}{2}). \quad (115)$$

Next, we construct the next-nearest-neighbor group-invariant symmetric anisotropic exchange vector groups. Beginning with $\hat{\mathbf{z}}_{13}$ of the form of Eq. (13), we require invariance under the parallel diagonal mirror plane, $\mathcal{O}_4^{D_{2d}} \hat{\mathbf{z}}_{13} = \pm \hat{\mathbf{z}}_{13}$. This leads to either $\sin \theta_{13}^{D_{2d}} = 0$ or $\cos \theta_{13}^{D_{2d}} = 0$, and we take $\theta_{13}^{D_{2d}} = 0$. Then, we similarly require $\mathcal{O}_4^{D_{2d}} \hat{\mathbf{x}}_{13} = \pm \hat{\mathbf{x}}_{13}$, and require $\sin \chi_{13}^{D_{2d}} = \cos \chi_{13}^{D_{2d}}$, choosing $\chi_{13}^{D_{2d}} = \pi/4$, where $\chi_{13}^{D_{2d}} = \phi_{13}^{D_{2d}} + \psi_{13}^{D_{2d}}$. Thus, the next-nearest-neighbor symmetric anisotropic exchange vector group elements are found to be

$$\hat{\mathbf{x}}_{n,n+2} = \frac{1}{\sqrt{2}} (-\gamma_n^+ \hat{\mathbf{x}} + \gamma_n^- \hat{\mathbf{y}}), \quad (116)$$

$$\hat{\mathbf{y}}_{n,n+2} = \frac{1}{\sqrt{2}} (\gamma_n^+ \hat{\mathbf{x}} + \gamma_n^- \hat{\mathbf{y}}), \quad (117)$$

$$\hat{\mathbf{z}}_{n,n+2} = (-1)^{n+1} \hat{\mathbf{z}}, \quad (118)$$

and the associated parameter set is

$$\{\mu_{13}^{D_{2d}}\} = (\theta_{13}^{D_{2d}}, \chi_{13}^{D_{2d}}) = (0, \frac{\pi}{4}). \quad (119)$$

We note that these vector groups are consistent with $J_{n,n+m}^{f,D_{2d}} = J_{f,m}$ and $J_{n,n+m}^{c,D_{2d}} = J_{c,m}$, as for the previous tetramer group symmetries studied.

C. D_{2d} antisymmetric exchange

We first consider the next-nearest-neighbor antisymmetric anisotropic exchange, which couples the spins at sites 1,3 and at 2,4, which lie parallel to the xy plane, and hence, the roles of the diagonal mirror planes are identical to that with C_{4v} symmetry. Thus, $\mathbf{d}_{13}^{D_{2d}} || (\hat{\mathbf{y}} - \hat{\mathbf{x}})$ and $\mathbf{d}_{24}^{D_{2d}} || (\hat{\mathbf{y}} + \hat{\mathbf{x}})$. Then, we require invariance under rotations about the x , y , and z axes. This leads to a single scalar parameter describing the next-nearest-neighbor antisymmetric anisotropic exchange interactions.

The near-neighbor antisymmetric anisotropic exchange Hamiltonian is obtained differently. We note that each position vector between each of the near-neighbor sites has an axis of rotation that bisects it. Thus, $\mathbf{d}_{n,n+1}^{D_{2d}}$ must be orthogonal to the respective axis of rotation. Specifically, $\mathbf{d}_{12}^{D_{2d}} = d_{12y}^{D_{2d}} \hat{\mathbf{y}} + d_{12z}^{D_{2d}} \hat{\mathbf{z}}$, $\mathbf{d}_{23}^{D_{2d}} = d_{23x}^{D_{2d}} \hat{\mathbf{x}} + d_{23z}^{D_{2d}} \hat{\mathbf{z}}$,

$\mathbf{d}_{34}^{D_{2d}} = d_{34y}^{D_{2d}} \hat{\mathbf{y}} + d_{34z}^{D_{2d}} \hat{\mathbf{z}}$, and $\mathbf{d}_{41}^{D_{2d}} = d_{41x}^{D_{2d}} \hat{\mathbf{x}} + d_{41z}^{D_{2d}} \hat{\mathbf{z}}$. Then, we rotate the near-neighbor antisymmetric exchange Hamiltonian about the x , y , and z axes, and impose invariance under the diagonal mirror planes. These combined symmetry operations result in the following restrictions upon the parameters: $d_{12y}^{D_{2d}} = d_{23x}^{D_{2d}} = -d_{34y}^{D_{2d}} = -d_{41x}^{D_{2d}}$ and $d_{12z}^{D_{2d}} = -d_{23z}^{D_{2d}} = d_{34z}^{D_{2d}} = -d_{41z}^{D_{2d}}$. Thus, there are only two free parameters describing the near-neighbor antisymmetric anisotropic exchange interactions. The combined antisymmetric exchange Hamiltonian for D_{2d} symmetry may then be written as

$$\begin{aligned} \mathcal{H}_{DM}^{D_{2d}} = & \sum_{n=1}^4 (\mathbf{S}_n \times \mathbf{S}_{n+1}) \cdot \left((-1)^{n+1} d_z \hat{\mathbf{z}} \right. \\ & \left. - \frac{d_{\perp}}{2} [(\gamma_n^+ + \gamma_n^-) \hat{\mathbf{x}} + (\gamma_n^+ - \gamma_n^-) \hat{\mathbf{y}}] \right) \\ & + d'_{\perp} \sum_{n=1}^2 [\hat{\mathbf{x}} + (-1)^n \hat{\mathbf{y}}] \cdot (\mathbf{S}_n \times \mathbf{S}_{n+2}), \end{aligned} \quad (120)$$

where d'_{\perp} is a scalar and we have set the other two scalars $d_z = d_{12z}^{D_{2d}}$ and $d_{\perp} = d_{12y}^{D_{2d}}$. The DM interactions for D_{2d} symmetry are similar to those for S_4 symmetry, except that the S_4 two-vectors, \mathbf{d}_{\perp} and \mathbf{d}_{\perp} , are just the one-vectors, $d_{\perp} \hat{\mathbf{y}}$ and $d'_{\perp} \hat{\mathbf{x}}$.

IX. T_d GROUP SYMMETRY

Aside from the restriction $c = a$, T_d is a very high symmetry group.[24] in addition to the identity operation, there are 23 other distinct operations,[24] all of which are necessary to include for our purposes. The operations $\mathcal{O}_{\lambda}^{T_d}$ for $\lambda = 1, 5$ are the same as for D_{2d} symmetry, rotations by π about the x , y , and z axis, and mirror planes containing the z axis and the lines $y = \pm x$. There are also four additional mirror planes, two of which contain the y axis and the lines $z = \pm x$ ($\lambda = 6, 7$), and two of which contain the x axis and the lines $y = \pm z$ ($\lambda = 8, 9$). These may be written as

$$\mathcal{O}_{6,7}^{T_d} = \begin{pmatrix} 0 & 0 & \pm 1 \\ 0 & 1 & 0 \\ \pm 1 & 0 & 0 \end{pmatrix}, \quad (121)$$

$$\mathcal{O}_{8,9}^{T_d} = \begin{pmatrix} 1 & 0 & 0 \\ 0 & 0 & \pm 1 \\ 0 & \pm 1 & 0 \end{pmatrix}. \quad (122)$$

In addition, there are four clockwise and four counter-clockwise rotations by $2\pi/3$ about the cube diagonals. These may be written as

$$\mathcal{O}_{10,12}^{T_d} = \begin{pmatrix} 0 & \pm 1 & 0 \\ 0 & 0 & 1 \\ \pm 1 & 0 & 0 \end{pmatrix}, \quad (123)$$

$$\mathcal{O}_{14,16}^{T_d} = \begin{pmatrix} 0 & \pm 1 & 0 \\ 0 & 0 & -1 \\ \mp 1 & 0 & 0 \end{pmatrix}, \quad (124)$$

and $\mathcal{O}_{2n+1}^{T_d} = (\mathcal{O}_{2n}^{T_d})^T = (\mathcal{O}_{2n}^{T_d})^{-1}$ for $n = 5, 6, 7, 8$. In addition, there are the six S_4 symmetries, which are clockwise and counterclockwise rotations about the x , y , and z axes.[24] The first two of these are $\mathcal{O}_{18,19}^{T_d} = \mathcal{O}_{1,2}^{S_4}$. The S_4 operations in which the axis of rotation are the x and y axes, respectively, are

$$\mathcal{O}_{20,21}^{T_d} = \begin{pmatrix} -1 & 0 & 0 \\ 0 & 0 & \pm 1 \\ 0 & \mp 1 & 0 \end{pmatrix}, \quad (125)$$

$$\mathcal{O}_{22,23}^{T_d} = \begin{pmatrix} 0 & 0 & \pm 1 \\ 0 & 1 & 0 \\ \mp 1 & 0 & 0 \end{pmatrix}, \quad (126)$$

respectively.

A. T_d single-ion anisotropy

We first examine the axial single-ion vector for site 1, making use of Eq. (13). We require that it remain invariant under the mirror planes $\mathcal{O}_{4,6,8}^{T_d}$. This forces the equations $\cos \theta - 1^{T_d} = \sin \theta_1^{T_d} \sin \phi_1^{T_d} = -\sin \theta_1^{T_d} \cos \phi_1^{T_d}$, which has the solution $\phi_1^{T_d} = 3\pi/4$ and $\theta_1^{T_d} = \tan^{-1}(\sqrt{2})$. Thus, $\hat{\mathbf{z}}_1^{T_d} = \hat{\mathbf{r}}_1$. By successive rotations about the x , y , and z axes, we generate the T_d axial vector set. We obtain

$$\hat{\mathbf{z}}_n^{T_d} = -\gamma_n^+ \hat{\mathbf{x}} + \gamma_n^- \hat{\mathbf{y}} + (-1)^{n+1} \hat{\mathbf{z}} \quad (127)$$

$$= \hat{\mathbf{r}}_n, \quad (128)$$

and the associated two-parameter set is

$$\{\mu_1^{T_d}\} = (\theta_1^{T_d}, \phi_1^{T_d}) = (\tan^{-1}(\sqrt{2}), 3\pi/4). \quad (129)$$

Since these axial vectors are identical to the position vectors, they automatically satisfy all of the remaining symmetry operations. Of course, $J_{a,n}^{T_d} = J_a$ is clearly independent of n , as it was for the lower symmetry D_{2d} group.

We have attempted to construct an azimuthal single-ion vector set, but there is no set other than the axial single-ion vector set that can satisfy all of the symmetry operations. Hence, there are no azimuthal single-ion vector groups, and we must infer $J_{e,n}^{T_d} = 0$.

B. T_d symmetric anisotropic exchange

For T_d symmetry, all six of the bond lengths are identical, as $c/a = 1$. Hence, there are at most three local

vector groups, each with six elements. From Eqs. (114) and (118), the axial vector group $\{\hat{\mathbf{z}}_{n,n+m}^{T_d}\}$ is found to have the six elements

$$\hat{\mathbf{z}}_{n,n+m}^{T_d} = \frac{\delta_{m,1}}{\sqrt{2}} \left[-\frac{1}{2} \left((\gamma_n^+ + \gamma_n^-) \hat{\mathbf{x}} + (\gamma_n^+ - \gamma_n^-) \hat{\mathbf{y}} \right) + (-1)^{n+1} \hat{\mathbf{z}} \right] + \frac{\delta_{m,2}}{\sqrt{2}} [\hat{\mathbf{x}} + (-1)^{n+1} \hat{\mathbf{y}}]. \quad (130)$$

It is easily verified that this axial vector set is a group satisfying all of the T_d symmetries. The reason this is true is actually pretty obvious: the axial exchange vector group consists of equally normalized differences between position vectors, and each position vector necessarily satisfies the group symmetry. However, there are no azimuthal anisotropic exchange groups for T_d , for the same reasons as for the single-ion group vectors. For T_d , there is therefore only one anisotropic exchange interaction $J_{n,n+m}^{f,T_d} = J_{f,1} = J_{f,2}$, since $J_{c,m} = 0$ for $m = 1, 2$.

C. T_d antisymmetric exchanges vanish

We now consider the possibility that there might be a non-vanishing antisymmetric exchange Hamiltonian for tetramers with T_d symmetry. From the mirror planes, the Moriya rules immediately restrict $\mathbf{d}_{12}^{T_d} = d_{12}(\hat{\mathbf{z}} - \hat{\mathbf{y}})/\sqrt{2}$, $\mathbf{d}_{23}^{T_d} = d_{23}(\hat{\mathbf{z}} + \hat{\mathbf{x}})/\sqrt{2}$, $\mathbf{d}_{34}^{T_d} = d_{34}(\hat{\mathbf{z}} + \hat{\mathbf{y}})/\sqrt{2}$, $\mathbf{d}_{41}^{T_d} = d_{41}(\hat{\mathbf{z}} - \hat{\mathbf{x}})/\sqrt{2}$, $\mathbf{d}_{13}^{T_d} = d_{13}(\hat{\mathbf{x}} - \hat{\mathbf{y}})/\sqrt{2}$, and $\mathbf{d}_{124}^{T_d} = d_{24}(\hat{\mathbf{x}} + \hat{\mathbf{y}})/\sqrt{2}$. Then, rotation by π about the x , y , and z axes ($\mathcal{O}_{1,2,3}^{T_d}$) forces $d_{24} = d_{13}$, $d_{41} = d_{23}$, and $d_{12} = d_{34}$. Then, we require the Hamiltonian to be invariant under the clockwise rotation by $2\pi/3$ about the cube diagonal passing through site 1, $\mathcal{O}_{12}^{T_d}$. This operation satisfies $\mathcal{O}_{12}^{T_d} \hat{\mathbf{x}} = \hat{\mathbf{z}}$, $\mathcal{O}_{12}^{T_d} \hat{\mathbf{y}} = \hat{\mathbf{x}}$, $\mathcal{O}_{12}^{T_d} \hat{\mathbf{z}} = \hat{\mathbf{y}}$, $\mathcal{O}_{12}^{T_d} \mathbf{S}_1 = \mathbf{S}_1$, $\mathcal{O}_{12}^{T_d} \mathbf{S}_2 = \mathbf{S}_3$, $\mathcal{O}_{12}^{T_d} \mathbf{S}_3 = \mathbf{S}_4$, and $\mathcal{O}_{12}^{T_d} \mathbf{S}_4 = \mathbf{S}_2$. Invariance of the Hamiltonian then requires $d_{12} = d_{23} = -d_{13}$. This reduces the number of parameters to just one, which we take to be d_{12} . We note that the rotation about the cube diagonal \mathcal{O}_{12} leaves this form of $\mathcal{H}_{DM}^{T_d}$ invariant, without any further restrictions. However, we must also have $\mathcal{H}_{DM}^{T_d}$ invariant under the six S_4 operations, and we choose $\mathcal{O}_{18}^{T_d} = \mathcal{O}_1^{S_4}$ as the first example. It is then easy to see that setting $\mathcal{O}_{18}^{T_d} \mathcal{H}_{DM}^{T_d} = \mathcal{H}_{DM}^{T_d}$ forces $d_{12} = -d_{12} = 0$. Hence, there are no DM interactions in tetramers exhibiting T_d group symmetry,

X. THE HAMILTONIAN IN THE MOLECULAR REPRESENTATION

A. The molecular single-ion Hamiltonian

To make contact with experiment, we use Eqs. (39)-(41), (63)-(65), (81)-(83), (97)-(99), (108)-(110), and

(128) to rewrite $\mathcal{H}_{si}^{g,\ell}$ in the molecular $(\hat{x}, \hat{y}, \hat{z})$ representation,

$$\mathcal{H}_{si}^g = - \sum_n \left(J_z^g(\mu_1^g) S_{n,z}^2 + (-1)^n J_{xy}^g(\mu_1^g) (S_{n,x}^2 - S_{n,y}^2) \right. \\ \left. + \frac{1}{2} \sum_{\alpha \neq \beta} K_{\alpha\beta}^g(n, \mu_1^g) \{S_{n,\alpha}, S_{n,\beta}\} \right), \quad (131)$$

where $\alpha, \beta = x, y, z$ and the $\mu_1^g \equiv \{\mu_1^g\}$ are given by Eqs. (43), (66), (84), (100), (111), and (129). In Eq. (131), $\{A, B\} = AB + BA$ and we subtracted an irrelevant constant. The easiest groups for which to evaluate the parameters in \mathcal{H}_{si}^g are D_{2d} and T_d . The site-independent interactions in the molecular representation are

$$J_z^{C_{4h}} = J_z^{D_{4h}} = J_a, \quad (132)$$

$$J_z^{C_{4v}}(\mu_1^{C_{4v}}) = \frac{1}{2} \left(J_a (3 \cos^2 \theta_1^{C_{4v}} - 1) + 3 J_e \sin^2 \theta_1^{C_{4v}} \right), \quad (133)$$

$$J_z^{S_4}(\mu_1^{S_4}) = \frac{J_a}{2} (3 \cos^2 \theta_1^{S_4} - 1) \\ - \frac{3}{2} J_e \sin^2 \theta_1^{S_4} \cos(2\psi_1^{S_4}), \quad (134)$$

$$J_z^{D_{2d}}(\mu_1^{D_{2d}}) = \frac{1}{2} \left(J_a (3 \cos^2 \theta_1^{D_{2d}} - 1) + 3 J_e \sin^2 \theta_1^{D_{2d}} \right), \quad (135)$$

$$J_z^{T_d}(\mu_1^{T_d}) = 0. \quad (136)$$

We note that the form of the site-independent interactions for D_{2d} and C_{4v} symmetry are identical, and can be obtained from that for the lowest symmetry, S_4 , by setting $\psi_1^{S_4} \rightarrow 3\pi/4$. In addition, that for the higher symmetry cases D_{4h} and C_{4h} are also obtained from that for S_4 by setting $\theta_1^g \rightarrow 0$. The vanishing site-independent single-ion interaction for the highest T_d symmetry is obtained from that of the lowest S_4 symmetry by setting both $\theta_1^{S_4} \rightarrow \tan^{-1}(\sqrt{2})$ and $J_e \rightarrow 0$.

In addition, \mathcal{H}_{si}^g contains the site-dependent interactions $(-1)^n J_{xy}^g(\mu_1^g)$ for $g = C_{4h}, S_4$ and $K_{\alpha\beta}^g(n, \mu_1^g)$ for $g = C_{4h}, D_{4h}, C_{4v}, S_4, D_{2d}$ and T_d , which are listed in the Appendix. These site-dependent interactions were generated from the site-independent interaction J_a for T_d , J_e for C_{4h} and D_{4h} , and both J_a and J_e for C_{4v} , D_{2d} , and S_4 in the local coordinates by the respective group operations. All of these site-dependent interactions average to zero, but they contribute to the eigenstate energies to second and higher orders in the interactions J_a and J_e . For C_{4v} and S_4 , the effective axial site-independent interactions $J_z^g(\mu_1^g)$ arise from a combination of the local axial and azimuthal interactions J_a and J_e , the details of the combination depending upon the precise effects of the ligand groups near to the ions. We also note that there is a substantial difference between T_d and the other three symmetries. For T_d symmetry, the average effective interaction vanishes. However, for C_{4v} , D_{2d} and S_4 symmetry,

the effective interactions can be large, even if the molecular structure is nearly T_d (that is, if $c/a \approx 1$). Once this symmetry is broken, the site-independent single-ion interactions J_z^g can become large.

B. Symmetric anisotropic exchange in the molecular representation

We then use these local exchange coordinates to construct the group-satisfying anisotropic exchange Hamiltonian in the molecular coordinates. For all four symmetries, there are similar effects. They first lead to renormalizations of the isotropic exchange interactions, modifying \mathcal{H}_0^g to

$$\mathcal{H}_0^{g,r} = -\frac{\tilde{J}_g}{2} \mathbf{S}^2 - \gamma \mathbf{B} \cdot \mathbf{S} - \frac{(\tilde{J}'_g - \tilde{J}_g)}{2} (\mathbf{S}_{13}^2 + \mathbf{S}_{24}^2), \quad (137)$$

where

$$\tilde{J}_g = J_g + \delta J_g, \quad (138)$$

$$\tilde{J}'_g \rightarrow J'_g + \delta J'_g, \quad (139)$$

where J'_g is given by Eqs. (9) and (10). For simplicity of presentation, we write

$$J_{m,\pm} = \frac{1}{2} (J_{c,m} \pm J_{f,m}) \quad (140)$$

for $m = 1, 2$. Then, the isotropic exchange renormalizations may be written as

$$\delta J_{C_{4h}} = \delta J_{D_{4h}} = 0, \quad (141)$$

$$\delta J_{C_{4v}} = \frac{1}{2} [J_{f,1} + J_{c,1} \cos(2\psi_{12}^{C_{4v}})], \quad (142)$$

$$\delta J_{D_{2d}} = -J_{1,-} \sin^2 \theta_{12}^{D_{2d}}, \quad (143)$$

$$\delta J_{S_4} = \frac{\sin^2 \theta_{12}^{S_4}}{2} [J_{f,1} + J_{c,1} \cos(2\psi_{12}^{S_4})] \quad (144)$$

$$\delta J_{T_d} = \frac{J_{f,1}}{4}, \quad (145)$$

$$\delta J'_{C_{4h}} = \delta J'_{D_{4h}} = \delta J'_{D_{2d}} = 0, \quad (146)$$

$$\delta J'_{C_{4v}} = \delta J'_{S_4} = J_{2,+}, \quad (147)$$

$$\delta J'_{T_d} = \frac{J_{f,1}}{2}. \quad (148)$$

They also lead to addition interactions $\delta \mathcal{H}_{ae}^g$ in the molecular frame. For $g = C_{4v}, S_4, D_{2d}$, and T_d , these may be written as

$$\delta \mathcal{H}_{ae}^g = \sum_{m=1}^2 \sum_{n=1}^{6-2m} \left[J_{m,z}^g(\mu_{1,m+1}^g) S_{n,z} S_{n+m,z} \right. \\ \left. + J_{m,xy}^g(\mu_{1,m+1}^g) (-1)^{n+1} \right. \\ \left. \times (S_{n,x} S_{n+m,x} - S_{n,y} S_{n+m,y}) \right]$$

$$\begin{aligned}
& + \sum_{n=1}^2 K_{2,xy}^g(\mu_{13}^g)(-1)^{n+1} \\
& \times (S_{n,x}S_{n+2,y} + S_{n,y}S_{n+2,x}) \\
& + \frac{1}{2} \sum_{n=1}^4 \sum_{\alpha,\beta} K_{1,\alpha\beta}^g(n, \mu_{12}^g) \\
& \times (S_{n,\alpha}S_{n+1,\beta} + S_{n,\beta}S_{n+1,\alpha}) \Big], \quad (149)
\end{aligned}$$

where $\alpha, \beta = x, y, z$, $\mu_{12}^g = \{\theta_{12}^g, \phi_{12}^g, \psi_{12}^g\}$, and $\mu_{13}^g = \{\theta_{13}^g, \phi_{13}^g, \psi_{13}^g\}$. The site-independent anisotropic exchange interactions are found to be

$$J_{1,z}^{C_{4h}} = J_{1,z}^{D_{4h}} = -J_{f,1}, \quad (150)$$

$$J_{1,z}^{C_{4v}}(\mu_{12}^{C_{4v}}) = \frac{1}{2}[J_{f,1} + 3J_{c,1} \cos(2\psi_{12}^{C_{4v}})], \quad (151)$$

$$\begin{aligned}
J_{1,z}^{S_4}(\mu_{12}^{S_4}) &= \frac{J_{f,1}}{2}(1 - 3\cos^2 \theta_{12}^{S_4}) \\
&+ \frac{3J_{c,1}}{2} \sin^2 \theta_{12}^{S_4} \cos(2\psi_{12}^{S_4}), \quad (152)
\end{aligned}$$

$$J_{1,z}^{D_{2d}}(\mu_{12}) = \frac{1}{4}[J_{f,1} + 3J_{1,-} \sin^2 \theta_{12}^{D_{2d}}], \quad (153)$$

$$J_{1,z}^{T_d} = -\frac{1}{4}J_{f,1} = -2J_{2,z}^{T_d}, \quad (154)$$

$$J_{2,z}^{C_{4h}} = J_{2,z}^{D_{4h}} = J_{2,z}^{D_{2d}} = -J_{f,2}, \quad (155)$$

$$J_{2,z}^{S_4} = J_{2,z}^{C_{4v}} = J_{2,+} + J_{c,2}, \quad (156)$$

where $J_{2,z}^g(\mu_{13}^g) = J_{2,z}^g$ has fully group-restricted μ_{13}^g sets for all symmetries. The site-dependent anisotropic exchange interactions are listed in the Appendix.

As we shall see in the following, to first order in the single-ion and anisotropic exchange interactions, only the site-independent interactions appear.

C. Antisymmetric exchange Hamiltonian

In Secs. IV-IX, we already presented the antisymmetric exchange Hamiltonians in the molecular representation. These may be combined into a single equation as

$$\begin{aligned}
\mathcal{H}_{DM}^g &= \sum_{n=1}^4 (\mathbf{S}_n \times \mathbf{S}_{n+1}) \cdot (d_z^g(n) \hat{\mathbf{z}} \\
&+ \frac{1}{2}(\gamma_n^- - \gamma_n^+) \mathbf{d}_\perp^g \\
&+ \frac{1}{2}(\gamma_n^+ + \gamma_n^-)(\hat{\mathbf{z}} \times \mathbf{d}_\perp^g)) \\
&+ \frac{1}{2} \sum_{n=1}^2 (\mathbf{S}_n \times \mathbf{S}_{n+2}) \cdot ((\gamma_n^- - \gamma_n^+) \mathbf{d}'_{\perp}{}^g \\
&+ (\gamma_n^+ + \gamma_n^-)(\hat{\mathbf{z}} \times \mathbf{d}'_{\perp}{}^g)), \quad (157)
\end{aligned}$$

where the relevant parameters are given in Eqs. (59), (77), (95), (106), (120), and they all vanish for $g = T_d$.

We find

$$d_z^{C_{4h}}(n) = d_z^{D_{4h}}(n) = d_z^{C_{4v}}(n) = d_z, \quad (158)$$

$$d_z^{S_4}(n) = d_z^{D_{2d}}(n) = d_z(-1)^{n+1}, \quad (159)$$

$$\mathbf{d}_\perp^{C_{4h}} = \mathbf{d}_\perp^{D_{4h}} = 0, \quad (160)$$

$$\mathbf{d}_\perp^{C_{4v}} = d_\perp \hat{\mathbf{x}}, \quad (161)$$

$$\mathbf{d}_\perp^{D_{2d}} = d_\perp \hat{\mathbf{y}}, \quad (162)$$

$$\mathbf{d}_\perp^{S_4} = \mathbf{d}_\perp = d_{\perp,x} \hat{\mathbf{x}} + d_{\perp,y} \hat{\mathbf{y}}, \quad (163)$$

$$\mathbf{d}'_{\perp}{}^{C_{4h}} = \mathbf{d}'_{\perp}{}^{D_{4h}} = 0, \quad (164)$$

$$\mathbf{d}'_{\perp}{}^{C_{4v}} = d'_\perp \hat{\mathbf{y}}, \quad (165)$$

$$\mathbf{d}'_{\perp}{}^{D_{2d}} = d'_\perp \hat{\mathbf{x}}, \quad (166)$$

$$\mathbf{d}'_{\perp}{}^{S_4} = \mathbf{d}'_{\perp} = d'_{\perp,x} \hat{\mathbf{x}} + d'_{\perp,y} \hat{\mathbf{y}}, \quad (167)$$

$$d_z^{T_d}(n) = \mathbf{d}_\perp^{T_d} = \mathbf{d}'_{\perp}{}^{T_d} = 0, \quad (168)$$

Tetramers with the lowest-symmetry group S_4 require five parameters to describe the full DM interactions, those with either D_{2d} or C_{4v} symmetry require three parameters, those with either C_{4h} or D_{4h} symmetry require just one parameter, and tetramers with T_d symmetry do not exhibit any DM interactions. We note that for C_{4v} , S_4 , and D_{2d} , the NNN DM interactions, while site-dependent, do not average to zero.

XI. EIGENSTATES OF THE FULL HAMILTONIAN

We assume a molecular Hamiltonian of $\mathcal{H} = \mathcal{H}_0^{g,r} + \mathcal{H}_{si}^g + \delta\mathcal{H}_{ae}$. To take proper account of \mathbf{B} in \mathcal{H}_0 , we construct our SMM eigenstates in the induction representation by

$$\begin{pmatrix} \hat{\mathbf{x}} \\ \hat{\mathbf{y}} \\ \hat{\mathbf{z}} \end{pmatrix} = \begin{pmatrix} \cos \theta \cos \phi & -\sin \phi & \sin \theta \cos \phi \\ \cos \theta \sin \phi & \cos \phi & \sin \theta \sin \phi \\ -\sin \theta & 0 & \cos \theta \end{pmatrix} \begin{pmatrix} \hat{\hat{\mathbf{x}}} \\ \hat{\hat{\mathbf{y}}} \\ \hat{\hat{\mathbf{z}}} \end{pmatrix}, \quad (169)$$

so that $\mathbf{B} = B\hat{\hat{\mathbf{z}}}$. A subsequent arbitrary rotation about $\hat{\hat{\mathbf{z}}}$ does not affect the eigenstates.[4] We then set $\hbar = 1$ and write

$$S^2 |\psi_{s,m}^{s_{13},s_{24}}\rangle = s(s+1) |\psi_{s,m}^{s_{13},s_{24}}\rangle, \quad (170)$$

$$S_{13}^2 |\psi_{s,m}^{s_{13},s_{24}}\rangle = s_{13}(s_{13}+1) |\psi_{s,m}^{s_{13},s_{24}}\rangle, \quad (171)$$

$$S_{24}^2 |\psi_{s,m}^{s_{13},s_{24}}\rangle = s_{24}(s_{24}+1) |\psi_{s,m}^{s_{13},s_{24}}\rangle, \quad (172)$$

$$S_{\hat{\hat{z}}} |\psi_{s,m}^{s_{13},s_{24}}\rangle = m |\psi_{s,m}^{s_{13},s_{24}}\rangle, \quad (173)$$

$$S_{\tilde{\sigma}} |\psi_{s,m}^{s_{13},s_{24}}\rangle = A_s^{\tilde{\sigma}m} |\psi_{s,m+\tilde{\sigma}}^{s_{13},s_{24}}\rangle, \quad (174)$$

$$A_s^m = \sqrt{(s-m)(s+m+1)}, \quad (175)$$

where $S_{\tilde{\sigma}} = S_{\hat{\hat{x}}} + i\tilde{\sigma}S_{\hat{\hat{y}}}$ with $\tilde{\sigma} = \pm$. For brevity, we denote $\nu = \{s, m, s_{13}, s_{24}, \{s_n\}\}$, and write $|\nu\rangle \equiv |\psi_{s,m}^{s_{13},s_{24}}\rangle$.

From Eqs. (170) to (173), $\langle \nu' | \tilde{\mathcal{H}}_0^{g,r} | \nu \rangle = E_{\nu,0}^g \delta_{\nu',\nu}$, where

$$E_{\nu,0}^g = -\frac{\tilde{J}_g}{2}s(s+1) - \gamma Bm - \frac{(\tilde{J}'_g - \tilde{J}_g)}{2}[s_{13}(s_{13}+1) + s_{24}(s_{24}+1)], \quad (176)$$

where the \tilde{J}_g and \tilde{J}'_g are given by Eqs. (9), (10), and (142)-(145).

A. Induction representation

We then transform the molecular $\mathcal{H}_{si}^g + \mathcal{H}_{ae}^g$ to the induction representation, yielding $\tilde{\mathcal{H}}_{si}^g + \tilde{\mathcal{H}}_{ae}^g$, and make a standard perturbation expansion for the six microscopic anisotropy energies $\{J_j\} \equiv (J_a, J_{c,m}, J_e, J_{f,m})$ for $m = 1, 2$ small relative to $|J_g|, |J'_g|$ and/or γB .^[4] To do so, the contain more interesting physics. Compact expressions for these matrix elements are given in the Appendix.

At arbitrary (θ, ϕ) , the first order corrections $E_{\nu,1}^g = \langle \nu | \tilde{\mathcal{H}}_{si}^g + \tilde{\mathcal{H}}_{ae}^g | \nu \rangle$ to the eigenstate energies for $g = C_{4v}, S_4, D_{2d}$, and T_d symmetries are

$$E_{\nu,1}^{g,\tilde{\mu}^g} = \frac{\tilde{J}_z^{g,\tilde{\nu}}(\tilde{\mu}^g)}{2}[m^2 - s(s+1)] - \delta\tilde{J}_z^{g,\tilde{\nu}}(\tilde{\mu}^g) - \frac{[3m^2 - s(s+1)]}{2}\tilde{J}_z^{g,\tilde{\nu}}(\tilde{\mu}^g)\cos^2\theta, \quad (177)$$

$$\tilde{J}_z^{g,\tilde{\nu}}(\tilde{\mu}^g) = J_z^g(\mu_1^g)a_{\tilde{\nu}}^+ - J_{1,z}^g(\mu_{12}^g)c_{\tilde{\nu}}^- - \frac{1}{2}J_{2,z}^ga_{\tilde{\nu}}^-, \quad (178)$$

$$\delta\tilde{J}_z^{g,\tilde{\nu}}(\tilde{\mu}^g) = J_z^g(\mu_1^g)b_{\tilde{\nu}}^+ - \frac{1}{4}J_{1,z}^g(\mu_{12}^g)(b_{\tilde{\nu}}^+ + b_{\tilde{\nu}}^-) - \frac{1}{4}J_{2,z}^gb_{\tilde{\nu}}^-, \quad (179)$$

where the $a_{\tilde{\nu}}^\pm$, $b_{\tilde{\nu}}^\pm$, and $c_{\tilde{\nu}}^\pm$ are given in the Appendix, and the interactions are given by Eqs. (133)-(134) and (151)-(156). We have used the notations

$$\tilde{\mu}^g = \{\theta_1^g, \phi_1^g, \psi_1^g, \theta_{12}^g, \phi_{12}^g, \psi_{12}^g\}, \quad (180)$$

$$\tilde{\nu} = \{s, s_{13}, s_{24}, s_1\}, \quad (181)$$

which excludes m . We note that the site-dependent interactions in Eqs. (131) and (149) and all of the DM interactions in Eq. (157) do not contribute to the first-order correction to the eigenstate energies. Second order corrections to the energies include contributions from both the site-independent and site-dependent interactions, and will be presented elsewhere.^[31]

For all four g symmetries, $E_{\nu,1}^{g,\tilde{\mu}^g}$ has a form analogous to that of the equal-spin dimer in the absence of azimuthal single-ion and anisotropic exchange interactions.^[4] For these high-symmetry tetramers, to first order in the anisotropy interactions, the azimuthal single-ion and anisotropic exchange interactions merely

renormalize the effective respective site-independent axial interactions. They do contribute directly to the second order eigenstate energies, but in rather complicated ways, which we will present elsewhere.^[31] Thus, to first order, we only have two effective isotropic exchange and three effective anisotropy interactions, \tilde{J}_g , \tilde{J}'_g , $J_z^g(\mu_1^g)$, $J_{1,z}^g(\mu_{12}^g)$, and $J_{2,z}^g$, which are fixed for a particular SMM. Nevertheless, the first-order eigenstate energies $E_\nu^g = E_{\nu,0}^g + E_{\nu,1}^{g,\tilde{\mu}^g}$, given by Eqs. (176) and (177), contain these five effective interaction strengths in ways that depend strongly upon the quantum numbers $\tilde{\nu}$ and θ . These different $\tilde{\nu}, \theta$ dependencies can be employed to provide definitive measures of the five $\tilde{\nu}$ -independent effective isotropic exchange and anisotropy interactions. To determine the precise values of the microscopic interactions, one needs to study the second order eigenstate energies in detail.

B. AFM level crossing inductions

For AFM tetramers, $\tilde{J}_g < 0$. There will be $2s_1 + 1$ level crossings, provided that the lowest energy state in each s manifold does not exhibit level repulsion. Letting $E_{s,m}^{g,\tilde{\mu}^g}(s_{13}, s_{24}, s_1) = E_{\nu,0}^g + E_{\nu,1}^{g,\tilde{\mu}^g}$, these occur when

$$E_{s,s}^{g,\tilde{\mu}^g}(s_{13}, s_{24}, s_1) = E_{s-1,s-1}^{g,\tilde{\mu}^g}(s_{13}, s_{24}, s_1). \quad (182)$$

There are two types of AFM level-crossings, depending upon the sign of $\tilde{J}'_g - \tilde{J}_g$, as seen from Eq. (176). For Type I, $\tilde{J}_g < 0$ and $\tilde{J}'_g - \tilde{J}_g > 0$, the lowest energy state in each s manifold occurs for $s_{13} = s_{24} = 2s_1$, their maximum values. Hence, the tetramer effectively acts as an AFM dimer with equal spins $2s_1$. The parameters for Type I are given for general s, s_1 in the Appendix. For the frustrated Type II, $\tilde{J}_g < 0$ and $\tilde{J}'_g - \tilde{J}_g < 0$, the level crossing occurs for the minimum values of s_{13} and s_{24} . It is easy to see that for even s values, these minima occur at $s_{13} = s_{24} = s/2$. For odd s values, the situation is doubly degenerate, and the minima occur at $s_{13}, s_{24} = (s \pm 1)/2, (s \mp 1)/2$. Hence, this level-crossing behavior differs substantially from that of equal spin dimers.^[4] In the Appendix, we also listed the formulas for the level-crossing parameters for Type II.

For both signs of $\tilde{J}_g - \tilde{J}'_g$, the s th AFM level-crossing induction in the first-order approximation may be written as

$$\begin{aligned} \gamma B_{s_1,s}^{g,\text{lc}(1)}(\theta) = & -\tilde{J}_gs + (\tilde{J}_g - \tilde{J}'_g)\Theta(\tilde{J}_g - \tilde{J}'_g)E\left(\frac{s+1}{2}\right) \\ & - \frac{J_z^g(\mu_1^g)}{2}(a_2^+ + 2b^+ + a_1^+ \cos^2\theta) \\ & + \frac{J_{1,z}^g(\mu_{12}^g)}{2}[c_2^- + \frac{1}{2}(b^+ + b^-) + c_1^- \cos^2\theta] \\ & + \frac{J_{2,z}^g}{4}(a_2^- + b^- + a_1^- \cos^2\theta), \end{aligned} \quad (183)$$

where $\Theta(s)$ is the standard Heaviside step function, $E(x)$ is the largest integer in x and

$$a_1^\pm = s(2s-1)a_{s,s_{13},s_{24}}^{s_1,\pm} - (s-1)(2s-3)a_{s-1,s_{13},s_{24}}^{s_1,\pm}, \quad (184)$$

$$a_2^\pm = sa_{s,s_{13},s_{24}}^{s_1,\pm} - (s-1)a_{s-1,s_{13},s_{24}}^{s_1,\pm}, \quad (185)$$

$$b^\pm = b_{s,s_{13},s_{24}}^{s_1,\pm} - b_{s-1,s_{13},s_{24}}^{s_1,\pm}, \quad (186)$$

$$c_1^- = s(2s-1)c_{s,s_{13},s_{24}}^{s_1,-} - (s-1)(2s-3)c_{s-1,s_{13},s_{24}}^{s_1,-}, \quad (187)$$

$$c_2^- = sc_{s,s_{13},s_{24}}^{s_1,-} - (s-1)c_{s-1,s_{13},s_{24}}^{s_1,-}. \quad (188)$$

These a_j^\pm , b^\pm , and c_j^- for $j = 1, 2$ are functions of s, s_1 and the case. For Type II, the functions are different for even and odd s . These functions are given for both cases with arbitrary s, s_1 in the Appendix.

Most notable is that for Type I, the symmetric anisotropic exchange interactions combine into a simple form, yielding the effective interaction $J_{\text{eff}}^g(s_1)$ given by

$$J_{\text{eff}}^g(s_1) = \frac{J_{1,z}^g(\mu_{12}^g)}{2} + \frac{s_1 J_{2,z}^g}{4s_1 - 1}. \quad (189)$$

Moreover, the symmetric anisotropic exchange contributions to Eq. (183) combine to yield the single term $-c_1^- J_{\text{eff}}^g(s_1)(1-3\cos^2\theta)/3$ for Type I, where c_1^- is a function of s, s_1 . However, the single ion interactions are more complicated, even for Type I, as the θ -independent and θ -dependent contributions have different s, s_1 dependencies, except for $s_1 = 1/2$, for which they both vanish.

One simplification that does occur for Type II AFM tetramers is the level crossing that occurs as a result of near-neighbor anisotropic exchange interactions $J_{1,z}^g(\mu_{12}^g)$. As shown in the Appendix, the contributions $\gamma B_{1,z}^{g,\text{lc}(1)} = J_{1,z}^g(\mu_{12}^g)f_{1,z}(s, \theta)$ to $\gamma B_{s_1,s}^{g,\text{lc}(1)}(\theta)$ from these terms are independent of s_1 , where

$$f_{1,z}(s, \theta) = \begin{cases} \frac{(s-1)}{4s} \left(1 + (2s-1)\cos^2\theta\right), & s \text{ odd} \\ \frac{s}{4(s-1)} \left(1 + (2s-3)\cos^2\theta\right), & s \text{ even.} \end{cases} \quad (190)$$

Note in particular that for $s = 1$, $f_{1,z}(1, \theta) = 0$, independent of s_1 . However, the single-ion and next-nearest neighbor anisotropic exchange contributions to the level crossing inductions depend both upon s, s_1 in different ways for both odd and even s , as shown in the Appendix.

$$s_1 = 1/2 \text{ AFM level crossings}$$

For the simplest case $s_1 = 1/2$, as in AFM Cu_4 tetramers, the single-ion terms in Eq. (183) vanish for both cases, as for the dimer of equal $s_1 = 1/2$ spins.[4] Using the results given in the Appendix, the expressions

for the $\gamma B_{1/2,s}^{g,\text{lc}(1)}(\theta)$ functions are particularly simple. For the effective dimer Type I, $\tilde{J}'_g - \tilde{J}_g > 0$,

$$\gamma B_{1/2,1}^{g,\text{lc}(1)}(\theta) = -\tilde{J}_g + \frac{1}{6}J_{\text{eff}}^g(1/2)(1-3\cos^2\theta), \quad (191)$$

$$\gamma B_{1/2,2}^{g,\text{lc}(1)}(\theta) = -2\tilde{J}_g - \frac{1}{2}J_{\text{eff}}^g(1/2)(1-3\cos^2\theta) \quad (192)$$

where $J_{\text{eff}}^g(1/2)$ is given by Eq. (189) with $s_1 = 1/2$, and for the frustrated Type II, $\tilde{J}_g - \tilde{J}'_g > 0$,

$$\gamma B_{1/2,1}^{g,\text{lc}(1)}(\theta) = -\tilde{J}'_g + \frac{1}{4}J_{2,z}^g(1+\cos^2\theta), \quad (193)$$

$$\gamma B_{1/2,2}^{g,\text{lc}(1)}(\theta) = -\tilde{J}_g - \tilde{J}'_g + \left(J_{\text{eff}}^g(1/2) - \frac{J_{2,z}^g}{4}\right)(1+\cos^2\theta) \quad (194)$$

Even in this simplest of all tetramer cases, for which single-ion interactions do not affect the thermodynamics, there is still a qualitative difference between Type I and Type II AFM $s_1 = 1/2$ tetramers. For Type I, there is only one effective isotropic interaction, \tilde{J}_g and one effective anisotropic interaction, $J_{\text{eff}}^g(1/2)$ that affect the level crossing. However, for Type II $s_1 = 1/2$ tetramers, the level crossing is different for the near-neighbor and next-nearest-neighbor anisotropic exchange interactions, and both effective isotropic interactions \tilde{J}_g and \tilde{J}'_g affect the spacing of the level crossings. The only effect of the group symmetry is to provide the particular value of J_{eff}^g . For example, $J_{\text{eff}}^{Td}(1/2) = J_{f,1}/8$. These expressions also show that Type II has a more complex level-crossing induction variation than does Type I, as the level-crossing behavior of Type I is fully described by two parameters \tilde{J}_g and J_{eff}^g , whereas the level-crossing behavior of Type II depends \tilde{J}_g , \tilde{J}'_g , $J_{1,z}^g(\mu_{12}^g)$, and $J_{2,z}^g$ separately. On the other hand, for this special $s_1 = 1/2$ example, the θ dependencies of the first and second $\gamma B_{1/2,s}^{g,\text{lc}(1)}$ are opposite in sign for Type I, but have the same sign for Type II. In Fig. 4, we illustrated these behaviors for $J_{\text{eff}}^g(1/2)/\tilde{J}_g = 0.2$ and for the general Type I and for Type II also with $J_{2,z}^g/\tilde{J}_g = 0.1$ and $\tilde{J}_g - \tilde{J}'_g = 0.5|\tilde{J}_g|$.

$$s_1 \geq 1 \text{ AFM level crossings}$$

For $s_1 > 1/2$, single-ion anisotropies are allowed, and the situation becomes much more complex than for $s_1 = 1/2$. We first consider the simplest $s_1 > 1/2$ case, $s_1 = 1$, appropriate for AFM Ni_4 tetramers. Exact expressions for the $s = 1, 2, 3, 4$ first-order level-crossing parameters are given in the Appendix. In Figs. 5 and 6, we plotted the θ -dependence of the first-order level crossing induction $\gamma B_{1,s}^{g,\text{lc}(1)}(\theta)/|\tilde{J}_g|$ for three special AFM cases of the general Type I, $\tilde{J}'_g - \tilde{J}_g > 0$, and for the particular Type II example, $\tilde{J}_g - \tilde{J}'_g = 0.5|\tilde{J}_g|$, respectively. In

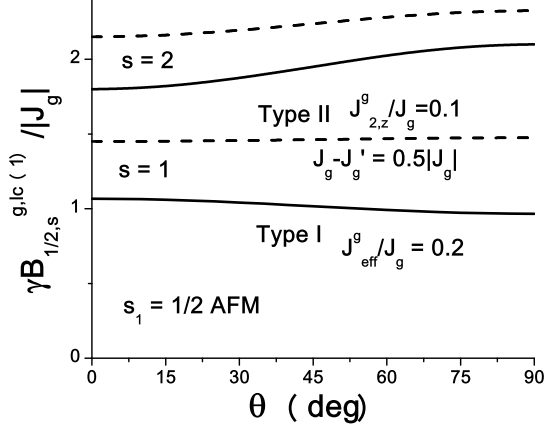


FIG. 4: Plots of the $s_1 = 1/2$ first-order level-crossing $\gamma B_{1/2,s}^{g,lc(1)}(\theta)/|\tilde{J}_g|$ with $J_{\text{eff}}^g/\tilde{J}_g = 0.2$, $\tilde{J}_g' - \tilde{J}_g > 0$ (solid, Type I) and $J_{2,z}^g/\tilde{J}_g = 0.1$, $\tilde{J}_g - \tilde{J}_g' = 0.5|\tilde{J}_g|$ (dashed, Type II).

each curve, we allow only one of the anisotropy interactions (or effective interactions) to be non-vanishing. In Fig. 3, the solid curves are for $J_z^g(\mu_1)/\tilde{J}_g = 0.2$ for $g = C_{4h}, D_{4h}, C_{4v}, S_4$, and D_{2d} . The dashed curves in Fig. 5 are for $J_{\text{eff}}^g(1)/\tilde{J}_g = 0.2$ with $g = C_{4h}, D_{4h}, C_{4v}, S_4, D_{2d}$, and T_d . For $g = T_d$, these dashed curves correspond to $J_{f,1}/(24\tilde{J}_g) = 0.2$, a huge axial symmetric exchange anisotropy, but still accessible in our first-order perturbation due to the small coefficient. We note from Fig. 5 that for Type I, the single-ion and symmetric exchange anisotropies lead to opposite θ -dependencies, both having a change in sign just before the second level crossing.

In Fig. 6, we illustrate the $s_1 = 1$ level crossings for Type II, setting $\tilde{J}_g - \tilde{J}_g' = 0.5|\tilde{J}_g|$. The solid curves are for $J_z^g(\mu_1)/\tilde{J}_g = 0.2$ for $g = C_{4h}, D_{4h}, C_{4v}, S_4$, and D_{2d} , as in Fig. 5. Except for $g = T_d$, Type II does not exhibit a unique effective symmetric anisotropic exchange interaction, so we plotted the two different symmetric exchange anisotropy interactions separately. The dashed and dotted curves are for $J_{1,z}^g(\mu_{12})/\tilde{J}_g = 0.4$ and $J_{2,z}^g/\tilde{J}_g = 0.4$, respectively, which apply for $g = C_{4h}, D_{4h}, C_{4v}, S_4$, and D_{2d} . The dash-dotted curves correspond to $J_{f,1}/\tilde{J}_g = 0.4$ for $g = T_d$. We note that for each curve, the Type II isotropic exchange parameters lead to a larger gap between the $s = 2$ and $s = 3$ level crossings. The sign of the θ -dependencies of the single-ion (solid) curves changes between $s = 2$ and $s = 3$. The NN symmetric anisotropic exchange interactions vanish for $s = 1$, but increase in magnitude with increasing s for $s = 2, 3, 4$. The sign of the θ -dependence of the level crossing due to the NNN symmetric anisotropic exchange interactions does not change, but its magnitude increases monotonically. For T_d , there is a sign change in the θ -dependence of between the $s = 3$ and $s = 4$ level crossings. Thus, Type

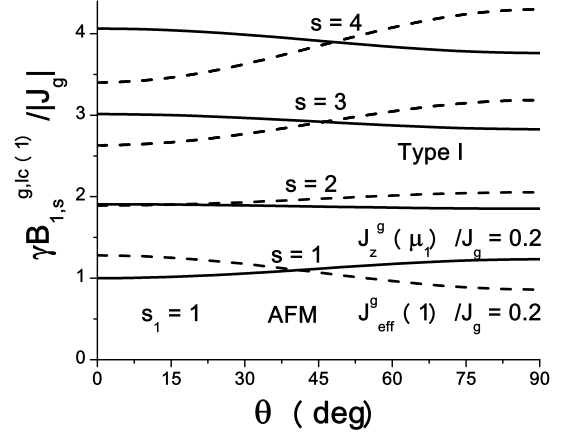


FIG. 5: Plots of the first-order level-crossing $B_{1,s}^{g,lc(1)}(\theta)/|\tilde{J}_g|$ for Type I, $\tilde{J}_g - \tilde{J}_g' < 0$ and $s_1 = 1$. Solid curves: $J_z^g(\mu_1^g)/\tilde{J}_g = 0.2$. Dashed curves: $J_{\text{eff}}^g(1)/\tilde{J}_g = 0.2$.

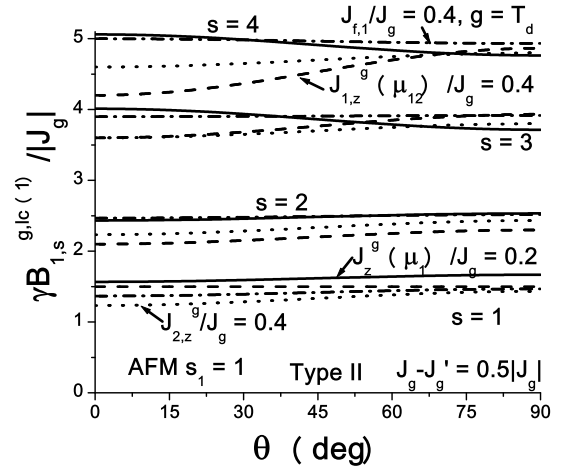


FIG. 6: Plots of the first-order level-crossing $\gamma B_{1,s}^{g,lc(1)}(\theta)/|\tilde{J}_g|$ for Type II with $\tilde{J}_g - \tilde{J}_g' = 0.5|\tilde{J}_g|$ and $s_1 = 1$. Solid curves: $J_z^g(\mu_1^g)/\tilde{J}_g = 0.2$. Dashed curves: $J_{1,z}^g(\mu_{12}^g)/\tilde{J}_g = 0.4$, $g = C_{4h}, D_{4h}, C_{4v}, S_4, D_{2d}$. Dotted curves: $J_{2,z}^g/\tilde{J}_g = 0.4$ for $g = C_{4h}, D_{4h}, C_{4v}, S_4, D_{2d}$. Dash-dotted curves: $J_{f,1}/\tilde{J}_g = 0.4$ for $g = T_d$.

II AFM $s_1 = 1$ tetramers have a richer set of first-order level-crossing behaviors than do Type I AFM $s_1 = 1$ tetramers.

In Figs. 7 and 8, the analogous Type I and Type II AFM level crossing inductions are plotted versus θ for $s_1 = 3/2$ equal-spin tetramers, such as Cr_4 . The notation is the same as in Figs. 5 and 6. For Type I $s_1 = 3/2$ AFM tetramers, the single-ion and symmetric anisotropic exchange interactions lead to different θ -dependencies of

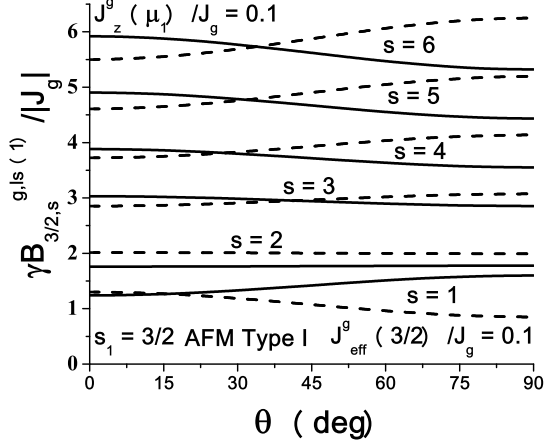


FIG. 7: Plots of the first-order level-crossing $\gamma B_{3/2,s}^{g,lc(1)}(\theta)/|\tilde{J}_g|$ for Type I, $\tilde{J}_g - \tilde{J}'_g < 0$ and $s_1 = 3/2$. Solid curves: $J_z^g(\mu_1^g)/\tilde{J}_g = 0.1$. Dashed curves: $J_{\text{eff}}^g(3/2)/\tilde{J}_g = 0.1$.

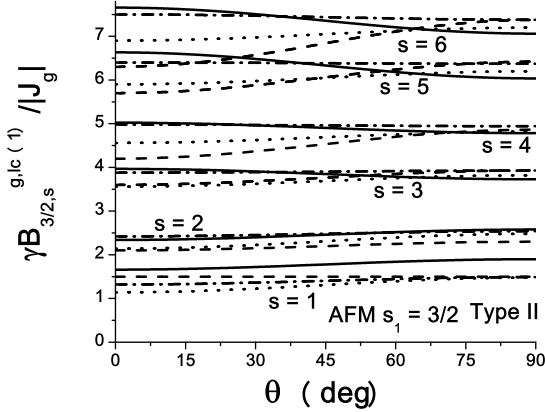


FIG. 8: Plots of the first-order level-crossing $\gamma B_{3/2,s}^{g,lc(1)}(\theta)/|\tilde{J}_g|$ for Type II with $\tilde{J}_g - \tilde{J}'_g = 0.5|\tilde{J}_g|$ and $s_1 = 3/2$. Solid curves: $J_z^g(\mu_1^g)/\tilde{J}_g = 0.2$. Dashed curves: $J_{1,z}^g(\mu_{12}^g)/\tilde{J}_g = 0.4$, $g = C_{4h}, D_{4h}, C_{4v}, S_4, D_{2d}$. Dotted curves: $J_{2,z}^g(\mu_{12}^g)/\tilde{J}_g = 0.4$ for $g = C_{4h}, D_{4h}, C_{4v}, S_4, D_{2d}$. Dash-dotted curves: $J_{f,1}/\tilde{J}_g = 0.4$ for $g = T_d$.

the level-crossing inductions, each with a change in sign in the θ dependence at about the second level crossings, as seen in Fig. 7. For Type II $s_1 = 3/2$ AFM tetramers, the sign changes appear between the second and third level crossings, as shown in Fig. 8.

XII. THE SELF-CONSISTENT HARTREE APPROXIMATION

The self-consistent Hartree approximation, or strong exchange limit,[27] provides accurate results for the \mathbf{B} dependence of the specific heat and magnetization at low $k_B T/|J|$ and $\gamma B/|J|$ not too small,[4] where k_B is Boltzmann's constant. In this approximation, $E_\nu^g = E_{\nu,0}^g + E_{\nu,1}^g$ is given by Eqs. (176) and (177), respectively. We shall present the self-consistent Hartree approximation of four measurable quantities in the induction representation. We first define the trace in a way sufficiently general as to encompass the four group symmetries under consideration,

$$\text{Tr}_\nu \equiv \sum_\nu = \sum_{s_{13}, s_{24}=0}^{2s_1} \sum_{m=-s}^s \sum_{s=|s_{13}-s_{24}|}^{s_{13}+s_{24}}, \quad (195)$$

The partition function in the self-consistent Hartree approximation may then be written

$$Z_g^{(1)} = \text{Tr}_\nu e^{-\beta E_\nu^g}, \quad (196)$$

where $\beta = 1/(k_B T)$, and $E_\nu^g = E_{\nu,0}^g + E_{\nu,1}^g$ is given by Eqs. (176) and (177). In this compact notation, the self-consistent Hartree magnetization $M_g^{(1)}(\mathbf{B}, T)$ and specific heat $C_{g,V}^{(1)}(\mathbf{B}, T)$ are given by

$$M_g^{(1)}(\mathbf{B}, T) = \gamma \text{Tr}_\nu \left(m e^{-\beta E_\nu^g} \right) / Z_g^{(1)}, \quad (197)$$

$$\frac{C_{g,V}^{(1)}(\mathbf{B}, T)}{k_B \beta^2} = \frac{\text{Tr}_\nu \left((E_\nu^g)^2 e^{-\beta E_\nu^g} \right)}{Z_g^{(1)}} - \left[\frac{\text{Tr}_\nu \left(E_\nu^g e^{-\beta E_\nu^g} \right)}{Z_g^{(1)}} \right]^2. \quad (198)$$

We note that there are strong differences between the low- T behavior of FM and AFM tetramers. We assume $|\tilde{J}_g| > |\tilde{J}'_g|$. For FM tetramers with $\tilde{J}_g > 0$, the low- T thermodynamic behavior is dominated by the $s = 4s_1$, $m = -4s_1$ state, leading to

$$M_g^{(1)}(\mathbf{B}, T) \underset{T \rightarrow 0}{\approx} \gamma \hat{\mathbf{B}} B_{4s_1}(\beta \gamma B), \quad (199)$$

where $B_S(x)$ is the Brillouin function. The universality of this function renders thermodynamic studies useless for the determination of the microscopic parameters. For AFM tetramers with $\tilde{J}_g < 0$, however, there will be interesting level-crossing effects, which can be employed to measure the microscopic interaction parameters, as discussed in detail in Sec. V. As for dimers, $C_V(B, T)$ for AFM tetramers at sufficiently low T exhibit $2s_1$ central minima at the level-crossing inductions $B_{s_1,s}^{g,lc}(\theta) \approx B_{s_1,s}^{g,lc(1)}(\theta)$ that vanish as $T \rightarrow 0$, equally surrounded by peaks of equal height.[4] As for the magnetization, $C_V(B, T)$ for FM tetramers at low T reduces

to that of a monomer with spin $4s_1$, yielding a rather uninteresting Schottky anomaly.

However, the microscopic nature of FM tetramers can be better probed either by EPR or INS techniques. The self-consistent Hartree EPR absorption $\Im\chi_{-\sigma,\sigma}^{g,(1)}(\mathbf{B},\omega)$ for clockwise ($\sigma = 1$) or counterclockwise ($\sigma = -1$) circularly polarized oscillatory fields normal to \mathbf{B} is

$$\begin{aligned} \Im\chi_{-\sigma,\sigma}^{g,(1)} &= \frac{\gamma^2}{Z_g^{(1)}} \text{Tr}_\nu \text{Tr}_{\nu'} e^{-\beta E_\nu^g} |M_{\nu,\nu'}|^2 \\ &\times [\delta(E_\nu^g - E_{\nu'}^g + \omega) - \delta(E_{\nu'}^g - E_\nu^g + \omega)], \end{aligned} \quad (200)$$

where $M_{\nu,\nu'} = A_s^{\sigma m} \delta_{m',m+\sigma} \delta_{s',s} \delta_{s'_{13},s_{13}} \delta_{s'_{24},s_{24}}$ and $\text{Tr}_{\nu'} = \sum_{\nu'}$. The strong resonant inductions for appear at

$$\gamma_{\text{res}}^{B^{g,(1)}} = \pm\omega + \frac{(2m+\sigma)}{2}(1 - 3\cos^2\theta)\tilde{J}_z^{g,\overline{\nu}}(\tilde{\mu}^g), \quad (201)$$

where $\tilde{J}_z^{g,\overline{\nu}}(\tilde{\mu}^g)$ is given by Eq. (178). We note that $\tilde{J}_z^{g,\overline{\nu}}(\tilde{\mu}^g)$ contains the three effective microscopic interactions, $J_z^g(\mu_1^g)$, $J_{1,z}^g(\mu_{12}^g)$, and $J_{2,z}$, multiplied by the constants $a_{\overline{\nu}}^+$, $-c_{\overline{\nu}}^-$, and $-a_{\overline{\nu}}^-/2$. Thus, for an experimental determination of all three microscopic parameters, it is necessary to perform EPR experiments in three different quantum state manifolds. At low T , the Boltzmann factor favors the ground state manifold, so to obtain the desired measurements of three manifolds, one needs to access the excited $s = 4s_1 - 1$ states, as well.

As shown in the Appendix, for a FM tetramer with $\tilde{J}_g > 0$ in the lowest energy manifold of states, nominally $(s, s_{13}, s_{24}) = (4s_1, 2s_1, 2s_1)$, has the highest population at very low T . In this ground state manifold with $-4s_1 \leq m \leq 4s_1$, the constants reduce to

$$a_{\overline{\nu}}^\pm \rightarrow \frac{s-1 \mp 1}{2(2s-1)}, \quad (202)$$

$$c_{\overline{\nu}}^- \rightarrow \frac{s-1}{2(2s-1)}, \quad (203)$$

where $s = 4s_1$. We note, of course, that when the single-ion and anisotropic exchange interactions are sufficiently large, s is not really a good quantum number, as the actual ground state, while mostly the nominal $s = 4s_1$, contains a mixture of $s = 4s_1 - 2$ states, to leading order in those interactions.[4] Additional mixtures are likely to be relevant for the excited states, as well.

However, assuming for simplicity that we can safely neglect such mixing, and take (s, s_{13}, s_{24}) to be a good quantum number set, there is still some ambiguity in the determination of the order of the lowest manifolds of excited states. From Eq. (176), it is evident that if $\tilde{J}_g > 0$ and $\tilde{J}'_g = \tilde{J}_g > 0$, the states $(s, s_{13}, s_{24}) = (s, 2s_1, 2s_1)$ are energetically favored for each s value. We denote this a Type I FM tetramer. However, for a Type II FM

tetramer with $\tilde{J}_g > 0$ and $\tilde{J}'_g - \tilde{J}_g < 0$, the states with minimal allowed values of s_{13}, s_{24} are favored. Thus, for even s , these are $(s, s/2, s/2)$, and for odd s are $(s, (s+1)/2, (s-1)/2)$.

Thus, there are two inequivalent lowest energy excited state manifolds with $s = 4s_1 - 1$ and $-4s_1 \leq m \leq 4s_1 - 1$ of excited states with $s = 4s_1 - 1$. For $|\tilde{J}_g - \tilde{J}'_g| \ll \tilde{J}_g$, these are ordinarily both accessible. One of these is non-degenerate (at fixed m) with $(s, s_{13}, s_{24}) = (4s_1 - 1, 2s_1, 2s_1)$ and the other is doubly degenerate with $(s, s_{13}, s_{24}) = (4s_1 - 1, 2s_1 - 1, 2s_1)$, $(4s_1 - 1, 2s_1, 2s_1 - 1)$. In Type I FM tetramers, the $(4s_1 - 1, 2s_1, 2s_1)$ states have lower energy than the next excited manifold with $(4s_1 - 1, 2s_1 - 1, 2s_1)$, $(4s_1 - 1, 2s_1, 2s_1 - 1)$ states. In Type II FM tetramers, the reverse order occurs. From the results presented in the Appendix, for the $(4s_1 - 1, 2s_1 - 1, 2s_1)$, $(4s_1 - 1, 2s_1, 2s_1 - 1)$ manifold of states with $-4s_1 + 1 \leq m \leq 4s_1 - 1$, the constants are

$$a_{\overline{\nu}}^\pm \rightarrow \frac{(s^2 - s + 1) \mp (2s - 1)}{2s(2s - 1)}, \quad (204)$$

$$c_{\overline{\nu}}^- \rightarrow \frac{(s+1)(s-1)^2}{2s^2(2s-1)}, \quad (205)$$

where $s = 4s_1 - 1$. For the $(4s_1 - 1, 2s_1, 2s_1)$ manifold of states, also with $-4s_1 + 1 \leq m \leq 4s_1 - 1$, the constants are

$$a_{\overline{\nu}}^\pm \rightarrow \frac{(s-1)(s \mp 1)}{s(2s-1)}, \quad (206)$$

$$c_{\overline{\nu}}^- \rightarrow \frac{(s-2)}{2(2s-1)}, \quad (207)$$

where again $s = 4s_1 - 1$. We note that these three sets of constants are all distinct. Thus, either by operating at higher temperature or by some special pumping technique, it is possible to probe these low-lying state manifolds, and thereby obtain a full measurement of the first-order microscopic parameters.

The Hartree INS cross-section $S_g^{(1)}(\mathbf{B}, \mathbf{q}, \omega)$ is

$$\begin{aligned} S_g^{(1)} &= \text{Tr}_\nu \text{Tr}_{\nu'} e^{-\beta E_\nu^g} \sum_{\tilde{\alpha}, \tilde{\beta}} (\delta_{\tilde{\alpha}, \tilde{\beta}} - \hat{q}_{\tilde{\alpha}} \hat{q}_{\tilde{\beta}}) \sum_{n, n'} \\ &\times e^{i\mathbf{q} \cdot (\mathbf{r}_n - \mathbf{r}_{n'})} \langle \nu | S_{n, \tilde{\alpha}}^\dagger | \nu' \rangle \langle \nu' | S_{n, \tilde{\beta}} | \nu \rangle \\ &\times \delta(\omega + E_\nu^g - E_{\nu'}^g), \end{aligned} \quad (208)$$

where $\tilde{\alpha}, \tilde{\beta} = \tilde{x}, \tilde{y}, \tilde{z}$, $\hat{q}_{\tilde{x}} = \sin\theta_{b,q} \cos\phi_{b,q}$, $\hat{q}_{\tilde{y}} = \sin\theta_{b,q} \sin\phi_{b,q}$, and $\hat{q}_{\tilde{z}} = \cos\theta_{b,q}$, $\theta_{b,q}$ and $\phi_{b,q}$ describe the relative orientations of \mathbf{B} and \mathbf{q} , [4] the \mathbf{r}_n and $\langle \nu' | S_{n, \tilde{\alpha}} | \nu \rangle$ are given by Eqs. (1), (255), and (256) respectively, and the scalar $\mathbf{q} \cdot (\mathbf{r}_n - \mathbf{r}_{n'})$ is invariant under the rotation, Eq. (169). After some algebra, we rewrite $S_g^{(1)}(\mathbf{q}, \omega)$ as

$$S_g^{(1)} = \text{Tr}_\nu^g e^{-\beta E_\nu^g} \sum_{\nu'} \delta(\omega + E_\nu^g - E_{\nu'}^g)$$

$$\times \left(\sin^2 \theta_{b,q} L_{\nu,\nu'}(\mathbf{q}) + \frac{(2 - \sin^2 \theta_{b,q})}{4} M_{\nu,\nu'}(\mathbf{q}) \right), \quad (209)$$

where the Hartree functions $L_{\nu,\nu'}(\mathbf{q})$ and $M_{\nu,\nu'}(\mathbf{q})$ are given in the Appendix. They are independent of \mathbf{B} . Since E_ν^g is well-behaved as $\mathbf{B} \rightarrow 0$, Eq. (209) is accurate for all \mathbf{B} .

As for the dimer,[4] additional EPR and INS transitions with amplitudes higher order in the anisotropy parameters $J_z^g(\mu_1^g)$, $J_{1,z}^g(\mu_{12}^g)$, and $J_{2,z}^g$ relative to \tilde{J}_g are obtained in the extended Hartree approximation, but will be presented elsewhere for brevity.[31]

XIII. DISCUSSION

We note that the phenomenological total spin anisotropy model widely used in fitting experimental data on SMM's is

$$\mathcal{H}_p = -J_b S_z^2 - J_d (S_x^2 - S_y^2), \quad (210)$$

containing axial and azimuthal contributions, respectively,[1] sometimes with additional quartic terms.[19, 36] The terms are generally defined relative to the total spin principal axes, which for equal spin, high symmetry systems are the molecular axis vectors. It is easy to evaluate $E_\nu^p = \langle \nu | \hat{\mathcal{H}}_p | \nu \rangle$ in the induction representation. One obtains Eq. (177) with

$$\tilde{J}_z^{g,\bar{\nu}} \rightarrow J_b, \quad (211)$$

$$J_d = 0, \quad (212)$$

$$\delta \tilde{J}_z^{g,\bar{\nu}} \rightarrow 0. \quad (213)$$

A non-vanishing J_d would lead to a term in Eq. (177) proportional to $\sin^2 \theta \cos(2\phi)$, as for the dimer,[4] which does not arise in the first-order calculation for the high-spin tetramers under consideration, based upon the microscopic parameters alone. Hence, J_b alone describes the θ and m dependencies of $E_{\nu,1}^g$ correctly.

In addition, for the lowest energy states of FM tetramers, we have $s = 4s_1$, $s_{13} = s_{24} = 2s_1$, so $\bar{\nu}$ is restricted to a single set of values. In this high-spin case, J_b can provide a correct phenomenology of the $s = 4s_1$ ground state energy manifold. However, if applied to the two low-lying excited state manifolds with $s = 4s_1 - 1$, for instance, one would infer two different J_b values from that obtained in the ground state manifold. For AFM tetramers, the phenomenological model also correctly provides a vanishing first-order correction to the $s = 0$ manifold of states with $s_{13} = s_{24} = 0, 1, \dots, 2s_1$. However, it also has problems describing the first excited manifold of AFM states with $s = 1$, because it leads to the unphysical choice of $\delta J_z^{g,\bar{\nu}}(\bar{\mu}) = 0$ (or a constant, independent of the quantum numbers $\bar{\nu}$). Hence, the phenomenological model works best in describing only a

single manifold of states with fixed (s, s_{13}, s_{24}) . This is more restrictive than the usual assumption of its applicability to a fixed set of s states.[15, 36, 37, 38]

We note that for the FM Fe_4 SMM with D_3 symmetry, $\text{Fe}_4(\text{thme})_2(\text{dpm})_6$, where H_3thme is 1,1,1-tris(hydroxymethyl)ethane and Hdpm is dipivaloylmethane,[36, 37] the D_3 symmetry also precludes the J_d term. Nevertheless, in fits to INS data, it was necessary to assume $J_d \neq 0$,[36, 38] to obtain the appropriate anticrossing gaps, so that either the powdered sample did not have pure D_3 symmetry, or the phenomenological model they used, Eq. (210) plus two quartic terms obeying D_3 symmetry, was not appropriate. Since single-ion interactions appeared to be important,[36] the total spin might not have been a well-defined quantum number, as in at least one Fe_2 dimer and in Fe_8 . [4, 5, 7, 8] In addition, second order effects might also provide a possible explanation.[31] To investigate this symmetry, it would be necessary to evaluate the single-ion matrix elements for that symmetry in compact form.[31]

For simplicity, we have neglected biquadratic exchange and higher order anisotropic interactions. Of these, those of the simplest form are the isotropic biquadratic exchange interactions, which for the symmetries under consideration take the form

$$\mathcal{H}_{bq}^g = -J_{2,g} \sum_{n=1}^4 (\mathbf{S}_n \cdot \mathbf{S}_{n+1})^2 - J'_{2,g} \sum_{n=1}^2 (\mathbf{S}_n \cdot \mathbf{S}_{n+2})^2, \quad (214)$$

where $J'_{2,g} \neq J_{2,g}$ for $g = C_{4h}, D_{4h}, C_{4v}, S_4$, and D_{2d} , $J'_{2,T_d} = J_{2,T_d}$. The $J'_{2,g}$ term is diagonal in the $|\nu\rangle$ representation, but the remaining term proportional to $J_{2,g}$ is not. However, it is important to note that these isotropic interactions are rotationally invariant, so they are independent of θ in the induction representation. Hence, they modify the positions but not the θ -dependencies of the AFM level-crossing inductions. Although the diagonal $J'_{2,g}$ term does not affect the EPR transitions, the non-diagonal $J_{2,g}$ term will modify the positions but not the θ -dependencies of the EPR resonant inductions.

We note that our formulation of the single-ion matrix elements in terms of a pair of dimers is applicable to low-symmetry systems such as $\text{Mo}_{12}\text{O}_{30}(\mu_2\text{-OH})_{10}\text{H}_2\{\text{Ni}(\text{H}_2\text{O})_3\}_4$, abbreviated as $\{\text{Ni}_4\text{Mo}_{12}\}$, [39] systems such as Ni_4 tetramers obtained from salts of $[\text{Ni}_4(\text{H}_2\text{O})_2(\text{PW}_9\text{O}_{34})_2]^{10-}$ with C_{2v} symmetry,[40] and the unequal-spin systems $\text{Mn}_2^{II}\text{Mn}_2^{III}$ and $\text{Ni}_2^{II}\text{Mn}_2^{III}$. [41, 42] In the first system with C_{1v} symmetry, one would expect many more single-ion, symmetric anisotropic exchange, and DM interactions, making definitive fits to the existing powder magnetization data problematic.[39] However, to improve the fits to the C_{3v} or D_3 symmetry systems, such as the Fe_4 compound $\text{Fe}_4(\text{thme})_2(\text{dpm})_6$

and the $\text{Cr}^{III}\text{Ni}_3^{II}$ tetramer with an $s = 9/2$ ground state,[36, 43] would require a reformulation of the single-ion matrix elements as a trimer plus a monomer.[31]

SUMMARY

We presented a microscopic theory of high-symmetry single molecule magnets, including a compact form for the exact single-spin matrix elements for four general spins. We used the local axial and azimuthal vector groups to construct the invariant single-ion and symmetric anisotropic exchange Hamiltonians, and the molecular representation to obtain the Dzyaloshinskii-Moriya interactions, for equal-spin s_1 tetramers with site point group symmetries T_d , D_{4h} , D_{2d} , S_4 , C_{4h} , or C_{4v} . Each vector group introduces site-dependent molecular single-ion and anisotropic exchange interactions. Assuming weak effective site-independent single-ion and exchange anisotropy interactions, we evaluated the first-order corrections to the eigenstate energies, and provided analytic results and illustrations of the antiferromagnetic level-crossing inductions. We also provided Hartree expressions for the magnetization, specific heat, EPR absorption, and INS cross-section, which are accurate at low temperatures and arbitrary magnetic fields. For ferromagnetic tetramers, we provided a procedure for a precise EPR determination of the microscopic anisotropy parameters. Our procedure is extendable to more general systems.

We thank N. S. Dalal for helpful comments. This work was supported by the NSF under contract NER-0304665.

APPENDIX

1. Site-dependent single-ion interactions

For $g = D_{4h}$, the only non-vanishing site-dependent single-ion interaction is

$$K_{xy}^{D_{4h}}(n, \mu_1^{D_{4h}}) = (-1)^{n+1} J_e. \quad (215)$$

For $g = C_{4h}$, the two non-vanishing site-dependent single-ion interactions are

$$J_{xy}^{C_{4h}}(\mu_1^{C_{4h}}) = J_e \cos(2\chi_1^{C_{4h}}), \quad (216)$$

$$K_{xy}^{C_{4h}}(n, \mu_1^{C_{4h}}) = (-1)^{n+1} J_e \sin(2\chi_1^{C_{4h}}). \quad (217)$$

For $g = C_{4v}$, the non-vanishing site-dependent single-ion interactions in Eq. (131) are

$$K_{xy}^{C_{4v}}(n, \mu_1^{C_{4v}}) = \frac{(-1)^{n+1}}{2} \left(J_a \sin^2 \theta_1^{C_{4v}} - J_e (1 + \cos^2 \theta_1^{C_{4v}}) \right), \quad (218)$$

$$K_{xz}^{C_{4v}}(n, \mu_1^{C_{4v}}) = -\frac{\gamma_n^+}{2\sqrt{2}} \sin(2\theta_1^{C_{4v}}) (J_a - J_e), \quad (219)$$

$$K_{yz}^{C_{4v}}(n, \mu_1^{C_{4v}}) = -\frac{\gamma_n^-}{2\sqrt{2}} \sin(2\theta_1^{C_{4v}}) (J_a + J_e). \quad (220)$$

For S_4 , the single-ion site-dependent interactions are

$$J_{xy}^{S_4}(\mu_1^{S_4}) = J_1(\mu_1^{S_4}) \cos(2\phi_1^{S_4}) + J_2(\mu_1^{S_4}) \sin(2\phi_1^{S_4}), \quad (221)$$

$$K_{xy}^{S_4}(n, \mu_1^{S_4}) = (-1)^n \left(J_1(\mu_1^{S_4}) \sin(2\phi_1^{S_4}) - J_2(\mu_1^{S_4}) \cos(2\phi_1^{S_4}) \right), \quad (222)$$

$$K_{xz}^{S_4}(n, \mu_1^{S_4}) = (-1)^{n+1} \left(J_3(\mu_1^{S_4}) \delta_n^-(\phi_1^{S_4}) - J_4(\mu_1^{S_4}) \delta_n^+(\phi_1^{S_4}) \right), \quad (223)$$

$$K_{yz}^{S_4}(n, \mu_1^{S_4}) = (-1)^{n+1} \left(J_3(\mu_1^{S_4}) \delta_n^+(\phi_1^{S_4}) + J_4(\mu_1^{S_4}) \delta_n^-(\phi_1^{S_4}) \right), \quad (224)$$

$$J_1(\mu_1^{S_4}) = \frac{1}{2} \left(J_a \sin^2 \theta_1^{S_4} - J_e (1 + \cos^2 \theta_1^{S_4}) \cos(2\psi_1^{S_4}) \right), \quad (225)$$

$$J_2(\mu_1^{S_4}) = J_e \cos \theta_1^{S_4} \sin(2\psi_1^{S_4}), \quad (226)$$

$$J_3(\mu_1^{S_4}) = \frac{1}{2} \sin(2\theta_1^{S_4}) [J_a + J_e \cos(2\psi_1^{S_4})], \quad (227)$$

$$J_4(\mu_1^{S_4}) = J_e \sin \theta_1^{S_4} \sin(2\psi_1^{S_4}). \quad (228)$$

For D_{2d} , the non-vanishing site-dependent single-ion interactions are

$$K_{xy}^{D_{2d}}(n, \mu_1^{D_{2d}}) = \frac{(-1)^{n+1}}{2} \left(J_a \sin^2 \theta_1^{D_{2d}} + J_e (1 + \cos^2 \theta_1^{D_{2d}}) \right), \quad (229)$$

$$K_{xz}^{D_{2d}}(n, \mu_1^{D_{2d}}) = \frac{\gamma_n^-}{2\sqrt{2}} (J_a - J_e) \sin(2\theta_1^{D_{2d}}), \quad (230)$$

$$K_{yz}^{D_{2d}}(n, \mu_1^{D_{2d}}) = \frac{-\gamma_n^+}{2\sqrt{2}} (J_a - J_e) \sin(2\theta_1^{D_{2d}}). \quad (231)$$

The site-dependent interactions for T_d symmetry are easily obtained from those Eqs. (229)-(231) by setting $\theta_1^{D_{2d}} \rightarrow \tan^{-1}(\sqrt{2})$ and $J_e \rightarrow 0$.

2. Site-dependent symmetric anisotropic exchange interactions

For $g = C_{4h}$, the non-vanishing site-dependent symmetric anisotropic exchange interactions in Eq. (149) are

$$J_{m,xy}^{C_{4h}}(\mu_{1,m+1}^{C_{4h}}) = J_{c,m} \cos(2\chi_{1,m+1}^{C_{4h}}) \quad (232)$$

for $m = 1, 2$. For D_{4h} , the non-vanishing site-dependent symmetric anisotropic exchange interactions are

$$J_{1,xy}^{D_{4h}}(\mu_{12}^{D_{4h}}) = J_{c,1}, \quad (233)$$

$$K_{2,xy}^{D_{4h}}(\mu_{13}^{D_{4h}}) = -J_{c,2}. \quad (234)$$

For C_{4v} , the non-vanishing site-dependent anisotropic exchange interactions are

$$J_{1,xy}^{C_{4v}}(\mu_{12}^{C_{4v}}) = \frac{1}{2}[J_{f,1} - J_{c,1} \cos(2\psi_{12}^{C_{4v}})], \quad (235)$$

$$K_{2,xy}^{C_{4v}}(\mu_{13}^{C_{4v}}) = J_{2,-}, \quad (236)$$

$$K_{1,xz}^{C_{4v}}(n, \mu_{12}^{C_{4v}}) = -\frac{1}{2}(\gamma_n^+ - \gamma_n^-)J_{c,1} \sin(2\psi_{12}^{C_{4v}}) \quad (237)$$

$$K_{1,yz}^{C_{4v}}(n, \mu_{12}^{C_{4v}}) = \frac{1}{2}(\gamma_n^+ + \gamma_n^-)J_{c,1} \sin(2\psi_{12}^{C_{4v}}). \quad (238)$$

Again, the more interesting group is $g = S_4$. We find

$$J_{1,xy}^{S_4}(\mu_{12}^{S_4}) = -\tilde{J}_1(\mu_{12}^{S_4}) \cos(2\phi_{12}^{S_4}) + \tilde{J}_2(\mu_{12}^{S_4}) \sin(2\phi_{12}^{S_4}), \quad (239)$$

$$J_{2,xy}^{S_4}(\mu_{13}^{S_4}) = -J_{2,-} \sin(2\phi_{13}^{S_4}), \quad (240)$$

$$K_{2,xy}^{S_4}(\mu_{13}^{S_4}) = J_{c,-} \cos(2\phi_{13}^{S_4}), \quad (241)$$

$$K_{1,xy}^{S_4}(n, \mu_{12}^{S_4}) = (-1)^{n+1} \left(\tilde{J}_1(\mu_{12}^{S_4}) \sin(2\phi_{12}^{S_4}) + \tilde{J}_2(\mu_{12}^{S_4}) \cos(2\phi_{12}^{S_4}) \right), \quad (242)$$

$$K_{1,xz}^{S_4}(n, \mu_{12}^{S_4}) = (-1)^n \left(\tilde{J}_3(\mu_{12}^{S_4}) \delta_n^-(\phi_{12}^{S_4}) - \tilde{J}_4(\mu_{12}^{S_4}) \delta_n^+(\phi_{12}^{S_4}) \right), \quad (243)$$

$$K_{1,yz}^{S_4}(n, \mu_{12}^{S_4}) = (-1)^n \left(\tilde{J}_3(\mu_{12}^{S_4}) \delta_n^+(\phi_{12}^{S_4}) + \tilde{J}_4(\mu_{12}^{S_4}) \delta_n^-(\phi_{12}^{S_4}) \right), \quad (244)$$

where

$$\tilde{J}_1(\mu_{12}^{S_4}) = \frac{1}{2} \left(J_{f,1} \sin^2 \theta_{12}^{S_4} - J_{c,1} (1 + \cos^2 \theta_{12}^{S_4}) \cos(2\psi_{12}^{S_4}) \right) \quad (245)$$

$$\tilde{J}_2(\mu_{12}^{S_4}) = J_{c,1} \cos \theta_{12}^{S_4} \sin(2\psi_{12}^{S_4}), \quad (246)$$

$$\tilde{J}_3(\mu_{12}^{S_4}) = \frac{1}{2} \sin(2\theta_{12}^{S_4}) [J_{f,1} + J_{c,1} \cos(2\psi_{12}^{S_4})], \quad (247)$$

$$\tilde{J}_4(\mu_{12}^{S_4}) = J_{c,1} \sin \theta_{12}^{S_4} \sin(2\psi_{12}^{S_4}), \quad (248)$$

and the $\delta_n^\pm(\phi)$ are given by Eqs. (34) and (35), and listed in Table II.

For $g = D_{2d}$, the non-vanishing site-dependent anisotropic exchange interactions are

$$J_{1,xy}^{D_{2d}}(\mu_{12}^{D_{2d}}) = J_{1,+} + J_{1,-} \cos^2 \theta_{12}^{D_{2d}}, \quad (249)$$

$$K_{2,xy}^{D_{2d}}(\mu_{13}^{D_{2d}}) = -J_{c,2}, \quad (250)$$

$$K_{1,xz}^{D_{2d}}(n, \mu_{12}^{D_{2d}}) = -(\gamma_n^+ + \gamma_n^-) \frac{J_{1,-}}{4} \sin(2\theta_{12}^{D_{2d}}), \quad (251)$$

$$K_{1,yz}^{D_{2d}}(n, \mu_{12}^{D_{2d}}) = (\gamma_n^+ - \gamma_n^-) \frac{J_{1,-}}{4} \sin(2\theta_{12}^{D_{2d}}). \quad (252)$$

For $g = T_d$, the non-vanishing site-dependent anisotropic exchange interactions reduce to

$$J_{1,xy}^{T_d} = \frac{J_{f,1}}{4}, \quad (253)$$

$$K_{2,xy}^{T_d} = -\frac{J_{f,1}}{2}. \quad (254)$$

3. Compact single-ion matrix elements

By using the Schwinger boson technique of representing a spin by two non-interacting bosons, and checking our results using the standard Clebsch-Gordan algebra with the assistance of symbolic manipulation software, we find the single-spin matrix elements with general $\{s_n\} = (s_1, s_2, s_3, s_4)$ to be

$$\begin{aligned} \langle \nu' | S_{n,\bar{z}} | \nu \rangle = & \delta_{m',m} \left(m \delta_{s',s} \Gamma_{s_{13},s'_{13},s_{24},s'_{24}}^{\{s_n\},s,n} \right. \\ & + \delta_{s',s+1} C_{-s-1}^m \Delta_{s_{13},s'_{13},s_{24},s'_{24}}^{\{s_n\},-s-1,n} \\ & \left. + \delta_{s',s-1} C_s^m \Delta_{s_{13},s'_{13},s_{24},s'_{24}}^{\{s_n\},s,n} \right), \quad (255) \end{aligned}$$

$$\begin{aligned} \langle \nu' | S_{n,\bar{\sigma}} | \nu \rangle = & \delta_{m',m+\bar{\sigma}} \left(A_s^{\bar{\sigma}m} \delta_{s',s} \Gamma_{s_{13},s'_{13},s_{24},s'_{24}}^{\{s_n\},s,n} \right. \\ & - \delta_{s',s+1} D_{-s-1}^{\bar{\sigma},m} \Delta_{s_{13},s'_{13},s_{24},s'_{24}}^{\{s_n\},-s-1,n} \\ & \left. + \delta_{s',s-1} D_s^{\bar{\sigma},m} \Delta_{s_{13},s'_{13},s_{24},s'_{24}}^{\{s_n\},s,n} \right) \quad (256) \end{aligned}$$

$$C_s^m = \sqrt{s^2 - m^2}, \quad (257)$$

$$D_s^{\bar{\sigma},m} = \bar{\sigma} \sqrt{(s - \bar{\sigma}m)(s - \bar{\sigma}m - 1)}, \quad (258)$$

$$\begin{aligned} \Gamma_{s_{13},s'_{13},s_{24},s'_{24}}^{\{s_n\},s,n} = & \delta_{s'_{24},s_{24}} \epsilon_n^- \alpha_{s_{13},s_{24}}^{s_{24},s,n} (s_{13}, s'_{13}) \\ & + \delta_{s'_{13},s_{13}} \epsilon_n^+ \alpha_{s_{24},s_{13}}^{s_{13},s,n} (s_{24}, s'_{24}), \quad (259) \end{aligned}$$

$$\begin{aligned} \Delta_{s_{13},s'_{13},s_{24},s'_{24}}^{\{s_n\},s,n} = & \delta_{s'_{24},s_{24}} \epsilon_n^- \beta_{s_{13},s_{24}}^{s_{24},s,n} (s_{13}, s'_{13}) \\ & + \delta_{s'_{13},s_{13}} \epsilon_n^+ \beta_{s_{24},s_{13}}^{s_{13},s,n} (s_{24}, s'_{24}), \quad (260) \end{aligned}$$

$$\begin{aligned} \alpha_{s_{13},s_{24}}^{s_{24},s,n}(s_{13}, s'_{13}) = & \frac{1}{4} (1 + \xi_{s,s_{13},s_{24}}) \delta_{s'_{13},s_{13}} \\ & + \gamma_n^+ \left(F_{s_{13},s_{24}}^{s_{13},s_{24}} \delta_{s'_{13},s_{13}-1} \right. \\ & \left. + F_{s_{13},s_{24}}^{s_{13}+1,s_{24}} \delta_{s'_{13},s_{13}+1} \right), \quad (261) \end{aligned}$$

$$\begin{aligned} \beta_{s_{13},s_{24}}^{s_{24},s,n}(s_{13}, s'_{13}) = & -\frac{(-1)^n}{4} \eta_{s,s_{13},s_{24}} \delta_{s'_{13},s_{13}} \\ & - \gamma_n^+ \left(G_{s_{13},s_{24}}^{s_{13},s_{24}} \delta_{s'_{13},s_{13}-1} \right. \\ & \left. + G_{s_{13},s_{24}}^{s_{13}+1,s_{24}} \delta_{s'_{13},s_{13}+1} \right), \quad (262) \end{aligned}$$

$$F_{s_{13},s_{24}}^{s_{13},s_{24}} = \frac{\eta_{s_{13},s_{13},s_{24}} A_{s+s_{13}}^{s_{24}} A_{s_{24}}^{s-1}}{4s(s+1)}, \quad (263)$$

$$G_{s_{13},s_{24}}^{s_{13},s_{24}} = \frac{\eta_{s_{13},s_{13},s_{24}} A_{s+s_{13}}^{s_{24}} A_{s+s_{13}-1}^{s_{24}}}{4s\sqrt{4s^2-1}}, \quad (264)$$

$$\eta_{z,x,y} = \frac{A_{x+z}^y A_y^{x-z}}{\sqrt{z^2(4z^2-1)}}, \quad (265)$$

$$\xi_{z,x,y} = \frac{x(x+1) - y(y+1)}{z(z+1)}, \quad (266)$$

where γ_n^+ and A_s^m are given by Eqs. (2) and (175). The prefactors m , $A_s^{\tilde{\sigma}m}$, C_s^m , C_{-s-1}^m , $D_s^{\tilde{\sigma},m}$, and $D_{-s-1}^{\tilde{\sigma},m}$ are consequences of the Wigner-Eckart theorem for a vector operator.[24] The challenge was to obtain the coefficients $\Gamma_{s_{13},s'_{13},s_{24},s'_{24}}^{\{s_n\},s,n}$ and $\Delta_{s_{13},s'_{13},s_{24},s'_{24}}^{\{s_n\},s,n}$. Their hierarchical structure based upon the unequal-spin dimer suggests that analogous coefficients with $n > 4$ may be obtainable.[4] Details will be presented elsewhere.[31]

4. First-order eigenstate energy constants

The constants appearing in the first-order eigenstate energies (177) are

$$\begin{aligned} c_{\nu}^{\pm} &= \frac{1}{4} \left(1 \pm \xi_{s,s_{13},s_{24}}^2 - \eta_{s,s_{13},s_{24}}^2 - \eta_{s+1,s_{13},s_{24}}^2 \right) \\ a_{\nu}^{\pm} &= c_{\nu}^{\pm} \pm 2 \left(\sum_{\sigma=\pm 1} \left[\left(F_{s_1,s_1,s}^{s_{13}+(1+\sigma)/2,s_{24}} \right)^2 \right. \right. \\ &\quad \left. \left. - \sum_{\sigma'=\pm 1} \left(G_{s_1,s_1,\sigma\sigma's+\sigma(1+\sigma')/2}^{s_{13}+(1+\sigma)/2,s_{24}} \right)^2 \right] \right. \\ &\quad \left. + (s_{13} \leftrightarrow s_{24}) \right), \end{aligned} \quad (267)$$

$$\begin{aligned} b_{\nu}^{\pm} &= \frac{1}{8} \sum_{\sigma'=\pm 1} (2s+1+\sigma')^2 \left(\eta_{s+(1+\sigma')/2,s_{13},s_{24}}^2 \right. \\ &\quad \left. \pm 8 \sum_{\sigma=\pm 1} \left[\left(G_{s_1,s_1,\sigma\sigma's+\sigma(1+\sigma')/2}^{s_{13}+(1+\sigma)/2,s_{24}} \right)^2 \right. \right. \\ &\quad \left. \left. + (s_{13} \leftrightarrow s_{24}) \right] \right), \end{aligned} \quad (268)$$

where the $F_{s_1,s_3,s}^{s_{13},s_{24}}$, $G_{s_1,s_3,s}^{s_{13},s_{24}}$, $\eta_{z,x,y}$, and $\xi_{z,x,y}$, are given by Eqs. (263)-(266), respectively.

5. Type I First-order AFM level-crossing constants

The Type I relevant both for $\tilde{J}'_g - \tilde{J}_g > 0$ AFM level-crossing inductions some low energy FM manifold states (with $\tilde{J}'_g > \tilde{J}_g > 0$) is $s_{13} = s_{24} = 2s_1$ with s arbitrary. Since all spins have s_1 , we let $a_{s,s_{13},s_{24}}^{\pm} \equiv a_{\nu}^{\pm}$, etc. For Type I, we have

$$a_{s,2s_1,2s_1}^{s_1,\pm} = c_{s,2s_1,2s_1}^{s_1,-} \left(1 \mp \frac{1}{4s_1-1} \right), \quad (269)$$

$$\begin{aligned} b_{s,2s_1,2s_1}^{s_1,\pm} &= \frac{1}{2(2s+3)(2s-1)} \left[s(s+1) \right. \\ &\quad \left. + [2s(s+1)-1][8s_1(2s_1+1)-s(s+1)] \right. \\ &\quad \left. \pm \frac{1}{4s_1-1} \left(2[16s_1^2+s(s+1)][s(s+1)-1] \right. \right. \\ &\quad \left. \left. - 8s_1[2s(s+1)-1] \right) \right], \end{aligned} \quad (270)$$

$$c_{s,2s_1,2s_1}^{s_1,\pm} = \frac{3[s(s+1)-1]-8s_1(2s_1+1)}{2(2s-1)(2s+3)}. \quad (271)$$

From these expressions, we may evaluate the Type I first-order level-crossing inductions for AFM tetramers. From the definitions of the level-crossing constants in Eqs. (184)-(188), we rewrite them to explicitly indicate the s_1 , s and type dependencies, and for Type I, it is easy to show that

$$a_{I,j}^{s_1,\pm}(s) = c_{I,j}^{s_1,-}(s) \left(1 \mp \frac{1}{4s_1-1} \right), \quad (272)$$

$$\begin{aligned} b_I^{s_1,\pm}(s) &= -\frac{2s[8s_1(2s_1+1)+4s^4-10s^2+3]}{(4s^2-1)(4s^2-9)} \\ &\quad \times \left(1 \mp \frac{1}{4s_1-1} \right), \end{aligned} \quad (273)$$

$$c_{I,1}^{s_1,-}(s) = \frac{3[4s^3+5s^2-3s-3-8s_1(2s_1+1)]}{2(2s+1)(2s+3)}, \quad (274)$$

$$c_{I,2}^{s_1,-}(s) = \frac{c_{20}(s) + (4s^2-4s+3)8s_1(2s_1+1)}{2(4s^2-1)(4s^2-9)}, \quad (275)$$

$$c_{20}(s) = 3(4s^4-9s^2-s+3), \quad (276)$$

for $j = 1, 2$. For $s_1 = 1/2$, it is easy to see that $a_{I,j}^{1/2,+}(s) = b_I^{1/2,+}(s) = 0$ for $s = 1, 2$, as expected.

Moreover, it is easy to show that for Type I,

$$c_2^- + \frac{1}{2}(b^+ + b^-) = -\frac{1}{3}c_1^-, \quad (277)$$

$$a_2^- + b^- = -\frac{1}{3}a_1^- = -\frac{4s_1}{3(4s_1-1)}c_1^-. \quad (278)$$

This implies that for Type I, the axial near-neighbor and next-nearest-neighbor axial anisotropic exchange interactions may be combined to yield an effective axial anisotropic exchange interaction given by Eq. (189). We emphasize that this is an exact expression for the effective interactions affecting the first-order level-crossing inductions, and is independent of the level-crossing number s , provided that Type I applies.

For the single-ion contributions to the level-crossing inductions, no such simple relation can be found. We note that

$$a_2^+ + b^+ = -\frac{1}{3}a_1^+, \quad (279)$$

but the overall quantity $a_2^+ + 2b^+ + a_1^+ \cos^2 \theta$ in Eq. (183) contains the extra quantity b^+ , which depends upon s , s_1 .

6. Type II First-order AFM level-crossing constants

For AFM tetramers with $\tilde{J}_g < 0$, $\tilde{J}'_g - \tilde{J}_g < 0$, Type II, there are two classes of minimum energy configurations for each s manifold, depending upon whether s is even or

odd. For even s , the relevant states have $s_{13} = s_{24} = s/2$, and for s odd, they are $s_{13}, s_{24} = (s \pm 1)/2, (s \mp 1)/2$. This type is also relevant for FM tetramers with $\tilde{J}_g > \tilde{J}'_g > 0$, especially for the first excited manifold of states with $s = 4s_1 - 1$. For even s the relevant parameters are

$$a_{s,s/2,s/2}^{s_1,\pm} = \frac{1}{2(2s-1)} \left[s-1 \mp \frac{f_1(s, s_1)}{2(s+3)} \right], \quad (280)$$

$$f_1(s, s_1) = 16s_1(s_1+1) - s^2 - 2s + 6, \quad (281)$$

$$b_{s,s/2,s/2}^{s_1,\pm} = \frac{1}{2(2s-1)} \left[s^2 \pm \frac{f_2(s, s_1)}{s+3} \right], \quad (282)$$

$$f_2(s, s_1) = 16s_1(s_1+1)(s^2+2s-1) - s(s^3+4s^2+s-4), \quad (283)$$

$$c_{s,s/2,s/2}^{\pm} = \frac{s-1}{2(2s-1)}. \quad (284)$$

For odd s , the relevant parameters are

$$a_{s,(s+1)/2,(s-1)/2}^{s_1,\pm} = \frac{1}{2s(2s-1)} \left[s^2 - s + 1 \mp \frac{f_3(s, s_1)}{2(s+2)(s+4)} \right], \quad (285)$$

$$f_3(s, s_1) = 16s_1(s_1+1)(s^2+3s-1) - s^4 - 5s^3 + 11s - 11, \quad (286)$$

$$b_{s,(s+1)/2,(s-1)/2}^{s_1,\pm} = \frac{1}{2(2s-1)} \left[s^2 - 1 \pm \frac{f_4(s, s_1)}{(s+2)(s+4)} \right], \quad (287)$$

$$f_4(s, s_1) = 16s_1(s_1+1)(s^3+5s^2+4s-3) - (s+1)(s^4+6s^3+7s^2-3s+1),$$

$$c_{s,(s+1)/2,(s-1)/2}^{+} = \frac{s^2 - s + 1}{2s(2s-1)}, \quad (288)$$

$$c_{s,(s+1)/2,(s-1)/2}^{-} = \frac{(s+1)(s-1)^2}{2s^2(2s-1)}. \quad (289)$$

From these expressions, we obtain the level-crossing inductions for the AFM type $\tilde{J}_g < 0$ and $\tilde{J}'_g - \tilde{J}_g < 0$.

For s even, we have

$$a_{IIe,1}^{s_1,\pm}(s) = s(2s-1)a_{s,s/2,s/2}^{s_1,\pm} - (s-1)(2s-3)a_{s-1,s/2,(s-2)/2}^{s_1,\pm}, \quad (290)$$

$$a_{||e,2}^{s_1,\pm}(s) = sa_{s,s/2,s/2}^{s_1,\pm} - (s-1)a_{s-1,s/2,(s-2)/2}^{s_1,\pm}, \quad (291)$$

$$b_{IIe}^{s_1,\pm}(s) = b_{s,s/2,s/2}^{s_1,\pm} - b_{s-1,s/2,(s-2)/2}^{s_1,\pm}, \quad (292)$$

$$c_{IIe,1}^{s_1,\pm}(s) = s(2s-1)c_{s,s/2,s/2}^{\pm} - (s-1)(2s-3)c_{s-1,s/2,(s-2)/2}^{\pm}, \quad (293)$$

$$c_{IIe,2}^{\pm}(s) = sc_{s,s/2,s/2}^{\pm} - (s-1)c_{s-1,s/2,(s-2)/2}^{\pm}. \quad (294)$$

For s odd, we have

$$a_{IIo,1}^{s_1,\pm}(s) = s(2s-1)a_{s,(s+1)/2,(s-1)/2}^{s_1,\pm}$$

$$- (s-1)(2s-3)a_{s-1,(s-1)/2,(s-1)/2}^{s_1,\pm}, \quad (295)$$

$$a_{IIo,2}^{s_1,\pm}(s) = sa_{s,(s+1)/2,(s-1)/2}^{s_1,\pm} - (s-1)a_{s-1,(s-1)/2,(s-1)/2}^{s_1,\pm}, \quad (296)$$

$$b_{IIo}^{s_1,\pm}(s) = b_{s,(s+1)/2,(s-1)/2}^{s_1,\pm} - b_{s-1,(s-1)/2,(s-1)/2}^{s_1,\pm}, \quad (297)$$

$$c_{IIo,1}^{s_1,\pm}(s) = s(2s-1)c_{s,(s+1)/2,(s-1)/2}^{\pm} - (s-1)(2s-3)c_{s-1,(s-1)/2,(s-1)/2}^{\pm}, \quad (298)$$

$$c_{IIo,2}^{s_1,\pm}(s) = sc_{s,(s+1)/2,(s-1)/2}^{\pm} - (s-1)c_{s-1,(s-1)/2,(s-1)/2}^{\pm}. \quad (299)$$

From these expressions, we may obtain the Type II AFM level-crossing induction parameters. For even s , we find

$$a_{IIe,1}^{s_1,\pm}(s) = \frac{2s-3}{2} \mp \frac{48s_1(s_1+1) + a_{10}^e(s)}{4(s+1)(s+3)}, \quad (300)$$

$$a_{10}^e(s) = -2s^3 - 5s^2 + 6s + 18, \quad (301)$$

$$a_{IIe,2}^{s_1,\pm}(s) = \frac{1}{2(2s-1)(2s-3)} \left[2s^2 - 6s + 3 \pm \frac{16s_1(s_1+1)(2s^2-4s+3) + a_{20}^e(s)}{2(s+1)(s+3)} \right], \quad (302)$$

$$a_{20}^e(s) = 2s^4 + 2s^3 - 9s^2 - 18s + 18, \quad (303)$$

$$b_{IIe}^{s_1,\pm}(s) = \frac{s}{(2s-1)(2s-3)} \left[s-1 \pm \frac{16s_1(s_1+1)(s-2) + b_0^e(s)}{2(s+1)(s+3)} \right], \quad (304)$$

$$b_0^e(s) = -4s^4 - 7s^3 + 20s^2 + 14s - 18, \quad (305)$$

$$c_{IIe,1}^{-}(s) = \frac{s(2s-3)}{2(s-1)}, \quad (306)$$

$$c_{IIe,2}^{-}(s) = \frac{s(2s^2-4s+1)}{2(s-1)(2s-1)(2s-3)}. \quad (307)$$

Combining $a_{IIe,2}^{s_1,-}(s)$ and $b_{IIe}^{s_1,-}(s)$, we find

$$a_{IIe,2}^{s_1,-} + b_{IIe}^{s_1,-} = \frac{1}{2} - \frac{16s_1(s_1+1) - d_0^e(s)}{4(s+1)(s+3)}, \quad (308)$$

$$d_0^e(s) = 2s^3 + 7s^2 + 2s - 6. \quad (309)$$

We note that this expression differs substantially from that for $a_{IIe,1}^{s_1,-}(s)$, except for $s_1 = 1/2$ and $s = 2$. Similarly, it is elementary to combine $c_{IIe,2}^{-}(s)$ and $[b_{IIe}^{s_1,+}(s) + b_{IIe}^{s_1,-}(s)]/2$. We find

$$c_{IIe,2}^{-}(s) + \frac{1}{2} (b_{IIe}^{s_1,+}(s) + b_{IIe}^{s_1,-}(s)) = \frac{s}{2(s-1)} \quad (310)$$

This simple expression differs from that for $c_{IIe,1}^{-}(s)$ by the factor $2s-3$. However, at $s = 2$, the only even s

value for $s_1 = 1/2$, they are equivalent. In addition, as for Type I, there is no simple relation between the single-ion parameters $a_{IIe,2}^{s_1,+}(s) + 2b_{IIe}^{s_1,+}(s)$ and $a_{IIe,1}^{s_1,+}(s)$.

For odd s , the Type II level-crossing induction parameters are

$$a_{IIo,1}^{s_1,\pm}(s) = \frac{2s-1}{2} \mp \frac{48s_1(s_1+1) + a_{10}^o(s)}{4(s+2)(s+4)}, \quad (311)$$

$$a_{10}^o(s) = -2s^3 - 11s^2 - 10s + 17, \quad (312)$$

$$a_{IIo,2}^{s_1,\pm}(s) = \frac{1}{2(2s-1)(2s-3)} \left[2s^2 - 2s - 1 \pm \frac{16s_1(s_1+1)(2s^2+1) + a_{20}^o(s)}{2(s+2)(s+4)} \right], \quad (313)$$

$$a_{20}^o(s) = 2s^4 + 10s^3 + 9s^2 - 22s - 5, \quad (314)$$

$$b_{IIo}^{s_1,\pm}(s) = \frac{1}{(2s-1)(2s-3)} \left[(s-1)(s-2) \pm \frac{16s_1(s_1+1)(s^2-4s+1) + b_0^o(s)}{2(s+2)(s+4)} \right], \quad (315)$$

$$b_0^o(s) = -4s^5 - 19s^4 + 54s^2 - 2s - 5, \quad (316)$$

$$c_{IIo,1}^-(s) = \frac{(s-1)(2s-1)}{2s}, \quad (317)$$

$$c_{IIo,2}^-(s) = \frac{(s-1)(2s^2-4s+3)}{2s(2s-1)(2s-3)}. \quad (318)$$

We note that $a_{IIe,j}^{1/2,+}(2) = a_{IIo,j}^{1/2,+}(1) = b_{IIe}^{1/2,+}(2) = b_{IIo}^{1/2,+}(1) = 0$ for $j = 1, 2$, as expected. However, by combining $a_{IIo,2}^{s_1,-}(s)$ and $b_{IIo}^{s_1,-}(s)$, we have

$$a_{IIo,2}^{s_1,-} + b_{IIo}^{s_1,-} = \frac{1}{2} - \frac{16s_1(s_1+1) - d_0^o(s)}{4(s+2)(s+4)}, \quad (319)$$

$$d_0^o(s) = 2s^3 + 13s^2 + 22s + 5, \quad (320)$$

which differs substantially from the version with $s_1 = 1/2$. In addition, it is elementary to combine $c_{IIo,2}^-(s) + [b_{IIo}^{s_1,+}(s) + b_{IIo}^{s_1,-}(s)]/2$. We find

$$c_{IIo,2}^-(s) + \frac{1}{2} (b_{IIo}^{s_1,+}(s) + b_{IIo}^{s_1,-}(s)) = \frac{(s-1)}{2s} \quad (321)$$

which differs from $c_{IIo,1}^-(s)$ by the factor $2s-1$. At $s = 1$, the only relevant odd s value for $s_1 = 1/2$, these are equivalent. In addition, as for Type I and the even crossings of Type II, there is no simple relation between the single-ion parameters $a_{IIo,2}^{s_1,+}(s) + 2b_{IIo}^{s_1,+}(s)$ and $a_{II|rmc,1}^{s_1,+}(s)$.

7. Hartree INS functions

The functions $L_{\nu,\nu'}(\mathbf{q})$ and $M_{\nu,\nu'}(\mathbf{q})$ in the self-consistent Hartree INS $S_g^{(1)}(\mathbf{q}, \omega)$ in the induction representation are given by

$$\begin{aligned} L_{\nu,\nu'}(\mathbf{q}) = & \delta_{m',m} \delta_{s'_{24},s_{24}} \left[m^2 \delta_{s',s} \right. \\ & \times \left(\delta_{s'_{13},s_{13}} f_{\bar{\nu},0}(\mathbf{q}) + \sum_{\sigma''=\pm 1} \delta_{s'_{13},s_{13}+\sigma''} f_{\bar{\nu},1}^{\sigma''}(\mathbf{q}) \right) \\ & + \sum_{\sigma'=\pm 1} \delta_{s',s+\sigma'} \left(C_{-\sigma's-(\sigma'+1)/2}^m \right)^2 \\ & \times \left(\delta_{s'_{13},s_{13}} f_{\bar{\nu},2}^{\sigma'}(\mathbf{q}) \right. \\ & \left. \left. + \sum_{\sigma''=\pm 1} \delta_{s'_{13},s_{13}+\sigma''} f_{\bar{\nu},3}^{\sigma',\sigma''}(\mathbf{q}) \right) \right] \\ & + \left(\begin{matrix} s_{13} \leftrightarrow s_{24} \\ s'_{13} \leftrightarrow s'_{24} \\ q_y \rightarrow -q_y \end{matrix} \right), \end{aligned} \quad (322)$$

$$\begin{aligned} M_{\nu,\nu'}(\mathbf{q}) = & \sum_{\sigma=\pm 1} \delta_{m',m+\sigma} \delta_{s'_{24},s_{24}} \left[\left(A_s^{\sigma m} \right)^2 \delta_{s',s} \right. \\ & \times \left(\delta_{s'_{13},s_{13}} f_{\bar{\nu},0}(\mathbf{q}) + \sum_{\sigma''=\pm 1} \delta_{s'_{13},s_{13}+\sigma''} f_{\bar{\nu},1}^{\sigma''}(\mathbf{q}) \right) \\ & + \sum_{\sigma'=\pm 1} \delta_{s',s+\sigma'} \left(D_{-\sigma's-(\sigma'+1)/2}^{\sigma,m} \right)^2 \\ & \times \left(\delta_{s'_{13},s_{13}} f_{\bar{\nu},2}^{\sigma'}(\mathbf{q}) \right. \\ & \left. \left. + \sum_{\sigma''=\pm 1} \delta_{s'_{13},s_{13}+\sigma''} f_{\bar{\nu},3}^{\sigma',\sigma''}(\mathbf{q}) \right) \right] \\ & + \left(\begin{matrix} s_{13} \leftrightarrow s_{24} \\ s'_{13} \leftrightarrow s'_{24} \\ q_y \rightarrow -q_y \end{matrix} \right), \end{aligned} \quad (323)$$

$$\begin{aligned} f_{\bar{\nu},0}(\mathbf{q}) = & \frac{1}{8} \left(f_+(\mathbf{q}) + \xi_{s,s_{13},s_{24}}^2 f_-(\mathbf{q}) \right. \\ & \left. - 2\xi_{s,s_{13},s_{24}} \sin(q_x a) \sin(q_y a) \right), \end{aligned} \quad (324)$$

$$\begin{aligned} f_{\bar{\nu},1}^{\sigma''}(\mathbf{q}) = & 2 \left(1 - \cos[a(q_x + q_y)] \right) \\ & \times \left(F_{s_1,s_1,s}^{s_{13}+(\sigma''+1)/2,s_{24}} \right)^2 \end{aligned} \quad (325)$$

$$f_{\bar{\nu},2}^{\sigma'}(\mathbf{q}) = \frac{1}{8} f_-(\mathbf{q}) \eta_{s+(\sigma'+1)/2,s_{13},s_{24}}^2, \quad (326)$$

$$\begin{aligned} f_{\bar{\nu},3}^{\sigma',\sigma''}(\mathbf{q}) = & 2 \left(1 - \cos[a(q_x + q_y)] \right) \\ & \times \left(G_{s_1,s_1,\sigma'\sigma''s+\sigma''(\sigma'+1)/2}^{s_{13}+(\sigma''+1)/2,s_{24}} \right)^2, \end{aligned} \quad (327)$$

$$\begin{aligned} f_{\pm}(\mathbf{q}) = & 1 + \cos(q_x a) \cos(q_y a) \\ & \pm \cos(q_z c) [\cos(q_x a) + \cos(q_y a)], \end{aligned} \quad (328)$$

where the A_s^m , C_s^m , $D_s^{\sigma,m}$, $F_{s_1,s_3,s}^{s_{13},s_{24}}$, $G_{s_1,s_3,s}^{s_{13},s_{24}}$, $\eta_{z,x,y}$, $\xi_{z,x,y}$, are given by Eqs. (175), (257), (258), and (263)-(266), respectively.

-
- * Electronic address: klemm@phys.ksu.edu
 † Electronic address: efremov@theory.phy.tu-dresden.de
- [1] R. Sessoli, D. Gatteschi, A. Caneschi, and M. Novak, *Nature (London)*, **365**, 141 (1993); W. Wernsdorfer and R. Sessoli, *Science* **284**, 133 (1999).
 - [2] M. N. Leuenberger and D. Loss, *Nature (London)*, **410**, 789 (2001).
 - [3] D. V. Efremov and R. A. Klemm, *Phys. Rev. B* **66**, 174427 (2002).
 - [4] D. V. Efremov and R. A. Klemm, *Phys. Rev. B (cond-mat/0601591)*, to be published.
 - [5] Y. Shapira, M. T. Liu, S. Foner, C. E. Dubé, and P. J. Bonitatebus, Jr., *Phys. Rev. B* **59**, 1046 (1999).
 - [6] C. Mennerich, H.-H. Klauss, M. Broekelmann, F. J. Litterst, C. Golze, R. Klingeler, V. Kataev, B. Büchner, S.-N. Grossjohann, W. Brenig, M. Goiran, H. Rakoto, J.-M. Broto, O. Kataeva, and D. J. Price, *cond-mat/0601305* (unpublished).
 - [7] D. Zipse, J. M. North, N. S. Dalal, S. Hill, and R. S. Edwards, *Phys. Rev. B* **68**, 184408 (2003).
 - [8] S. Carretta, E. Livioti, N. Magnani, P. Santini, and G. Amoretti, *Phys. Rev. Lett.* **92**, 207205 (2004).
 - [9] A. Bino, D. C. Johnston, D. P. Goshorn, T. R. Halbert, and E. I. Stiefel, *Science* **241**, 1479 (1988).
 - [10] R. S. Rubins, T. D. Black, and J. Barak, *J. Chem. Phys.* **85**, 3770 (1985).
 - [11] T. D. Black, R. S. Rubins, D. K. De, R. C. Dickinson, and W. A. Baker, Jr., *J. Chem. Phys.* **80**, 4620 (1984).
 - [12] R. C. Dickinson, W. A. Baker, Jr., T. D. Black, and R. S. Rubins, *J. Chem. Phys.* **79**, 2609 (1983).
 - [13] E. Buluggiu, *J. Chem. Phys.* **84**, 1243 (1986).
 - [14] E.-C. Yang, D. N. Hendrickson, W. Wernsdorfer, M. Nakano, L. N. Zakharov, R. D. Sommer, A. L. Rheingold, M. Ledezma-Gairaud, and G. Christou, *J. Appl. Phys.* **91**, 7382 (2002).
 - [15] A. Sieber, C. Boskovic, R. Bircher, O. Waldmann, W. T. Ochsenein, G. Chaboussant, H. U. Güdel, N. Kirchner, J. van Slageren, W. Wernsdorfer, A. Neels, H. Stoeckli-Evans, S. Jannsen, F. Juranyi, and H. Mutka, *Inorg. Chem.* **44**, 4315 (2005), and references therein.
 - [16] M. Moragues-Cánovas, M. Helliwell, L. Ricard, Éric Rivière, W. Wernsdorfer, E. Brechin, and T. Mallah, *Eur. J. Inorg. Chem.* **2004**, 2219.
 - [17] R. S. Edwards, S. Maccagnano, E.-C. Yang, S. Hill, W. Wernsdorfer, D. Hendrickson, and G. Christou, *J. Appl. Phys.* **93**, 7807 (2003).
 - [18] E. del Barco, A. D. Kent, E.-C. Yang, and D. N. Hendrickson, *Polyhedron* **24**, 2695 (2005).
 - [19] D. N. Hendrickson, E.-C. Yang, R. M. Isidro, C. Kirman, J. Lawrence, R. S. Edwards, S. Hill, A. Yamaguchi, H. Ishimoto, W. Wernsdorfer, C. Ramsey, N. Dalal, and M. M. Olmstead, *Polyhedron* **24**, 2280 (2005).
 - [20] C. Boskovic, R. Bircher, P. L. W. Tregenna-Piggott, H. U. Güdel, C. Paulsen, W. Wernsdorfer, A.-L. Barra, E. Khatsko, A. Neels, and H. Stoeckli-Evans, *J. Am. Chem. Soc.* **125**, 14046 (2003).
 - [21] S. Hill, private communication.
 - [22] R. Boča, *Theoretical Foundations of Molecular Magnetism*, (Elsevier, Amsterdam, 1999).
 - [23] O. Waldmann and H. Güdel, *Phys. Rev. B* **72**, 094422 (2005).
 - [24] M. Tinkham, *Group Theory and Quantum Mechanics*, (McGraw-Hill, New York, 1964).
 - [25] D. M. Barnhart, D. L. Clark, J. C. Gordon, J. C. Huffman, J. G. Watkin, and B. D. Zwick, *J. Am. Chem. Soc.* **115**, 8461 (1993).
 - [26] R. A. Klemm and M. Luban, *Phys. Rev. B* **64**, 104424 (2001).
 - [27] A. Bencini and D. Gatteschi, *Electron Paramagnetic Resonance of Exchange Coupled Systems*, (Springer, Berlin, 1990).
 - [28] O. Waldmann, J. Hassmann, P. Müller, D. Volkmer, U. S. Schubert, and J.-M. Lehn, *Phys. Rev. B* **58**, 3277 (1998).
 - [29] T. Moriya, *Phys. Rev.* **120**, 91 (1960); I. Dzyaloshinskii, *J. Phys. Chem. Solids* **4**, 241 (1958).
 - [30] R. Valenti, C. Gros, and W. Brenig, *Phys. Rev. B* **62**, 14164 (2000).
 - [31] D. V. Efremov and R. A. Klemm, unpublished.
 - [32] H. Goldstein, *Classical Mechanics*, (Addison-Wesley, Reading, MA, 1965), p. 109.
 - [33] M. Alcántara Ortigoza, R. A. Klemm, and T. S. Rahman, *Phys. Rev. B* **72**, 174416 (2005).
 - [34] J. D. Jackson, *Classical Electrodynamics, 3rd Edition* (Wiley & Sons, Hoboken, NJ, 1999), p. 186.
 - [35] C. Kittel, *Introduction to Solid State Physics* (Wiley & Sons, Third Edition, New York, 1968), pp. 149, 173.
 - [36] S. Carretta, P. Santini, G. Amoretti, T. Guidi, R. Caciuffo, A. Candini, A. Cornia, D. Gatteschi, M. Plazanet, and J. A. Stride, *Phys. Rev. B* **70**, 214403 (2004).
 - [37] A. Cornia, A. C. Fabretti, P. Garrisi, C. Mortalò, D. Bonacchi, D. Gatteschi, R. Sessoli, L. Sorace, W. Wernsdorfer, and A.-L. Barra, *Angew. Chem. Int. Ed.* **43**, 1136 (2004).
 - [38] G. Amoretti, S. Carretta, R. Caciuffo, H. Casalta, A. Cornia, M. Affronte, and D. Gatteschi, *Phys. Rev. B* **64**, 104403 (2001).
 - [39] J. Schnack, M. Brüger, M. Luban, P. Kögerler, E. Morosan, R. Fuchs, R. Modler, H. Nojiri, R. C. Rai, J. Cao, J. L. Musfeldt, and X. Wei, *Phys. Rev. B* **73**, 094401 (2006).
 - [40] J. M. Clemente-Juan, H. Andres, J. J. Borrás-Almenar, E. Coronado, H. U. Güdel, M. Aebbersold, G. Kearly, H. Büttner, and M. Zolliker, *J. Am. Chem. Soc.* **121**, 10021 (1999).
 - [41] L. Lecren, W. Wernsdorfer, Y.-G. Li, O. Roubeau, H. Miyasaka, and R. Clérac, *J. Am. Chem. Soc.* **127**, 11311 (2005).
 - [42] M. Koikawa, M. Ohba, and T. Tokii, *Polyhedron* **24**, 2257 (2005).
 - [43] J.-N. Rebilly, L. Catala, E. Rivière, R. Guillot, W. Wernsdorfer, and T. Mallah, *Inorg. Chem.* **44**, 8194 (2005).